Pharmacological targeting of the Treg/Th17 axis using *in vitro* cell cultures derived from patients with autoimmune Addison's disease

Adrianna Jebrzycka

This thesis is submitted in partial fulfillment for the degree of Master's in Biomedical Sciences

Department of Biomedicine

KG Jebsen Center for Autoimmune Diseases, Department of Clinical Science

University of Bergen

Spring 2022

Acknowledgements

First and foremost, I would like to express my most sincere gratitude to my supervisors Anette Susanne Bøe Wolff, Bergithe Eikeland Oftedal and Thea Sjøgren, for the knowledge you have shared and the patience you have shown when helping me to navigate this journey. I am very thankful for the time and effort you have dedicated to my scientific training and for always being available to answer my questions and give feedback on my writing. Your encouragement has been invaluable, especially towards the submission of this thesis. I could have not wished for better mentors. And to you Anette, I certainly would not have made it this far without your faith in me.

Furthermore, I would like to thank all members of the Endocrine Medicine group, led by prof. Eystein Sverre Husebye for creating such a lovely and inclusive environment. Many thanks to head engineer Lars Breivik for making sure that all the equipment was always available and to the lab technicians Marie Karlsen, Hajirah Muneer and Elisabeth Halvorsen for technical support and method training. To my fellow master's and Erasmus students at the lab: Emina, Ifunanya, Abtin, Stephan and Didac, cheers for the laughs and great company. I would also like to thank head engineer Brith Bergum at the Flow Cytometry Core Facility for valuable advice during flow cytometry analyses and to Marianne Sponheim and Charlotte Quist Månsson Svendsen at AH diagnostics for technical advice on xCELLigence RTCA.

To my friends and family who have supported me through this process, I am very grateful to have you. Finally, to my best friends and fellow classmates with whom I have shared the most fun times throughout the two years, Marthe and Patrick, I could not have made it without you.

Bergen, June 2022

Adrianna Jebrzycka

Table of contents

Selected abbreviations

AAD	Autoimmune Addison's disease
AIRE	Autoimmune regulator
ACT	Adoptive cell therapy
BCR	B cell receptor
CD	Cluster of differentiation
CI	Cell index
CTL	Cytotoxic T cell
cTEC	Cortical thymic epithelial cell
DC	Dendritic cell
DMSO	Dimethyl sulfoxide
FOXP3	Forkhead box P3
GATA3	Gata binding protein 3
IFN	Interferon
IL	Interleukin
iTregs	*in vitro* induced Tregs
mTEC	Medullary thymic epithelial cell
PBMC	Peripheral blood mononucleated cells
PBS	Phosphate buffered saline
PRR	Pattern recognition receptor
pTregs	Peripherally induced Tregs
PI	Proliferation index
RA	Rheumatoid arthritis
ROAS	Registry and biobank for organ specific autoimmune disorders
RORγt	Retinoic acid-related orphan receptor gamma t
RTCA	Real time cell analysis (or analyzer)
STAT3	Signal transducer and activator of transcription3
T1D	Type 1 diabetes
T-bet	T-box protein expressed in T cells
TCR	T cell receptor
TGF-β	Transforming growth factor β
TRA	Tissue restricted antigen
Teff	Effector T cell
Tconv	Conventional T cell
Treg	Regulatory T cell
Th	Helper T cell

Summary

Autoimmune Addison's disease (AAD) is a rare endocrine disorder characterized by an immune-mediated attack towards the cells of the adrenal cortex. The major self-antigen, targeted by autoantibodies and self-reactive T cells is the enzyme 21-hydroxylase, responsible for the production of life-essential hormones: cortisol and aldosterone. Over time, patients develop hormone insufficiency and depend on life-long hormone replacement therapy, which is currently the only treatment option available. AAD patients suffer from lower quality of life and risk earlier death and as such it is important to find treatment options that target the cause of AAD and not only manage the symptoms.

Regulatory T cells (Tregs) are natural immune suppressors that possess a range of immunomodulatory mechanisms to control overt immune responses, promoted by potentially self-reactive T cells. Their reduced numbers and impaired suppressive function are seen in autoimmune conditions, including autoimmune polyendocrine syndromes of which AAD is a frequent component. At the same time, Th17 cells and their signature cytokine IL-17A are frequently involved in the pathogenicity of autoimmune disorders, including psoriasis and rheumatoid arthritis. Intriguingly, peripheral induction of both Tregs and Th17 cells happens in response to TGF-β, and the presence of IL-6 skews this reciprocal interrelation towards Th17 cells. The IL-6R-inhibitor LMT-28 and the monoclonal antibody neutralizing IL-17A Secukinumab, have previously been shown to alter the Treg/Th17 axis by promoting the numbers and function of Tregs. Therefore, they offer an attractive strategy when attempting to restore self-tolerance with the possibility to alleviate or reverse the autoimmune reaction.

In this project, we aimed to study the effects of LMT-28 and Secukinumab using *in vitro* cultures of PBMCs and expanded Tregs from AAD patients and healthy controls. Prior to drug screenings, we optimized the xCELLigence RTCA platform for continuous monitoring of T cells in culture. The subsequent drug screening assays were followed by functional and phenotypical analyses of cells using flow cytometry, quantitative polymerase chain reaction (qPCR,) and enzyme-linked immunosorbent assay (ELISA).

Overall, we did not observe major influences of the selected drugs on *in vitro* cultures of PBMCs and Tregs. Although a slight increase in the number of FOXP3+ Tregs was seen in patients in the expanded LMT-28 treated cultures, these results were not verified on the RNA level. As no differences were observed in the expression levels of Treg and Th17 linage

markers FOXP3 and Rorγt following treatments, the Treg/Th17 axis was likely not affected by either of the drugs.

As for the effect of the drugs on Treg functional markers, we observed an increase in the protein expression of CD39 in Tregs from healthy controls after both treatments, not seen in AAD patients. The ectoenzyme has been connotated to Tregs with a higher suppressive capacity, indicating that patients' cells possibly did not respond optimally to this positive alteration of the treatments. To validate this finding, future studies with a larger cohort of patients and healthy controls must be conducted, to draw any firm conclusions about the effects of the *in vitro* treatments.

1. Introduction

1.1 The immune system

The human immune system plays a critical role in maintaining homeostasis by quickly responding to environmental stimuli and possible threats posed by a wide range of pathogens, as well as tissue injury and cancerous cells of the self. To achieve this goal, it is equipped with an impressive repertoire of immune cells, each type commonly characterized by the expression of cell surface molecules assigned with a number within the cluster of differentiation (CD) system. Based on the timescale and the specificity of the response, as well as the type of cells engaged, immune responses are commonly divided into innate and adaptive sub-compartments.

1.1.1 Innate immunity

In the early stages of infection, upon entrance through the airways or breakage of anatomical barriers like skin or mucosal epithelium, the first responders are cells of the innate immune system, including dendritic cells (DCs), macrophages, neutrophils, and innate lymphoid cells (ILCs). Using different classes of pattern recognition receptors (PRRs) they recognize conserved structural motifs on broad classes of microbes, collectively called pathogen associated molecular patterns (PAMPs). Activation of a specific PRR leads to enhanced expression of inflammatory genes, initiating the production of pro-inflammatory cytokines and chemokines [1]. Their subsequent release potentiates the immune responses, enhancing the ability of phagocytes to engulf the invaders, additionally inducing local inflammation [2], that aids in the recruitment of other immune cells from circulation. Among these are the B and T lymphocytes, cells of the adaptive immune system.

1.1.2 Adaptive immunity

Although slower to arise, the immune responses promoted by lymphocytes are much more potent and target-specific compared to the ones promoted by innate immune cells. The specificity of lymphocytes is achieved by their ability to express highly diverse antigen receptors [3]. These are generated during the early development and maturation of B cells in the bone marrow and T cells in the thymus, where segments of genes encoding variable regions of the B cell receptor (BCR) and the T cell receptor (TCR) rearrange at random. As a result, every B and T cell has a unique specificity to recognize a distinct antigen, providing an extremely large repertoire of diverse cells on a population level.

As opposed to B cells, T cells cannot bind antigens through direct contact of their TCR with a pathogen and instead depend on interactions with antigen presenting cells (APCs) which display antigens on their cell surface using major histocompatibility complex (MHC) molecules (human leukocyte antigens, HLA, in humans) [4]. Upon recognition of matching antigen in secondary lymphoid organs (specialized for filtering and trapping antigens) or the periphery, naïve lymphocytes get activated. Only lymphocytes with high specificity towards that antigen will effectively proliferate in a process of clonal expansion, migrate to the site of infection, and differentiate into either memory cells or effector cells [3]. The former stay in circulation following infection and can mount a faster and more efficient response to a repeated encounter of the same antigen. Effector functions of B cells are characterized by the production of antigen specific antibodies [5]. Effector T cells promote diverse cell-mediated responses, described in 1.2. As this thesis will focus on T cells and their subpopulations, the remaining introduction will concern T cells.

1.2 T cells

T cells are commonly subdivided into two major subsets, based on their expression of signalling co-receptors and specific effector functions [5]. TCRs of CD8 expressing T cells interact with antigens presented on MHC class I molecules, expressed by all nucleated cells. MHC class I molecules display cytosolic antigens, thus enabling $CD8^+$ T cells to "scan" host cells for viruses or indications of a cancerous phenotype. CD4 expressing cells in turn, recognize antigens bound to MHC class II molecules displayed by professional APCs like DCs, monocytes and B cells. Peptides loaded onto MHC class II stem from phagocytosed extracellular pathogens, which are the main target for CD4+ T cells. Activated CD4+ T cell cells (helper T cells or Th) are crucial orchestrators of immune responses, maximizing the function of other immune cells by secreting cytokines including interleukins (ILs) and interferons (IFNs).

1.2.1 Thymic T cell development and tolerance achievement

The thymus is a primary lymphoid organ located beneath the breastbone, specialized to promote the development and maturation of T cells. Following migration from the bone marrow to the thymus, the early T cell progenitors (now termed thymocytes), do not express a TCR, nor CD4/CD8 co-receptors, and thus exhibit a double negative (CD4-CD8-) phenotype [6]. Thereafter, expression of both CD4 and CD8 is promoted, while genes encoding the TCR's β and α chain are somatically recombined. At this point, the double-positive (CD4+CD8+) thymocytes undergo the process of positive selection ensuring that the newly assembled TCR

has an affinity for self-MHC I/II molecules, displayed by the cortical thymic epithelial cells (cTECs) [7]. Thymocytes incapable of binding self-MHC (which is a requirement for all mature T cell functions), do not receive the TCR signal needed to survive and thus undergo apoptosis. Followingly, surviving thymocytes progress to the single positive stage, downregulating either CD4 or CD8, depending on which class of self-MHC they recognized. Linage committed, single positive thymocytes then migrate to the thymic medulla where they are "taught" not to respond to antigens of the self, which they will frequently encounter once released to the periphery. Important in this context is the thymic presentation of otherwise tissue-restricted antigens (TRAs), driven by the transcription factor: Autoimmune Regulator (AIRE), predominantly expressed by the medullary thymic epithelial cells (mTECs) [8]. Thymocytes with a high TCR-affinity towards self-antigens displayed by mTECs, given their self-reactive propensity, are driven to apoptosis. On the other hand, thymocytes with low-affinity TCRs towards self, survive, mature, and ought to be released into the periphery as conventional naïve CD4+ or CD8+ T cells. Lastly, thymocytes with TCR affinities falling in the intermediate affinity range may become thymus-derived Tregs (described in 1.3.2), a generation of which is likely enforced by AIRE [9]. Thymic T cell development, including positive and negative selection, is shown in fig 1.1.

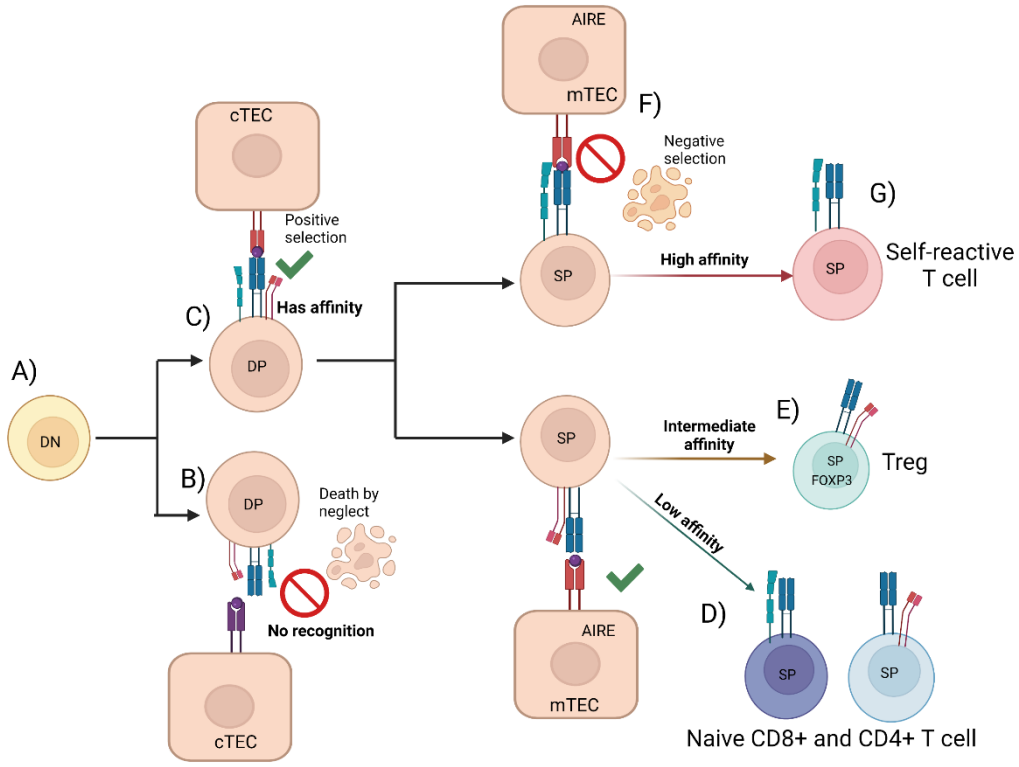

Figure 1.1 T cell development and central tolerance A) Early T cell progenitors do not express a TCR or the CD4/CD8 coreceptors (DN). In the thymic cortex, the expression of both CD4 and CD8 is promoted and the TCR is assembled. B) Thymocytes with no affinity for self-MHC die by neglect, while C) the ones that show TCR affinity towards self-MHC downregulate either CD4 or CD8 and become single positive (SP), migrating to the

thymic medulla. Medullary thymic epithelial cells (mTECs) express autoimmune regulator (AIRE) which promiscuously expresses antigens of the self that are otherwise tissue-restricted (TRAs). D) Upon low affinity TCR interaction towards self-antigens, the thymocytes become naïve CD4+ or CD8+ cells. E) Intermediate affinity promotes the generation of Tregs, while F) high affinity interactions indicate cells with propensities to become self-reactive and are thus driven to apoptosis. G) Some thymocytes evade negative selection, escape into the periphery, and may target tissues displaying cognate antigen. Figure created in Biorender.com

1.2.3 Activation of T cells

Initiation of T cell effector functions requires T cell activation and usually depends on at least two signalling events, the first consisting of TCR binding to an antigen peptide presented through an MHC class I or class II molecule, an interaction that is stabilized by CD4 and CD8 respectively (Fig. 1.2). The second signal is costimulatory and delivered by CD80/86 molecules found on the surfaces of APCs that bind CD28, another co-receptor expressed by T cells. APCs upregulate the expression of CD80/CD86 when stimulated by inflammatory cytokines produced by activated innate immune cells [10]. In the absence of pathogenic threat, the levels of the costimulatory molecules are kept low to not cause or augment unnecessary (and potentially harmful) T cell effector functions. Signal 2 provides T cells with necessary proliferation signals and is thought to induce expression of the IL-2Rα subunit (CD25) as well as the production of interleukin 2 (IL-2) [11], needed for their survival and further expansion [12].

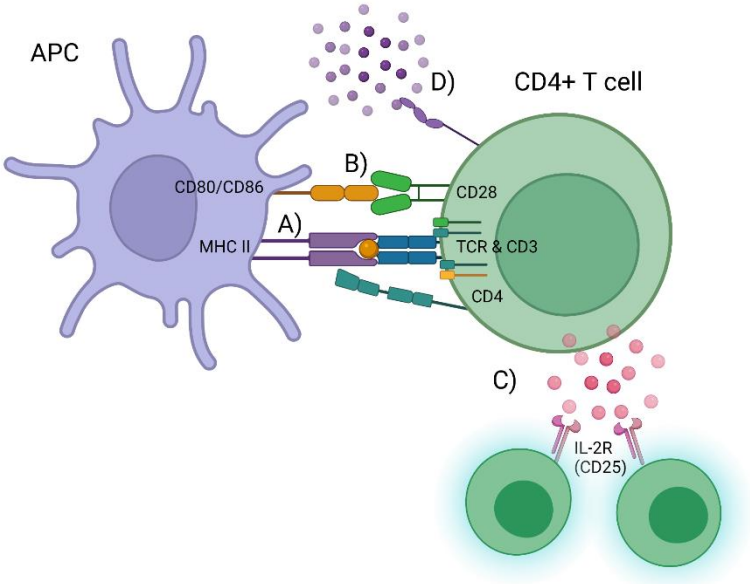

Figure 1.2 Signalling events during T cell activation, as exemplified by a CD4+ T cell. APC (here; dendritic cell) displays antigens on an MHC class II molecule to a $CD4^+$ T cell (signal 1). Co-stimulatory signaling where CD80/CD86 on an APC binds CD28 on T cells is needed for proper activation (signal 2). Activation transduced through the intracellular tails of the CD3 co-receptor induces C) production of IL-2, needed for T cell survival, proliferation, and differentiation as well as expression of high-affinity IL-2 receptor (CD25) that potentiates IL-2 capture D) Depending on the cytokines at the site, activated T cells will commit to a specific effector subpopulation and start exerting their respective effector functions. Figure created in Biorender.com, inspired by [13]

T cell activation induces a series of concerted cellular events, ranging from cytoskeletal rearrangements during T cell-APC/target cell contacts [14], to differentiation of T cells into distinct effector populations. Of notice here is that peripheral differentiation of CD4+ cells is largely influenced by their microenvironment, especially cytokines present at the site of their activation [15]. Signaling through cytokine receptors activates the Th linage-specific transcription factors, which yield them their specific effector functions [16]. Several major effector populations of helper T cells have been characterized including Th1, Th2, Th17 and follicular T helper cells, each with a distinct cytokine profile and specialties regarding the type of responses they promote. Lastly, immunosuppressive CD4+ T cells also exist, termed regulatory T cells (Tregs), important for controlling exaggerated or undesirable immune responses. including ones mounted to normal constituents of the host(self-antigens) [17].

1.3. Regulatory T cells

1.3.1 Treg phenotype

Regulatory T cells (Tregs) is a subpopulation comprising 5-10% of CD4+ T cells in peripheral blood [18]. They have the capacity to actively suppress activation and function of other immune cells, thus making them a central player in the maintenance of peripheral self-tolerance [17, 19]. Their thymic origin as well as pivotal contribution in preventing autoimmunity over self-reactive T cells were already indicated in the 80's [20, 21]. However, major advances in understanding Tregs were not made until the discoveries of cellular markers that delineated them from (most) conventional T cells (Tconvs). The first marker characterized was the high-affinity IL-2 receptor α chain (CD25) that Tregs constitutively express [19]. Followingly, the transcription factor Forkhead box P3 (FOXP3) was identified as a Treg master-regulator, crucial for Treg development, maintenance, and induction of their immunosuppressive properties [22, 23]. Currently, a combination of markers is typically used to distinguish Tregs from Tconvs including CD4+, CD25+, FOXP3+, and CD127-, where expression of the latter is thought to inversely correlate with FOXP3 [24].

1.3.2 Treg development

Most of the Tregs commit to their linage during development in the thymus (these are termed thymic or natural Tregs or tTregs/nTregs) where they are presumed to display an "intermediate TCR affinity" towards thymically expressed self-antigens during negative selection [25, 26]. This means that they recognize self-antigens with higher affinity than developing naïve Tconvs, but lower than what is needed to be eliminated. Their TCR affinities are therefore thought to

be "skewed" towards recognizing self [26-28], again pointing to their crucial role in preventing autoimmunity. Following the TCR engagement and co-stimulation by CD80/CD86 [29], signalling through IL-2 is thought to induce *FOXP3* expression and promote Treg effector phenotype [30-32] while its peripheral maintenance is supported by transforming growth factor β (TGF-β). Stable maintenance expression of *FOXP3* has been indicated to require a specific epigenomic landscape, recognized by demethylation of CpG islands in *FOXP3* conserved non-coding region 2 (CNS2) called Treg specific demethylation region (TSDR) [33].

1.3.3 Induced Tregs (iTregs and pTregs)

Intriguingly, Tregs can also be generated outside the thymus from naïve CD4+CD25- T cells in peripheral lymphoid organs or tissues (termed peripheral Tregs or pTregs) [34] or *in vitro* (iTregs) [35]. Generation of both pTregs and iTregs is thought to occur under non-inflammatory and "suboptimal" activation conditions. These are recognized by weak TCR stimulation [36] in the presence of IL-2 [37] and anti-inflammatory cytokines including IL-10 [38] and TGF-β, the latter being indispensable for Treg induction [39]. The binding of TGF-β to its receptor leads to a cascade of signalling events involving Smad2-3 [40], (NFAT) and FOXP3 enhancer CNS1 leading to an increase in FOXP3 expression [41]. Additionally, TGF-β restricts Smad7 [42] and methyltransferaserase (DNTM1) [43] that limit FOXP3 expression in non-Tregs.

Physiologically, pTregs richly locate mucosal surfaces including the lungs and gut [34]. They are thought to be important in mediating tolerance to antigens not displayed during thymic Treg generation, including food- and environmental antigens as well as commensal microbes [44]. nTregs and pTregs are therefore predisposed to different antigen niches, meaning that they likely synergize to accomplish optimal immunoregulation [45]. Phenotypically and functionally the two subsets are thought to share many of their characteristics [39], making it somewhat difficult to assess the suppressive contributions of each population *in vivo.* Two markers have however been suggested to be mainly confined to tTregs: the Ikaros transcription factor family member Helios (IKZF2) [46], as well as the cell surface receptor Neuropilin-1 (NRP1) [47].

Despite acquiring FOXP3 expression, TGF-β induced Tregs likely do not possess the full gene expression- and epigenetic profile of tTregs [48], making them more prone to lose their suppressive capacity (or even reverting them to acquire functions of effector Th cells).

1.3.4 Mechanisms of Treg suppression

Tregs express a variety of cell surface- (CD25, CTLA-4, CD39, CD73, TGF-β, GPR-15 ICOS) and secreted molecules (IL-10, TGF-β, and IL-35) which are suggested to mediate peripheral inactivation of effector T cells that managed to escape negative selection as well as other cell types [49]. Selected mechanisms by which they are thought to modulate inhibitory function are shown in fig. 1.3 and will be described in more detail below. Furthermore, Treg markers associated with increased suppressive abilities will also be underlined in this chapter.

IL-2Ra chain (CD25) and IL-2 deprivation

Since FOXP3 represses the *Il2* gene [50] Tregs are highly dependent on exogenous IL-2 for their survival, expansion and enhancement of effector functions [51, 52], which elegantly shows the need for constitutive expression of high affinity IL-2R α chain [19]. The main source of IL-2 providers during an immune response are believed to be activated Tconvs and it has therefore been suggested that colocalized Tregs would have a competitive advantage to acquire IL-2 [53]. By depriving potentially self-reactive Tconvs of IL-2, Tregs both support their own proliferation and suppress Tconvs nearby from further expansion and differentiation into effector cells [54] (fig. 1.3A). IL-2 together with TGF-β is also needed for generation and expansion of Tregs from peripheral naïve CD4+ T cells (pTregs and iTregs) [35] providing another mechanism for Treg expansion.

CTLA-4 (CD152)

Cytotoxic T lymphocyte associated protein 4 (CTLA-4) is a structural homolog of CD28 with opposite, inhibitory function [55]. It is constitutively expressed by Tregs under FOXP3 regulation [56, 57] and upregulated at lower dose in activated Tconvs [58]. By binding to CD80/CD86 ligands on APCs with approx. 10 times higher affinity than CD28 [59], it outcompetes Tconvs of the co-stimulatory signal, thus indirectly impeding their activation [60, 61] fig. 1.3 B). Furthermore, CTLA-4 mediated cell-to-cell contact is thought to both downregulate CD80/CD86 expression on DCs and B cells [62] and deplete the co-stimulators from the APC's cell surface by trans-endocytosis [63]. CTLA-4 deficiencies have been shown to induce lymphoproliferative and autoimmune diseases in mice [64] and humans [65] and thereby suggest the importance of CTLA-4 function in Treg immunoregulation.

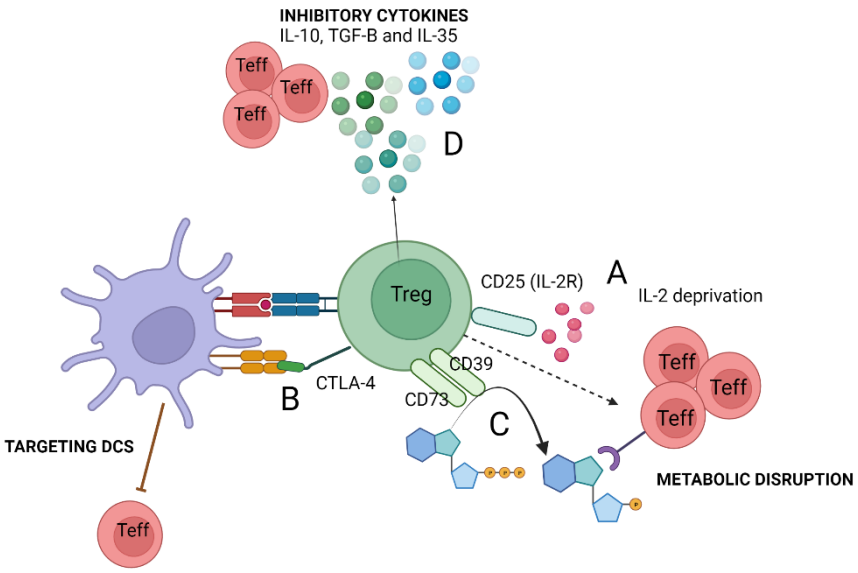

Figure 1.3 Selected mechanisms of Treg suppression. A) Tregs depriving T effector cells (Teffs) from IL-2 using IL-2Rα (CD25) B) CTLA-4 on Tregs binding co-stimulatory CD80/CD86 indirectly inhibiting Teff activation. C) CD73/CD39 expressed on Tregs are ectoenzymes that hydrolyse pro-inflammatory ATP to immunosuppressive adenosine which induce immunosuppressive signalling in Teffs. D) Tregs produce immunosuppressive cytokines IL-10, IL-35 and TGF-*β* inhibiting generation, activation and function of Teffs. Figure created in Biorender.com, inspired from [66]

CD73/CD39

Ecto-5'- Nucleotidase (CD73) and ectonucleoside triphosphate diphosphohydrolase 1 (ENTPD-1 or CD39) are enzymes expressed on the cell membranes of Tregs [67], involved in the conversion of pro-inflammatory ATP into immunosuppressive adenosine (fig.1.3 C). Adenosine binding to A2A receptors of Tconvs is thought to elevate intracellular cAMP levels and activate immunosuppressive signalling loops [67]. In addition, heightened expression of CD73 and co-expression of CD39 on Tregs expanded *in vitro*, has been shown to considerably induce their immunosuppressive function [68]. In line with that, a decrease in CD39 expression on Tregs has been indicated in several autoimmune diseases, especially those involving pathogenic Th17 cells [69, 70].

Cytokines: IL-10, IL-35 and TGF-β

Another proposed mechanism of Treg function is their ability to produce anti-inflammatory cytokines (fig. 1.3 D) including IL-10, IL-35 and TGF-β, mediating pleiotropic suppressive activities on a range of cell types. Both IL-35 and TGF-β are thought to pose direct suppression of generation [71], activation [72] and effector functions of Tconvs [71-73], whereas IL-10 is important in inhibiting functional antigen presentation by APCs, thereby indirectly inhibiting Tconv activation [74]. Importantly, all three cytokines have been implicated in the potentiating the functions of Tregs. TGF-β is associated to the maintenance of FOXP3 expression in both

nTregs and pTregs [75] and (together with IL-2) differentiation of naïve CD4+CD25- T cells into peripherally and *in vitro* induced Tregs [35], a process potentiated by IL-10 [38]. IL-10 is additionally suggested to facilitate its own expression in Tregs [76]. IL-35 is thought to promote Treg expression of CD39 and IL-10 production [77]. Additionally IL-35 has been associated to promote maximal suppressive capacity of Tregs [73].

Other molecules associated with Treg function

Other molecules and markers affecting Treg function have also been considered of interest in this thesis. The display of HLA-DR identifies a distinct population of Tregs, expressing higher levels of FOXP3 than HLADR-CD25+ Tregs, also connotated to a unique contact-dependent suppression mechanism [78]. Inducible T cell costimulator (ICOS) expressing Tregs have been associated with increased IL-10 production correlating with a higher suppressive capacity [79]. Differential expression of fatty acid synthase (FASN) and G protein-coupled receptor 15 (GPR15) have recently been observed in Tregs from patients with autoimmune polyendocrine syndrome 1 (APS-1), indicating Tregs with higher dependence on fatty acid metabolism as well as decreased gut-homing ability [80]. Intriguingly, both these properties relate to functional characteristics of Th17 cells [81, 82]. Lastly, CD31 is a marker of recent thymic emigrants [83] while surface expression of CD45RA marks naïve T cells [84]

1.3.5. IL-6 and the Treg/Th17 axis

A key feature of the immune system is that it rapidly adjusts to homeostatic alterations, especially when facing threats of invading pathogens or tissue injury. In this context, immune suppression promoted by Tregs must be reduced and simultaneously substituted by augmentation of T cell effector functions. This shift is efficiently regulated by cytokines exemplified by the pro-inflammatory IL-6. In combination with IL-1β [85] and IL-21 [86], IL-6 skews the differentiation of naïve CD4+ T cells towards Th17, simultaneously suppressing the generation of induced Tregs [87] by promoting methylation of the *FOXP3* locus [88]. Interestingly, like FOXP3, early induction of the Th17 master regulator RORγt also requires TGF-β [89]. This results in a reciprocal regulation of the developmental pathways for the two CD4+ linages, a balance which is controlled by the surrounding cytokine milieu.

Differentiation towards the Th17 linage is thought to be strongly enforced by phosphorylation and activation of the transcription factor STAT3, downstream of the IL-6R complex. Upon homodimerization STAT3 translocate to the nucleus, upregulating key genes needed for Th17 cell differentiation, activation and proliferation including *RORγt, IL6RA, IL23R and IL17.*

Furthermore, the increase in IL-17, stimulates proximal stromal cells [90] and colocalized APCs [91] to induce IL-6 production and thus the activation state of STAT3. This results in a circular IL-6/STAT3/IL-17 driven positive feedback loop of perpetuating Th17 differentiation [92], further maintained by IL-23 [93].

Th polarization through such an amplification loop is a useful mechanism to quickly mount a potent immune response. However, persistently high levels of proinflammatory cytokines can also lead to development of pathologies including autoimmune and autoinflammatory diseases [94]. Increased levels of IL-6 and IL-17 in particular have been associated to psoriasis and rheumatoid arthritis (RA) [95] and imbalance between Tregs and Th17 cells has also been indicated in the latter [96]. Targeting the Treg/Th17 disequilibrium might therefore be of therapeutic relevance, not only in diseases mediated by IL-17, but potentially conditions where increased levels of Th17 potentiating cytokines, including IL-6, have been indicated.

1.4 Autoimmunity

1.4.1 Loss of tolerance and autoimmune diseases

Negative selection during thymic T cell development is the first step in tolerance education, a process in which adaptive immune cells learn to remain non-responsive to self. Although efficient, it is not flawless and there are therefore secondary peripheral tolerance mechanisms in place. These include deletion of self-reactive T cells by apoptosis, immunosuppression by Tregs, and induction of anergy, by which antigen-primed T cells do not receive sufficient co-stimulation to get activated and promote responses [3]. If both central and peripheral mechanisms fail to eliminate self-reactive lymphocytes, these might get activated and mediate attack on host tissue resulting in pathological autoimmunity. About 80 different autoimmune diseases have so far been defined, affecting 3-5% of the general population [97] exemplified by type 1 diabetes, rheumatoid sclerosis, and psoriasis. Autoimmune diseases are subdivided into organ-specific and systemic, depending on whether the autoantigen is mainly confounded to a specific tissue or found in many. What underlies their development is however difficult to assess as they likely involve an interplay between genetic and environmental factors [98].

1.4.3 Autoimmune Addison's disease

Loss of tolerance towards self-antigens in the adrenal cortex progressively leads to overt adrenal insufficiency, or autoimmune Addison's disease (AAD). AAD is a rare endocrine disorder reported to affect 93-220 per million in the European population [99], being most common in the Nordic countries [100]. Notably, AAD patients often acquire other endocrine autoimmune components, and more than 50% have an autoimmune polyendocrine syndrome [99]. The major self-antigen targeted in AAD is the enzyme 21-hydroxylase (21OH) [101], responsible for the production of the life-essential hormones cortisol and aldosterone (fig.1.4) . The autoimmune mediated attack results in gradual destruction of the adrenals most likely promoted by self-reactive T cells [102] with contributions from antibodies against 21OH, the latter detected in almost all affected individuals [103] . Life-long hormone replacement therapy is currently the only treatment option available, attempting to restore the crucial functions of these hormones in regulating stress response, salt- and water balance and blood pressure. Their insufficiency, especially prone to occur in the context of physically or mentally stressful situations [104, 105] can lead to incidents of acute adrenal crisis. This is a potentially life-threatening condition requiring immediate medical care and associated with a substantial mortality risk, even in medicated individuals [104, 105].

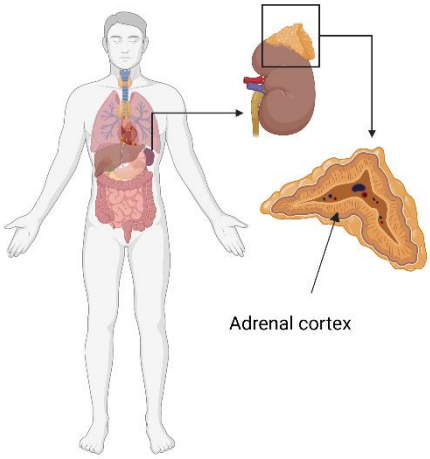

Figure 1.4 Anatomical depiction of the (left) adrenal and its cortex. Adrenal production of cortisol and aldosterone declines during the progression of adrenal insufficiency. Typical symptoms develop over time and include fatigue, dizziness, weight loss and nausea complemented by the mere disease specific; hunger for salt and darkening of the skin. Figure created in Biorender.com

Since AAD is both rare and polygenic, defining the possible genetic variants and their contribution to disease development, has been difficult. Several risk alleles for AAD have been identified through targeted studies investigating single gene variants previously found to be implicated in other autoimmune diseases. The strongest genetic association for AAD is connected to the inherited haplotypes of the highly polymorphic HLA alleles, enabling antigen recognition by T cells. Also, single nucleotide polymorphisms (SNPs) in genes tightly connected to T cell activation, differentiation, and regulation, including: *IKZF4*, *CTLA-4*, *PD-L1*, *PTPN22*, *STAT-4* and *BACH2* have been associated with AAD (reviewed in [106]).

Variants in the same genes have later also been confirmed in the recent GWAS study for AAD [107], where several novel risk loci were discovered, including the autoimmune regulator *AIRE*. Overall, genetic susceptibility to AAD appears to be strongly related to T cell function, overlapping with risk loci also found in the common autoimmune comorbidities of AAD patients.

Lastly, AAD patients experience lower quality of life [108] and have shorter life expectancy than the general public [109]. Therefore, it is important to develop novel therapy options not only manage the symptoms, but aid to target the autoimmune cause, potentially restoring self-tolerance.

1.4.3 Tregs in autoimmune diseases

The majority of healthy organisms harbor self-reactive T cells in their blood stream [110, 111], but only few develop autoimmune disease, pointing to the crucial role of peripheral tolerance to aid in their inhibition or elimination. Tregs exert dominant suppressive mechanisms in the periphery, and it has therefore been suggested that dysregulation of Tregs may be the factor that "tips the scale" in favor of self-targeting T cells leading some individuals to develop pathological autoimmunity. Indeed, early studies characterizing Tregs showed that depletion of CD4+CD25+ T cells in murine models leads to a range of experimentally induced autoimmune diseases [19]. Additionally, rarely occurring mutations in *FOXP3* cause severe and multi-organ autoimmune manifestations in both humans (Immunodysregulation polyendocrinopathy X-linked, IPEX syndrome) [112, 113] and IPEX model *scurfy* mice [112-114]. Intriguingly, symptoms in the latter can be prevented by subsequent transfer of CD4+CD25+ into FOXP3-deficient neonates [22].

In the more common (and polygenic) autoimmune disease, clinical and experimental evidence also suggest deficiencies in Tregs including their reduced number [115-117] and impaired suppressive function [115, 118-121]. Altered cytokine profiles found in autoimmune patients, recognized by deficiencies in Treg-promoting IL-2 and TGF-β [118] and increase in pro-inflammatory cytokines [122, 123] potentially further promotes/exaggerates this imbalance [124]. Lastly, proinflammatory cytokines have also been indicated to lead to Treg destabilization [125-127] exemplified by Tregs from patients with severe psoriasis that co-express *RORγt* and *IL17A* [128] followed by enhanced loss of *FOXP3* expression [127].

1.4.4 Treg enhancing therapies

The rationale behind the ongoing research of Treg-based therapies has been to increase Treg in numbers or enhance their suppressive capacities towards pathogenic, autoreactive effector cells (Teffs). Adoptive cell therapy (ACT) is a potential strategy for expanding the Treg compartment, by which Tregs from a patient are isolated, purified and stimulated to proliferate *in vitro,* and subsequently transferred back to the patient [129] ACT has yielded promising results in preclinical autoimmune models [130] as well as early clinical trials of type 1 diabetes (T1D) [131, 132]. However, this therapeutical strategy assumes that the function of patient Tregs is not impaired and requires further considerations including possible contamination of Tregs by potentially self-reactive Tconvs. Additionally, repeated *in vitro* stimulation can lead to Treg instability and loss of/reduced suppressive phenotype upon expansions and transfer [133-136].

1.4.5 LMT-28 (IL-6R inhibitor)

LMT-28 is a small molecule compound that binds to the extracellular part of gp130, the signal transducing subunit of the IL-6R complex [137]. Upon interaction, LMT-28 inhibits gp130 dimerization and assosiation to the IL-6Rα subunit thereby inhibiting signalling induced by IL-6, including the activation of STAT3 [137]. Given the importance of STAT3 for Th17 cell differentiation, LMT-28 might skew the Treg/Th17 axis and instead promote the expansion of Tregs. Efficacy of orally administered LMT-28 has been tested in mice models with collagen induced arthritis, showing substantial allevaition of disease severity [137]. Currently, the only approved anti-IL-6 agents are humanized monoclonal antibodies targeting IL-6R (Tocilizumab and Sarilumab) and IL-6 itself (Siltuximab) [138], mainly used to reduce autoimmune-mediated joint damage in RA patients.

1.4.6 Secukinumab (IL-17A inhibitor)

Secukinumab is a recombinant, fully human monoclonal antibody targeting the Th17 signature cytokine IL-17A. It is primarily used to treat patients with psoriasis, a chronic autoimmune skin disease recognized by lesional skin hyperplasia promoted by chronic inflammation [139]. The pathogenesis of psoriasis is associated with elevated levels of IL-6 [140] and IL-17A [127], cytokines involved in the Treg/Th17 axis favoring the latter. IL-17A has been indicated to downregulate *TGF-β* leading to a following decrease in the expression of *FOXP3* by Tregs [127, 141] as well as induced secretion of pro-inflammatory cytokines, including IFN-γ [127].

Flow cytometry analysis of Tregs isolated from psoriasis patients following 4-week Secukinumab treatment showed markedly restored levels of TGF-β and FOXP3 expression compared to the levels pre-treatment, being similar or higher than in untreated healthy controls [127]. In addition, Secukinumab has also shown to recover Treg suppressive capacity towards Teffs, correlating with improved clinical score in all patients [127].

2. Aims

We hypothesize that LMT-28 and Secukinumab may potentiate the number and function of Tregs, by skewing the Treg/Th17 axis towards Tregs. To examine the effects of the drugs on *in vitro* PBMC and Treg cell cultures from AAD patients and healthy controls, we performed drug screenings assays.

Specific aims:

1) Optimize and investigate the utility of xCELLigence RTCA platform for real time monitoring of immune cells (T cells & Tregs)

2) Employ xCELLigence to study the response of T cells and Tregs to LMT-28 and Secukinumab and compare with viability and proliferation estimates provided by flow cytometry

3) Assess the effect of LMT-28 and Secukinumab in-vitro treatments on the phenotype and function of Tregs and T cells from AAD patients compared to healthy controls using established endpoint assays: flow cytometry, qPCR, and ELISA

3. Materials

3.1 Reagents, antibodies, and primers

Reagent name	Producer	Cat. Number
2x PowerTrack SYBR Green Master Mix	Thermo Fischer	A46109
10X TBE	Invitrogen	15581-044
DEPC Treated Water	Ambio (Invitrogen)	AM9906
Dimethyl Sulfoxide (DMSO)	Sigma Aldrich	D2650
Dulbecco's phosphate buffered saline (PBS)	Sigma Aldrich	D8537
Fetal Bovine Serum	Gibco	16000-44
Ficoll-Paque PLUS	Cytiva	GE17-1440-02
Flow antibodies Target, fluorochrome and Ab clone **For PBMC and Treg panel:** Anti-CD3, V500, clone UCHT1 Anti-CD4, PerCP-Cy5, clone: RPA-T4 Anti-FOXP3, PE-CF594 clone: 236A/E7 **Solely for PBMC panel:** Anti-CD8, PE-Cy5, clone: RPA-T8 Anti-CD14, PE, clone: M5E2 Anti-CD20, APC-Cy7 clone: 2H7 **Solely for Tregs panel:** Anti-CD25, PE-Cy7, clone: 2A3 Anti-CD45RA, APC-H7, clone: HI100 Anti-CD152 (CTLA-4), BV421, clone: BNI3 Anti-CD39 (ENTPD-1), PE, clone: eBioA1 Anti-CD31 (PECAM-1), BV785, clone: L133.1 Anti-HLA-DR, BV650, clone: G46-6 Anti-CD127, PE-Cy5, clone: A019D5 Anti-IKZF2 (Helios), APC, clone: 22F6	 BD Biosciences Biolegend BD Biosciences BD Biosciences Biolegend Biolegend BD Biosciences BD Biosciences Biolegend Invitrogen BD Biosciences BD Biosciences Biolegend Biolegend	 561416 300570 563955 555368 301806 302314 335824 560674 369606 12-0399-42 744757 564231 351324 137222
Gelred Nucleic acid stain	Merck	SCT123
Generuler 50bp DNA Ladder, ready-to-use	Thermo Fischer	SM0373
Human IL-2 IS research grade, 50 µg	Miltenyi Biotec	130-097-743
Human serum	Sigma Aldrich	H4522
LMT-28 (C17H29NO4)	Sigma Aldrich	SML1628
PBS Tablets	Merck	524650-1EA
Primers for PBMC panel (primer sequences in appendix) **Gene target** Bcl6 Eomes T-bet GATA-3 RORyt1 FOXP3 B-actin	 Merck Merck Merck Merck Eurogentec Eurogentec Merck	
Rinsing buffer: AutoMACS rinsing solution 99,5% MACS BSA Stock Solution	 Miltenyi Biotec Miltenyi Biotec	 130-091-222 130-091-376

Mouse IgG (H+L)	Fisher	A11003
Secukinumab (MW: 147944,37 g/mol) Stock conc. 5 mg/mL	Seleckchem	A202501
SeaKem LE Agarose	Lonzo	50004
Superscript IV Vilo Master mix with EZ DNase	Invitrogen (Thermo Fischer Scientific)	11766050
TaqMan Gene expression assays **Treg panel** **Gene, assay number, reporter dye:** ACTB, HS01060665_g1, FAM B2M, HS00187842_m1, VIC CTLA-4, HS00175480_m1, FAM ENPD-1, HS00969556_m1, VIC FASN, HS01005622_m1, FAM FOXP3, HS01085834_m1, FAM GAPDH, HS9999905_m1, VIC GPR15, HS00922903_s1, FAM ICOS, HS00359999_m1, FAM IKZF2, HS00915979_m1, VIC	Thermo Fisher Scientific	 4331182 4331182 4331182 4448489 4331182 4331182 4448489 4331182 4331182 4448489
TaqMan Universal PCR Master Mix	Applied Biosystems (Thermo Fischer Scientific)	2108179
TexMACS medium	Miltenyi Biotec	130-097-196
Tryptan blue stain 0,4%	Invitrogen (Thermo Fischer Scientific)	T10282
UltraComp eBeads Compensation beads	Invitrogen	01-2222-42
Ultra-LEAF purified mouse anti-human CD28 Clone: CD28.2 conc. 1 mg/mL	BioLegend	302934
Ultra-LEAF purified mouse anti-human CD3 Clone: UCHT1 conc. 1 mg/mL	BioLegend	300438

2.2 Consumables, equipment and kits

Product name	**Producer**	**Cat. Number**
CellTrace CFSE Cell proliferation Kit	Invitrogen (Thermo Fischer Scientific)	C34554
C-Chip disposable hemocytometer Burker B	NanoEntek	DHC-B01
Coolcell freezing container	Corning	432001
Cryotubes 1,2 mL	VWR	479-1254
Dead cell removal Kit	Miyltenyi Biotec	130-090-101
Disposable Glass Pasteur pipettes 150mm	VWR	612-1701
E-plate 16	Agilent	5469830001
eBioscience FOXP transcription factor Fixation/Permabilization Kit	Invitrogen	00-5521-00
Eppendorf tubes DNA LoBind Tube 1,5 mL	Eppendorf	022431021
Falcon serological pipettes - 10 mL - 25 mL	Corning	 357551 P8250

Falcon tube - 15 mL - 50 mL	VWR	 525-1085 525-1109
Human IL-10 Quantikine HS ELISA Kit	R&D Systems	HS100C
Human Interleukin 35 ELISA Kit	Mybiosource	MBS2511987
Human TGF-B1 Picokine ELISA Kit	Mybiosource	MBS175889
LIVE/DEAD Fixable Yellow Dead Cell Stain Kit	Invitrogen	L34959
LS column	MyltenyiMiltenyi Biotec	130-042-401
MACS Multistand	MyltenyiMiltenyi Biotec	130-042-303
MACSxpress Whole Blood Treg Isolation Kit (human)	MyltenyiMiltenyi Biotec	130-109-557
MiniMACS separator	MyltenyiMiltenyi Biotec	130-042-102
MicroAmp Optical 384-Well reaction plate	Applied Biosystems (by Thermo Fischer Scientific)	4309849
Microtube 2 mL	Sarstedt	72.694.006
MS column	MyltenyiMiltenyi Biotec	130-042-201
OctoMACS separator	MyltenyiMiltenyi Biotec	130-042-109
Pipetboy acu 2 controller	Integra Biosciences	
Polysterene Round-Bottom Tube with Cell-Strainer Cap 5mL	Corning	352235
Pre-separation filters	Miltenyi Biotec	130-041-407
QIAshredder (250)	Qiagen	79656
QuadroMACS separator	MyltenyiMiltenyi Biotec	130-098-308
Scepter Sensors 40 uM	Millipore	PHCC40050
Treg expansion Kit human	MyltenyiMiltenyi Biotec	130-095-345
Vacuette K3EDTA tubes 9 mL	Greiner bio-one	455036
Vacuette Lithium Heparin tubes 9 mL	Greiner bio-one	455084

2.3 Instruments

Instrument name	**Producer**
BD LSR Fortessa	BD Biosciences
Centrifuge 5810	Eppendorf AG
CO2 incubator	Sanyo
GelDoc EZ Imager	Biorad
GeneAmp PCR System 9700	Thermo Fisher
Incubator 1000	Heidolph
Multifuge 3SR+ Centrifuge	Thermo Scientific
Nanodrop ND-1000 Spectrophotometer	BD
Olympus CKX53 microscope	Olympus
Scepter handheld automated cell counter	Merck (Millipore)
Shaker Unimax 1010	Heidolph
Testtube rotator	Labinco
Vacusafe inspiration system	Integra Biosciences
Vortex 1 S000	Ika
xCELLigence RTCA DP analyzer	Agilent
Quant Studio 5 Real-Time PCR Intrument (384- Well Block)	Thermo Fischer Scientific

2.4 Software

Software name	Developer
BD FACS Diva	BD Biosciences
Microsoft Excel v.2204	Microsoft
Flow Jo 10.8	FlowJo LLC
GelDoc EX Image Lab	Bio Rad
Graphpad Prism 9.0	GraphPad
QuantStudio Design & Analysis Software 1.5.2	Thermo Fisher
RTCA Software Pro	Agilent
Softmax Pro Software	Molecular Devices
Thermo Fisher connect	Thero Fisher Scientific

3. Methods

3.1 Experimental pipeline

In this project we utilized *in vitro* cultures of cells isolated from whole blood of five Addison's patients and five age/sex matched controls to assess the effect the two selected drugs, LMT-28 and Secukinumab on T cell subsets. For each drug, treated and non-treated cells were compared within and across the patient and control groups yielding four different conditions:

1) patient, treated
2) patient, non-treated
3) control, treated
4) control, non-treated

For both patients and controls, two types of cells were assayed following five-day culture with or without drug present in the medium. One consisted of isolated Tregs, providing valuable indication of the drugs direct effect on viability, proliferation and possible changes in phenotype and function of these cells. In addition, we assayed peripheral blood mononuclear cells (PBMCs) composing various lymphocytes and monocytes. These cells were included as a measure on how the drugs affected immune subpopulations, especially focusing on the balance between the Th17 and Treg cells. To reflect the range of possible changes in cell phenotype and function we utilized several well-established endpoint assays on cells post-culture, namely: flow cytometry, quantitative polymerase chain reaction (qPCR), and enzyme linked immunosorbent assay (ELISA). Additionally, for continuous monitoring of dynamic changes in cell behavior during the four days of culture, we utilized biosensor technology called xCELLigence Real Time Cell Analyzer (RTCA). The experimental pipeline including all the above-mentioned techniques is summarized in Fig. 3.1.

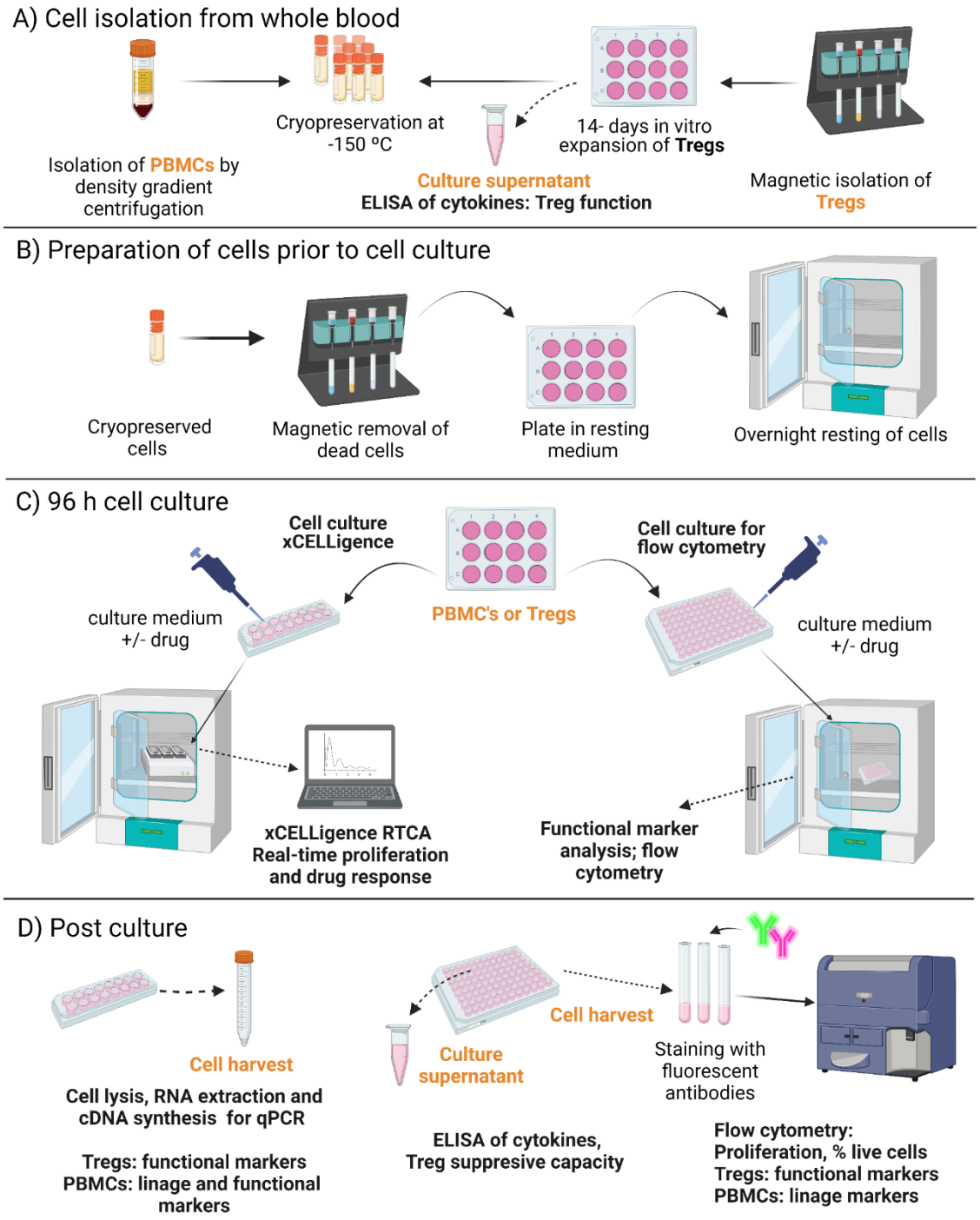

Figure 3.1 Experimental pipeline including key methods (highlighted in black) and biological materials used for each method (highlighted in orange). **A)** Isolation of cells (PBMCs and Tregs), Treg expansion and storage conditions **B)** Dead cell removal and resting of cells, day prior to cell culture. **C)** Cell culture; cells plated and treated on two parallel plates: one for continuous monitoring of cell behavior during culture using xCELLigence RTCA, the other with cells intended for flow cytometry. **D)** Endpoint assays examining the survival, phenotype, and functionality of Tregs after culture, with and without drug treatment. Figure created in Biorender.com

3.2 Overview and theory behind the methods

3.2.1 xCELLigence RTCA

Studies focusing on cell viability, proliferation, and possible signs and timing of drug toxicity are important in the early processes of drug validation. For this purpose, we have utilized a label-free xCELLigence RTCA biosensor technology [142] that measures the electron flow in cell suspension during culture. The biosensor employs specifically designed culture E-plates with gold microelectrodes situated on well-surfaces. Cells adhering to the bottom of the plates disrupt the interactions between the medium and electrodes, causing impedance of the electron flow [142] as shown in figure 3.2. Impedance values are recorded in real-time by an instrument located inside a CO2 incubator and transformed by the analyzer's software to an unitless value called Cell Index (CI). CI is defined as (Rn – Rb)/15 where Rn is the cell-electrode impedance of a well containing cells, and Rb is the background impedance of wells with medium alone. CI values are then presented as functions of time yielding a graph (as seen in figure 3.3), indicative of changes in cell behavior associated with cell- morphology, attachment, and number.

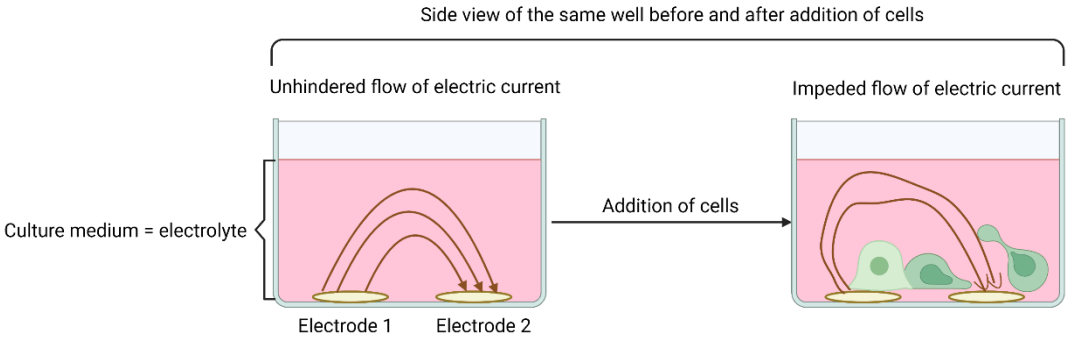

Figure 3.2 The principals behind measurements of relative electrical impedance. Side view of a single well on an xCELLigence E-Plate. Shown to left is the unhindered electron flow in a cell-free suspension (Rb), compared to an impeded electron flow due to adherence of cultured cells to the electrodes on the well-bottoms (Rn), as shown to the right. The difference between these two conditions is the basis for determination of relative impedance measurements which are transformed to Cell Index (CI). Figure created in Biorender.com, inspired by [143]

Due to the variability of the experiments for which the xCELLigence RTCA can be utilized, there is no universal culturing protocol or measurement scheme. Optimization of culturing conditions suited to the cell type and type of assay was therefore performed prior to the experiments and will be further described in 3.7.1.

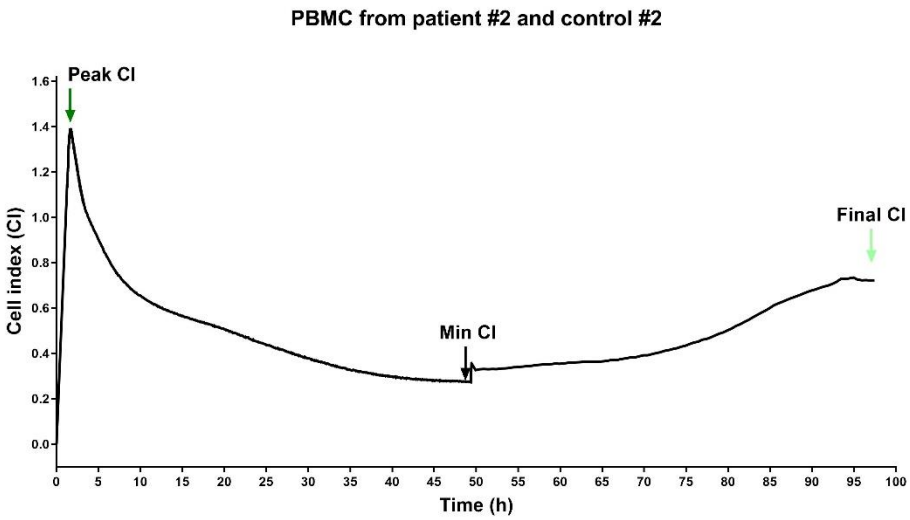

Figure 3.3 Characteristic CI-graph of activated T cells, here seen in PBMC culture. Increase in cell attachment and morphological changes upon activation result in a large CI increase during the first two hours of culture (denoted by the dark green arrow). A significant decrease in CI values is seen during the next 48 h, after which new medium is added (denoted by black arrow). A gradual increase in CI values is observed following cell feeding in a 96-h culture.

3.2.2 Flow cytometry

Flow cytometry was used to assess the effect of drugs on the relative number, phenotype, and functional characteristics of Tregs, as well as the population sizes of the different cell types present in PBMCs. Prior to flow analysis, cell samples were stained with specific fluorochrome-conjugated monoclonal antibodies targeting extra- and intracellular protein markers of interest expressed by these cells. In the cytometer (fig.3.4), the cell suspension is pressurized by a fluidics system to yield a stream of single cells. Followingly, these cells (termed events) pass a series of lasers with wavelengths falling within excitation energies of the fluorochromes, that upon absorption, will emit light at a slightly longer, but defined wavelength. Any light emitted from a passing cell will then be isolated by a series of bandpass filters and designated by photodetectors into channels, one for each fluorochrome present. Additionally, cells will diffract and reflect/refract some of the light by the means of forward scatter (FSC) and side scatter (SSC), yielding information about the cell's size and complexity, respectively. A pivotal data correction step during flow analysis includes compensation, where one attempts to account for possible fluorescence overlap of the light emitted by different fluorochromes that are mistakenly designated into the same channel. Data is then analyzed using a software by applying a gating strategy, where one discriminates between cells positive

and negative for each of the markers, yielding valuable information about phenotypic diversity of the cells present.

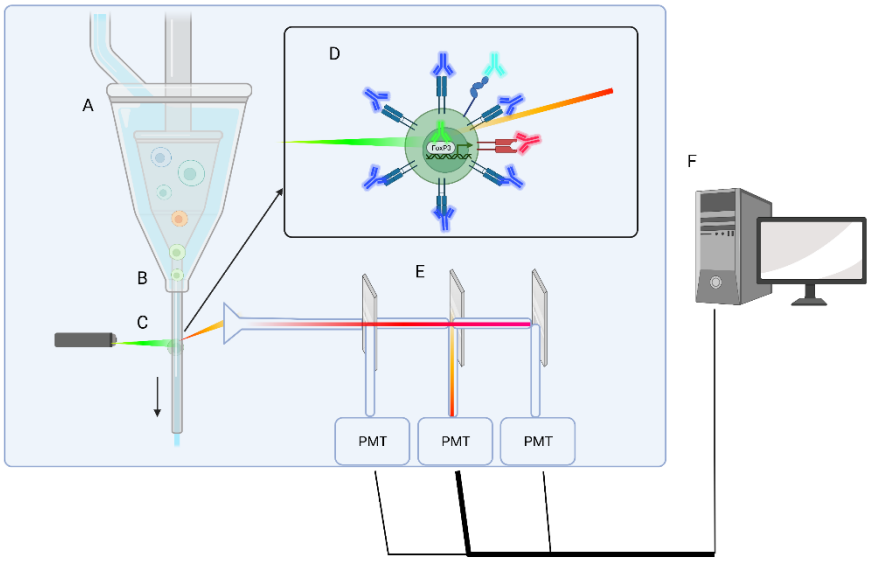

Figure 3.4 Principles behind flow cytometry. A) Cells are injected into the cytometer and focused into stream of B) single cells by a fluidics system. C) Cells pass a series of lasers exciting fluorophores bound to antibodies targeting selected phenotypical/functional markers, D) here exemplified by FOXP3, intracellular marker of Tregs. Following excitation, the fluorophore emits light with a longer wavelength E) The light then passes a series of mirrors and bandpass filters that deflect a narrow range of wavelengths towards matching detectors. Photomultiplier tubes (PMTs) convert light energy from photons into voltage pulses, F) providing readout to the software. Figure created using Biorender.com, modified from [144]

3.2.3 Quantitative polymerase chain reaction

Quantitative PCR (qPCR) is one of the most reliable methods to measure changes in gene expression. It was here used to quantify the amount of mRNA transcripts of selected marker genes, to be compared in drug treated and non-treated cells derived from patients and matched controls. In a RT-qPCR analysis, the RNA from cells is isolated and followingly used for synthesis of a complementary DNA (cDNA) strand by reverse transcription. cDNA is used as a basis for the qPCR reaction, which can be performed using either dye-based or probe-based assay, both of which have been utilized in this project (fig.3.5). SYBR green is a dye that fluoresces upon binding of dsDNA and will thus yield an increase in fluorescent signal that is proportional to the DNA product amplified per PCR cycle. TaqMan assay utilizes a hybridization probe, consisting of an oligonucleotide complementary to a short region specific for the target sequence, which will anneal to the single strands of the denatured target DNA during PCR cycling. Importantly, the probe is flanked by two proximal fluorescent dyes; a reporter attached to its 3’ end and a quencher at its 5’ end. A fluorescence signal is emitted only when the reporter is separated from the quencher, which takes place when the probe is

digested by Taq polymerase with 5'-3' exonuclease activity during the elongation step. The emitted signal is amplified proportionally to the amount of probe digested, equal to the amount of the separated DNA strands of the target gene that ideally doubles for every PCR cycle. Changes in gene expression are expressed relatively as fold changes with regards to housekeeping gene(s), calculated using the $2^{-\Delta\Delta Ct}$ method [145]

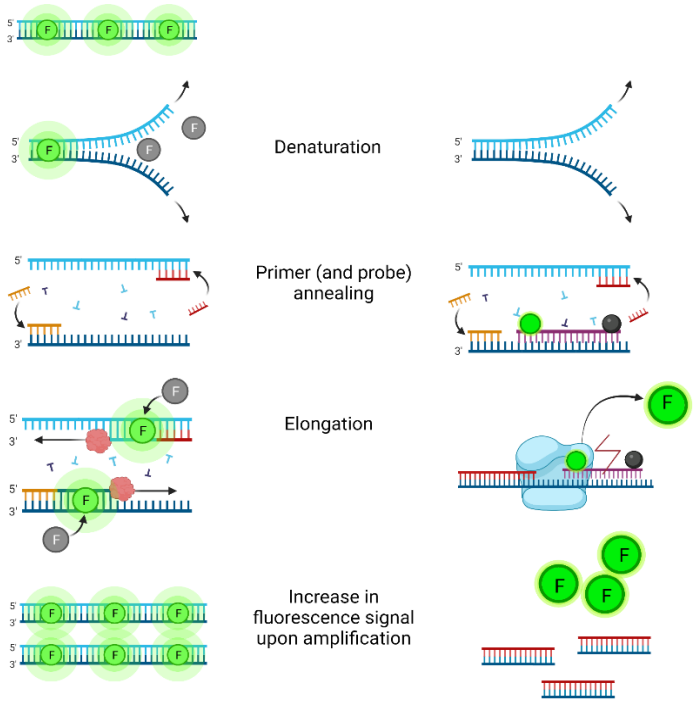

Figure 3.5 Principles behind qPCR. SYBR green based assay is shown to the left, while TaqMan based assay to the right. SYBR green dye fluoresces upon binding to double stranded DNA. TaqMan based assay utilizes sequence specific probes that release fluorescent signal upon digestion by TaqMan polymerase during the elongation step. For both assays signal increases exponentially, in line with amplification of the product. Figure created in Biorender.com, inspired by [146]

3.2.4 Enzyme-linked immunosorbent assay

Sandwich ELISA assays were used to measure secretion of Treg signature cytokines: TGF-β and IL-10. This was done to assess Treg function after expansion, as well as to measure Treg's suppressive capacity after cell culture with or without drug in medium. All three commercially available ELISA kits employ plates precoated with the immobilized capturing antibodies. The antibodies will specifically bind their respective antigen once the samples and known standards are added onto the plate. Bound cytokines are again complexed with a secondary, detection antibody conjugated to a molecule which permits an enzyme driven, color producing reaction to take place. For TGF-β the detection antibody is biotinylated, permitting binding of the

enzyme Avidin-Horseradish-Peroxidase (HRP) which produces blue color once its chromogenic substrate; 3,3', 5'5 tetramethylbenzidine (TMB) is added. For IL-10, the detection antibody is conjugated to alkaline phosphatase, which reacts with NADPH in the substrate solution producing color upon addition of the amplifier solution containing iodonitrotetrazolium (INT) violet. The colorimetric reactions are terminated by addition of strongly acidic stop solutions. The amounts of colored substrate produced are read using a spectrophotometer reflecting the concentrations of cytokines present in the samples.

3.3 Ethical aspects

This project was approved by the Regional Ethical Committee of Western Norway (approval number 2018/1417 and 2009/2555). All patients were recruited from the Registry and biobank for organ specific autoimmune disorders (ROAS), Haukeland University Hospital, Norway (approval number 2009/2555), and gave written informed consent for participation. Control samples were obtained from the Haukeland University Hospital blood bank and these individuals were anonymized when processed and analyzed.

3.4 Patients and controls

Whole blood from AAD patients 1-5 (3 females, 2 males, age range 55-76, mean age 63,4) as well as age and sex-matched healthy controls 1-5 (3 females, 2 males, age range 59-73, mean age: 64,6) was used for isolation of both PBMC's and Tregs (sampling of blood for both cell types was done on the same occasion). These cells were used for culturing experiments, xCELLigence RTCA and all subsequent end point assays following cell culture (fig.3.1). Additionally, PBMCs isolated from healthy controls 6-23 and Tregs from 4 healthy controls were used for optimization of culturing conditions and flow cytometry analyses.

All the 5 included patients (appendix I) had the diagnosis of AAD. Four out of five had antibodies against 21OH in their sera, a sensitive marker for AAD. Three of these also had other antibodies against endocrine targets like anti-side chain cleavage enzyme and anti-17-hydroxylase. All the four with autoantibodies against 21OH also had hypothyroidism in addition to AAD.

3.5 PBMC isolation

Approx. 18 mL fresh whole blood per donor was retrieved from patients and healthy controls in heparin tubes. The blood was transferred to a 50 mL Falcon tube and diluted 1:1 with PBS. The diluted blood was then layered on top of 12 mL of density gradient medium Ficoll-Paque and centrifuged at room temperature (RT), at 300xg for 30 min with break acceleration 1. The

PBMC layer was pipetted out into a new 50 mL Falcon tube, topped with PBS and washed at 400xg, RT for 10 min. The supernatant was removed, and the pellet resuspended in 10 mL PBS and the cells were counted using Scepter handheld automated cell counter. Another wash step followed at 400xg in RT for 5 min.

After centrifugation, the supernatant was removed, and the cell pellet was resuspended in human AB serum. Two hundred and fifty microliter of cell suspension was transferred to cryovials containing 250 uL 20% (v/v) DMSO in AB serum. The vials were left at RT for 10 min in a CoolCell cryogenic container in which they were transferred to -80 ºC freezer for one day, followed by long time storage at -150 ºC

3.6 Magnetic Treg isolation and expansion

Isolation was performed according to the protocol provided with the MACSxpress Treg Isolation Kit (Miltenyi Biotec), referred to for details. In short, 5 mL of MACSxpress buffer and 500 µL of Treg Isolation cocktail were added to 9 mL EDTA-blood in a 50 mL Falcon tube. The contents were gently mixed for 10 min using test tube rotator, then incubated in MACSxpress Separator for 15 min. Supernatant containing the $CD4^+CD127^{dim}$ cell fraction was collected and centrifuged at 300xg for 10 min. Cell pellet was resuspended in 2 mL of Separation buffer (5% v/v MACS BSA Stock Solution in AutoMACS Rinsing Solution).

An LS column was washed with 2 mL Separation buffer, before application of the cells and subsequent two washes to flush unlabelled cells ($CD4^+CD25^-$). $CD4^+CD25^+$ $CD127^{dim}$ Tregs were eluted with 2 mL Separation Buffer by pushing down the plunger supplied with the column.

Since the number of Tregs that can be obtained from donor whole blood is not sufficient for culturing experiments to follow, the isolated cells were expanded *in vitro* using Treg Expansion Kit human (Miltenyi Biotec). The starting number of isolated Tregs was estimated using a hemocytometer and the newly isolated cells were centrifuged at 300xg for 10 min at RT. The pellet was resuspended in culture medium (5% v/v AB serum in TexMACS medium supplemented with 500 U/mL IL-2) to a concentration of 10^6 Tregs/mL and the cells were seeded onto a 96-well round bottom plate with 10^5 cells/well. CD3/CD28 MACSiBeads were prepared to $2*10^7$ beads/mL as stated in the amended protocol and 20 µL of bead solution was added to each of 10^5 cells.

The day after seeding (day 1), an additional 100 µL fresh culture medium was added. Throughout the 14 days of expansion, the cell growth was closely observed, and the culture

medium was changed every second day. When the culture reached high confluence, the cells were split accordingly:

- Day 3-4: 48-well plate (1 mL of culture medium/well).
- Day 5-8: 24-well plate (1,5 mL of culture medium/well)
- Day 10-11: 12-well plate (2 mL culture medium/ well)
- Day 12-13: 6-well plate (4 mL culture medium/well)

Tregs were harvested on day 14. The cells were counted and then centrifuged at 300xg for 10 min at RT. The cell pellet was subsequently resuspended and frozen in 10% v/v DMSO in human AB serum, and the cells were cryopreserved in the same manner as PBMCs. Supernatant from day 14 was frozen down in cryovials at -80 ºC for later verification of Treg function using ELISA.

3.7 Cell culture

On the day prior to drug based cell culture, cryopreserved PBMCs or Tregs from patient and matching control were thawn in hand and transferred to 10 mL pre-heated medium before centrifugation at 300xg, RT for 10 min. Dead and dying cells, as well as cell debris were magnetically removed using Dead cell removal kit (Miltenyi Biotec) according to the protocol provided using an MS column and a miniMACS (or octoMACS) magnet. After the final wash the cells were counted and resuspended at a concentration of $2*10^6$ cells/mL in resting medium (5% v/v AB serum in TexMACS medium supplemented with 20 U/mL IL-2). Followingly, the cells were plated and put to rest overnight in the incubator: at 37 ºC and humidified 5% CO2/95% air atmosphere. All following incubation steps during cell culture were done in these incubator conditions.

3.7.1 Optimization of cell culture conditions for xCELLigence proliferation assay

To determine optimal culturing conditions, several optimization steps on PBMCs from healthy controls were performed prior to starting the drug screening assays (described in 3.7.2). Unless stated, the optimizations were performed according to the final protocol described in 3.7.3. The following conditions were optimized:

- Pre-coating agent: T cells grown in suspension are non-adherent to plastic, the E- plates must therefore be pre-coated with an agent that assists with immobilization of cells to the well bottoms (ref). We tried two different agents: goat anti-mouse IgG [147] and

mouse anti-human CD3 [148] The only exception for the trial with anti-CD3 was that there was no need for additional mouse anti-human CD3 in the activation medium.

- Number of cells per well (density of cells): Cell titration was performed, and the cells were added in parallels onto an IgG- coated E-plate in numbers spanning from 200.000 to 12.500 cells/well.
- IL-2 concentration: We initially tested culture medium supplemented with IL-2 concentrations spanning from 2500 U/mL to 160 U/mL and one with no IL-2 present (all with 1µL/mL of mouse anti-human CD3 and mouse anti-human CD28).

For all steps where the number of cells was not a parameter, 200.000 cell were plated per well. Additionally, the optimization assays were carried out for only 48 hours, thus without addition of fresh medium (except when optimizing IL-2 concentration, during which 100 µL fresh medium with 50 U/mL IL-2 was added after 24 h), as added on day 3 during the assays on patient and control cells.

3.7.2 Determination of optimal treatment concentrations of LMT-28 and Secukinumab

To find the concentrations of each drug which showed least cytotoxic effects while simultaneously providing the best proliferative capacity of the cultured cells, test runs of drug screening assays were performed on PBMCs and Tregs isolated from blood of healthy donors. The assays using drugs, both during screening and assays on patient/control cells had two plates cultured in parallel: an E-plate designated for xCELLigence RTCA as well as an additional 96-well plate with cells meant for flow cytometry analysis. Common drug dilutions, media as well as cells from the same individual were utilized on both plates, followed by 48-h culture.

For xCELLigence RTCA, the protocol was alike the one described 3.7.3, excluding the overnight resting of the cells described in 3.7. Five mg of oil suspended LMT-28 was reconstituted in 4,014 mL DMSO and aliquoted in concentrations of 20 mM. Five mg Secukinumab was received, suspended in 1 mL PBS and was aliquoted in the original stock conc. of 33,8 µM. Both were stored in aliquots at -20 ºC to be used for experiments to follow. Screenings were performed by making a dilution series of Secukinumab in growth medium, in 5 final concentrations collectively spanning between 1 µM and 1 nm [127] in a series of experiments.

Similarly, LMT-28 was tested in six concentrations 100 µM-1 nM, in a series of experiments, based on similar work performed by Hong S. et. al on TF-1 cells [137]. To equalize the potential cytotoxic effect of 0,5% (v/v) DMSO in 100 µM LMT-28 dilution, equal amount of DMSO was added to the rest of the wells, employing an additional parallel of non-treated controls where no DMSO was added. This step was omitted after screening assays as the amount of DMSO in the LMT-28 dilution chosen for further assays was negligible.

3.7.3 Cell culture for xCELLigence proliferation assay; the final protocol

Preparation of E-plates and resting of cells

On the day of cell culture, xCELLigence E-plates were prepared by pre-coating all but two wells with 50 µL of 5 µg/mL goat anti-mouse IgG antibody in PBS, and pure PBS in cells where no pre-coating was to be added (to serve as no pre-coat controls). The plate was then put in the incubator for 3 h. Rested cell were taken out, saving $2*10^5$ (for PBMCs) and 10^5 (for Tregs) to for latter RNA isolation and gene expression analysis of non-activated cells, procedures described closer in 3.9.

Starvation of cells for xCELLigence RTCA

The remaining rested cells were centrifuged at 300xg RT for 10 min. Cell pellet was resuspended to a concentration of $1,5*10^6$ cells/mL (for PBMCs) and $1*10^6$ (for Tregs) in starving medium (2% v/v feat bovine serum (FBS) in TexMACS medium). Half the volume of cell suspension was transferred to another tube, to be cultured in a parallel plate designated for flow cytometry analysis, closer described in 3.7.4. Cells for xCELLigence RTCA were starved for 2 h in the incubator to synchronize their cell cycle prior to proliferation assay. After starving and centrifugation at 300xg RT for 10 min, the cell pellet was resuspended in culture medium to yield a seeding concentration of $1,5*10^6$ cells/mL (for PBMCs) and $1*10^6$ (for Tregs).

Activation

The wells were filled with 50 µL activating medium (5% AB serum in TexMACS medium supplemented with 1 mg/mL mouse anti-human CD3, 1 mg/mL mouse anti-human CD28 and 500 U/mL IL-2 for PBMC, 50 U/mL IL-2 for Tregs). The plate was then inserted into the xCELLigence instrument for a medium-background measurement. 50 µL of the cell suspension was seeded into six wells for both patient and control, subsequently being left to settle at RT for 30 min. Next, 50 µL of activating medium containing 1 µM for LMT-28 (medium A in fig.

3.6), 0,3 µM Secukinumab (medium B in fig. 3.6) and pure activating medium (C in fig. 3.6) for non-treated cells was added to patient and control cells, in parallel for each condition. The plates were reinserted into the instrument scheduled to measure Cell Index values in given intervals: every 10 s for first 2 hours, every 5 min for next 46 h and every 30 min the last 48 h.

On day 3, 100 µL additional growth medium (5% v/v AB serum in TexMACS medium) containing drug for treated cell and 100 µL pure growth medium for non-treated cells was added to respective wells, both media also supplemented with 50 U/mL IL-2. On day 5, 150 µL of the supernatant from each well was collected, and the cells harvested by careful scraping of the well bottoms in 100 µL PBS. Further handling of cells for RNA isolation will be described in 3.9.1.

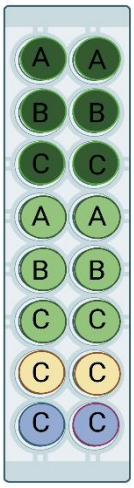

Fig. 3.6 E-plate layout All but blue wells we pre-coated with goat anti- mouse IgG Ab. Dark green: patient cells. Light green: healthy control cells. Yellow and blue: no cells. Medium contents denoted by letters are described in main text. Figure created in Biorender.com

3.7.4 Cell culture and preparation for flow cytometry

Prior to cell seeding, the cells were stained with the proliferation marker carboxyfluorescein succinimidyl ester (CFSE) using Invitrogen's CFSE Cell Proliferation Kit. CFSE is a membrane permeable dye that binds intracellular amines, the amount of which is approx. halved for every cell division [149]. This allows for quantification of the number of cell divisions undergone by cells in a population.

Half the volume of cells in starving medium (as mentioned in 3.7.3) was centrifuged at 300xg, RT for 10 min and resuspended in 1 mL warm PBS. CFSE working solution was prepared and added to the cell solution to final concentration of 5 µM. The cells were incubated for 10 min in the dark at 37 ºC. To quench the staining, 2 mL ice-cold FBS was added to the cell-CFSE solution, then put on ice for 5 min. The tube was topped with 5 volumes of growth medium and washed at 300xg, RT for 10 min.

Cells were resuspended in growth medium, followed by treatment with drug in the same manner as during culture for xCELLigence, this time in triplicate wells for each condition. The cells were put in the incubator for 5 days, split to double number of wells on day 3 by transferring 50 µL of cell suspension to a new well, followed by addition of 150 µL fresh media to all wells (same media as for cells on RTCA E-plate). Cells from all three wells for each

condition were harvested together and transferred to flow tubes on day 5 and subsequently stained with antibodies targeting either markers of Tregs (when staining Tregs) or subset lineage markers in PBMCs (described in detail in 3.8.3).

3.8 Flow cytometry

The antibody targets, dilution factors, their fluorochromes and the cell type stained are listed in appendix II. The Treg antibody panel was previously validated by Heimli in her master's project [150], inspired by the work of Santegoets et al [84]. Compensation files for the Treg panel as well as assessment of voltage settings were provided by candidate's co-supervisor Thea Sjøgren.

3.8.1 Titration experiments of antibodies

Titrations of CD14 and CD20 were performed in this project , as all other titrations were already available to the candidate [150]. Cryopreserved PBMCs were thawed and washed at 300xg, 20 ºC for 10 min (unless stated, all following washes were done in the same conditions) in 4 mL flow buffer (0,5% v/v Bovine serum albumin (BSA) in PBS). Following resuspension of the cell pellet in 4 mL PBS, cell aggregates were removed by filtering the cell suspension through pre-separation filters. Cells were counted and stained with live dead marker. Two hundred and fifty thousand cells were transferred to flow tubes and stained with Fc-block, followed by wash and resuspension in 100 µL flow buffer. Five serial dilutions of CD14 and CD20 (spanning 1:50 and 1:800 of the final suspension volume) were prepared and added to separate tubes. The cells were incubated in the dark at 4 ºC for 30 min, washed and resuspended in 1 mL 1x permeabilization buffer (from the eBioScience FOXP3 Fixation/Permeabilization Kit). Following incubation in the dark at 4 ºC for 1 h, cells were washed twice in 2 mL 1x permeabilization buffer and the cell pellet was resuspended in 250 µL 1x permeabilization buffer then kept in the dark at 4 ºC until flow analysis the following day.

3.8.2 Staining of harvested PBMCs and Tregs for flow cytometry

Cells were harvested and pelleted at 300xg, 20 ºC for 10 min. The supernatant was collected (and stored at -80 ºC for future ELISA analysis) while the cells resuspended in 1 mL PBS. Dead cells were stained using LIVE/DEAD Fixable Yellow Dead Cell Stain Kit, according to the manufacturer's protocol. The cells were then incubated for 20 min at RT in the dark, followed by quenching of the signal by adding 1 mL flow buffer subsequent wash at 300xg, 20 ºC for 10 min (all subsequent washing steps preformed in the same conditions). To prohibit unspecific antibody binding when staining PBMCs, 2 µL 0,5 mg/mL Fc-block was added to

each tube, which were then incubated at RT in the dark for 20 min and then washed in 2 mL flow buffer. The supernatant was removed by swift tipping of the tube and the cells were resuspended in remaining buffer (approx. 100 µL)

A master mix of antibodies targeting extracellular markers was prepared (according to the dilutions stated in appendix II) and added to each cell sample, then incubated in the dark at 4 ºC for 20 min before washing. Supernatant was removed and the cells were fixated and permeabilized using eBioscience FOXP3 Transcription Factor Fixation/Permeabilization Kit exactly as the manufacturer's protocol describes. One mL of Fix/perm buffer working solution was added to each sample and stored overnight in the dark at 4 ºC.

On the day of flow analysis, the samples were washed with 2 mL 1X permeabilization buffer from the eBioScience FOXP3 Fixation/Permeabilization Kit, and centrifuged for 5 min at RT and 500xg, followed by addition of intracellular markers: FOXP3 for both PBMCs and Tregs and Helios for Tregs only. The samples were incubated for 1 h at 4 ºC in the dark, before subsequent wash at 500xg, 20 ºC for 5 min. Lastly the supernatant was removed, and the cells resuspended in 250 µL permeabilization buffer.

To account for fluorescent spill over, single stained (compensation) controls were analyzed by using eCompensation beads followed by addition of 1 µL of each antibody to separate tubes (with one tube left unstained) for 20 min in the dark. Pelleted cells/beads were reconstituted in 100 µL flow buffer, ready for flow analysis. Followingly, to ensure accurate gating during flow data analysis, we analyzed fluorescence minus one controls (FMOs) of all antibodies on the multicolor PBMC and Treg panels using cryopreserved PBMCs and Tregs after 96 h culture. Flow analysis was then performed using BD LSR Fortessa flow cytometer, followed by data-analysis using Flow.Jo version 10.8

3.9 Relative quantification of gene expression from harvested cells

3.9.1 RNA isolation

RNA isolation was performed on both non-activated and activated cells from the drug assays, the first retrieved after resting while the latter after 96 h culture. Qiagen RNeasy Plus Micro Kit (Qiagen) was used according to the manufacturer's protocol, referred to for detailed description of the procedures. In short, the cell suspension harvested after culture was centrifuged at 300xg, RT for 10 min, followed by resuspension and lysis of the pelleted cells and homogenization of the lysate using shredder columns, prior to storage in -80 ºC. Cell lysates were then passed through a gDNA eliminator spin column. The flow through mixed

with one volume of 70 % ethanol and transferred to a RNeasy MiniElute column, before washed with 700 RPE µL, 500 µL RPE and 500 µL 80% ethanol. The membrane bound RNA was collected in a new tube by double elution in 14 µL DEPC treated water. The concentration of RNA in all samples was measured using Nano-drop ND-1000 spectrophotometer.

3.9.2 cDNA synthesis

First-strand cDNA synthesis was performed using Superscript IV Vilo Kit exactly as the protocol kit describes with 70 ng RNA input, for both PBMCs and Tregs. The synthesis was performed using GeneAmp PCR System 9700 with following steps: 25 ºC for 10 min, 50 ºC for 10 min, 85 ºC for 5 min. If not used directly for qPCR, the cDNA samples were stored at -20 ºC.

3.9.3 Optimization of the qPCR SYBR green assay

Optimal function of newly ordered primers for expression analysis of Tc and Th linage specific genes: *FOXP3, RORγt, BCL6, EOMES, GATA3* and *TBET* (sequences listen in Appendix III) was validated in preliminary qPCR runs. These were performed as described in 3.9.5 including primers in 10 µM concentration. To assess assay efficacy with regards to varying cDNA inputs, cDNA was added to the reaction mixes in 4 dilutions: 166 ng/µL, 83 ng/µL, 41,5 ng/µL and 8,3 ng/µL.

To verify the specificity of the primers for the genes of interest, a melting curve was established in the run. Additionally, gel electrophoresis was utilized in preliminary runs on the qPCR products. The gel was prepared by addition of 2 µL GelRed to 35mL of prewarmed 2% (w/v) agarose dissolved in 1x TBE buffer, which was left to stiffen in a caster for 30 min. Followingly, 10 µL of qPCR products with 20% (v/v) loading dye were loaded onto the gel, accompanied by 50-1,000 bp ladder and run in 1x TBE buffer at 100 V, 220 mA for 40-50 min until visible separation of the different sized amplicons. UV pictures of the gels were obtained using Image Lab software provided with the Gel Doc EZ imager.

3.9.4 qPCR SYBR green assay of PBMC gene panel

qPCR on the PBMC gene panel was performed using a SYBR Green based assay utilizing the 2x PowerTrack SYBR Green Master Mix diluted from stock to a concentration of 10 mM. A master mix was prepared containing 2x PowerTrack SYBR green master mix (50% v/v), forward and reverse primers (5% v/v each), and DEPC treated water (35% v/v). Subsequently (2,5 % v/v) Yellow sample buffer 40X was mixed with (diluted 1:10 from 3.9.2) cDNA (10% v/v) followed by addition to the above-described master mix, yielding a reaction mix with the

total volume of 30 µL. Alike the TaqMan based assay, 10 µL triplicates were transferred to a 384-well plate and centrifuged. A run was performed in the QuantStudio 5 Real-time PCR system including a preparative step at 95 ºC for 2 min, followed by 40 cycles denaturation at 95 ºC for 15 s and annealing/elongation at 60 ºC for 60 s of amplification

A non-template control for each reaction mix, as well as the housekeeping gene encoding B-actin was also included. Plate and run setup were prepared using Quant Studio Design and Analysis Software, providing amplification data as Ct values. For each gene of interest and the housekeeping gene, a mean of Ct values from three replicates was used to calculate ΔCt, whereas a mean of ΔCt values from non-treated samples of healthy controls served as the calibrator. Fold change values for all samples ($2^{-\Delta\Delta Ct}$) were calculated [145]. Further, the fold change values from treated samples were normalized to the the $2^{-\Delta\Delta Ct}$ value for non-treated samples within each individual (patient/control), and the relative increase/decrease in expression obtained was used for statistical analyses (described in 3.11).

3.9.5 qPCR TaqMan assay of Treg signature genes

For relative quantification of the expression of Treg genes: *FOXP3*, *HELIOS*, *CTLA-4*, *ENTPD-1*, *ICOS*, *FASN* and *GPR15* a standardized TaqMan based assay was used. For one reaction volume, a master mix was prepared containing 20X of a gene target specific probe/primer mix (5 % v/v), 2X TaqMan Universal PCR master mix (50 % v/v), DEPC treated water (28 % v/v), as well as cDNA (17% v/v) (diluted 1:10 from 3.9.2), yielding a total volume of 30 µL. Each reaction mix was transferred to a 384 well qPCR plate in 10 µL triplicates. The plate was covered with adhesive film and centrifuged at 3000 rpm for 60 s before analysis in the QuantStudio 5 Real-time PCR system. The program included two preparatory steps: first at 50 ºC for 2 min, second at 95 ºC for 10 min. Thereafter, two amplification steps were steps identical to the SYBR green assay. Additionally, a melt curve analysis was performed at the end of the run to verify presence of a simple amplicon.

A non-template control for each reaction mix, as well as GADPH as the housekeeping gene were also included. Plate and run setup were prepared using Quant Studio Design and Analysis Software, providing amplification data as Ct values, further analyzed using the $2^{-\Delta\Delta Ct}$ method [145] in Excel, where treated and non-treated samples were normalized as described in 3.9.4

3.10 ELISA

ELISAs were performed on culture supernatants preserved at -80 ºC after Treg expansion as well as following 96 h culture of treated and non-treated cells. The experiments were performed according to the amended protocols and are referred to for detailed description of the procedures. The two kits employed were: Picokine Human TGFβ-1 ELISA kit (Mybiosource) and Human IL-10 quantikine HS ELISA kit (R&D systems). TGF-β in 110 µL supernatant sample was diluted with activating solutions according to the protocol provided, yielding a 1,4x dilution factor. 200 µL supernatant was utilized in IL-10 ELISA. The absorbance values were measured using SpectraMaxPlus spectrophotometer at wavelengths: 450 nm for TGF-β and 490 nm for IL-10. The concentrations of the cytokines in added samples were calculated by the SoftMax Pro software based on the standard curve prepared from a dilution series of the protein standard that followed with the kits.

3.11 Statistical analysis and generation of graphical illustrations

Statistical analyses were performed using GraphPad Prism 9.0, also used to generate the graphical illustrations of the results presented in this thesis. When evaluating the effect of treatments, between LMT-28 versus “no drug” and Secukinumab versus “no drug” samples within individual patients and controls, one-way Anova (Friedman test) was used on flow cytometry and xCELLigence data, where significance was characterized by a p-value less than 0,05. For the data analysis of qPCR and ELISA results, effect of treatments within individuals was evaluated using multiple paired, non-parametric t tests (Wilcoxon test), where the significance p-value threshold was lowered to 0,01 to account for possibly exaggerated p-values due to multiple testing.

To compare effects of treatment between patients and controls for xCelligence, flow cytometry, qPCR and ELISA the data were normalized from treated samples to the “no drug” control of the same individual. To compare the response of patient and control groups to the respective *in vitro* treatments, unpaired non-parametric t test (Mann-Whitney test) where a p-value lower than 0,05 was used to indicate significance.

4. Results

4.1 Isolation of PBMCs

PBMCs from 23 healthy controls were isolated and the number of cells was estimated, ranging between $4{,}7*10^6$ and $1{,}47*10^7$ average $9{,}3*10^6$ cells from 10 mL of blood. Five of the samples were used as sex- and age-matching controls during culturing experiments and the following endpoint assays: flow cytometry, qPCR The rest were used for optimization of cell culturing experiments during xCELLigence optimization, drug screening assays, preliminary qPCR experiments and preliminary flow cytometry analyses. PBMCs from patients were retrieved from the ROAS biobank.

4.2 Isolation and expansion of Tregs

Tregs from 10 healthy controls were magnetically isolated and the cell number was estimated, ranging between $1{,}66*10^5$ and $4{,}0*10^5$ average $3{,}03*10^5$ Tregs. The cells were subsequently expanded for 14 days *in vitro*. Cell count was conducted post expansion, yielding numbers ranging between $1{,}07*10^7$ and $2{,}2*10^7$ Tregs per individual sample, corresponding to 25-94-fold increase as compared to the respective cell number pre-expansion. Confirmation of stable Treg phenotype reflected by high CD4, CD25 and low CD127 expression post-expansion was assessed by flow cytometry analysis in the group prior to this master's project (data not shown). Five of the samples were used as sex- and age-matching controls during culturing experiments and following endpoint assays: flow cytometry, qPCR. Tregs from patients were retrieved from the ROAS biobank. The five other samples were used in optimalisation experiments. Tregs from patients were retrieved from the ROAS biobank.

4.3 Real-time analysis of cell behavior using xCELLigence RTCA: optimizations and drug screening assays

4.3.1 Optimization of cell culturing conditions for xCELLigence RTCA

Since xCELLigence has not been widely used before to assess T cell behavior, limited information exists regarding the optimal culturing conditions to be used during assays. Therefore, we performed several preliminary runs to determine the optimal pre-coating agent, cell number and density as well as optimal IL-2 concentration in culture medium. To ensure satisfying quality of the experiments, the results were also discussed with the xCELLigence manufacturer. The results showing recorded CI values over the course of 48 h cell culture for each condition tested are presented below.

Optimization of pre-coating agent:

Since T cells are non-adherent to plastic, an immobilization agent must be used to mediate the attachment of these cells onto well bottoms of E-plates, where the CI-recording electrodes are situated. Figure 4.1 depicts CI values of PBMCs cultured on a common E-plate where half of wells are pre-coated with A) goat-anti mouse IgG and the other half with B) mouse anti-human CD3. To visualize how the other parameters influence the CI recordings in accordance with the type of coating used, the number of cells, medium volume, and IL-2 concentrations (500U/mL and 1000U/mL) were also varied, as indicated in the figure legends.

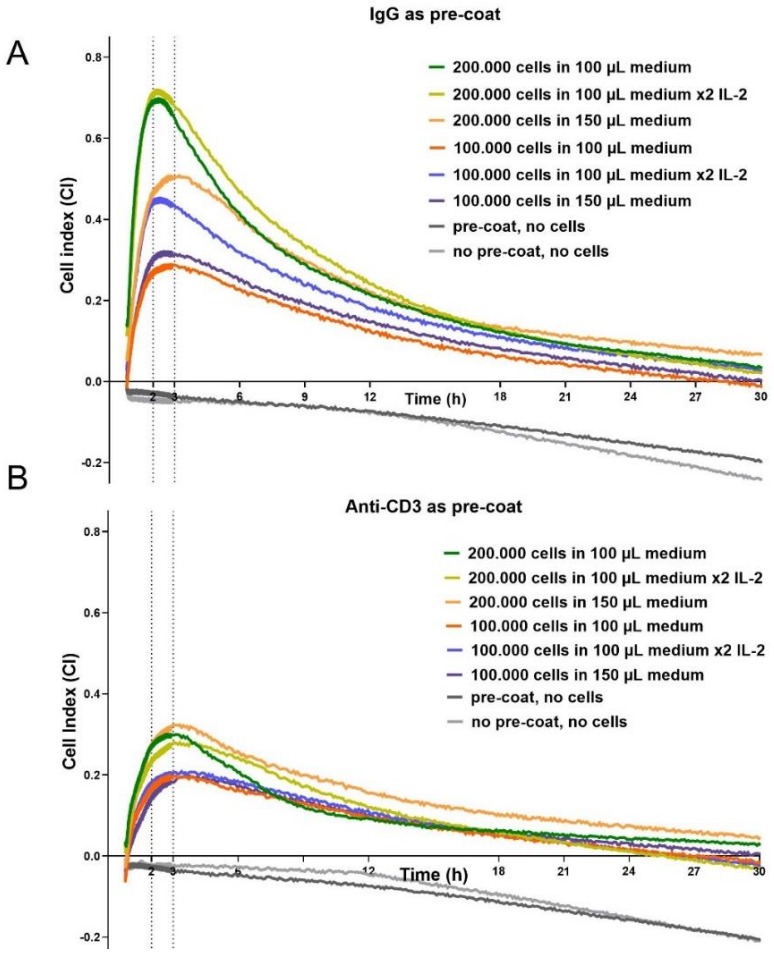

Figure 4.1 Cell index values recorded in real-time during 48 h PBMC culture using two different antibodies as pre-coat. PBMCs plated in single wells pre-coated with **A)** goat-anti mouse IgG coated wells yielding relatively high CI value-peaks in the interval 1-2 h post T cell activation (seen in the interval marked at 2-3 h). Varying CI values are seen, depending on the number of cells and the concentration of T-cell stimulating IL-2 in culture medium. **B)** Mouse anti-human CD3 wells yielding much lower CI-values following activation than the goat-anti mouse IgG counterparts with otherwise the same parameters. CI values for control wells without cells, with and without precoat are colored grey. Only the first recorded 30 h of culture are depicted in the figure.

Trends with regards to cell number, with $2*10^5$ cells yielding approx. twice as high CI as 10^5 cells can be observed for both agents. However, differences regarding media volume and IL-2 for anti-CD3 as pre-coat (fig 4.1 B) are much less prominent compared to what is seen in IgG

coated wells (fig. 4.1 A). Goat-anti mouse IgG was therefore deemed more appropriate to reflect changes in cell behavior during treatment with drug. It was hence used for the rest of the optimization experiments and culturing assays on patient and control cells.

Optimization of number of cells seeded per well:

As indicated already from the CI values observed in figure 4.1, cell number seeded seems to be the parameter which most critically influence on impedance measured by the biosensor. Similar effects can be observed following a cell titration experiment, outlined in figure 4.2. Each graph represents a mean of CI values from two parallel wells.

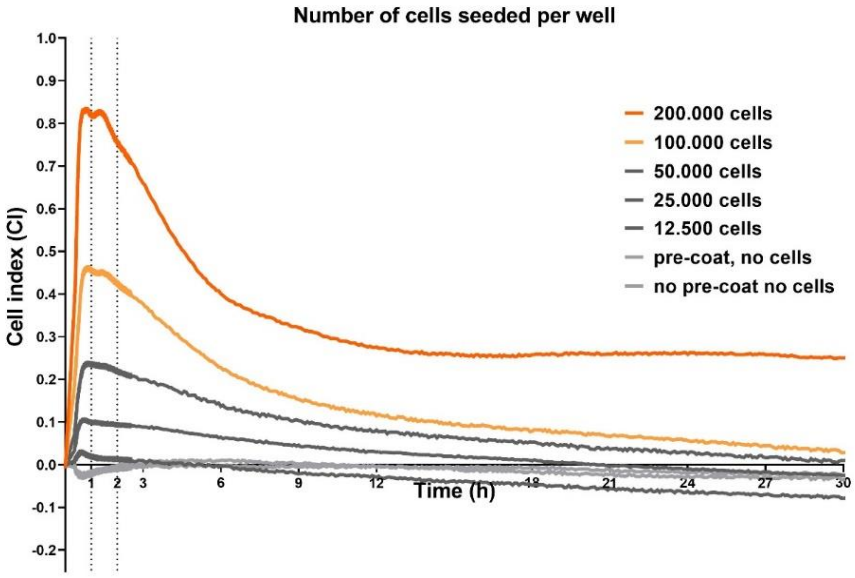

Figure 4.2 Cell index values recorded in real-time during 48 h PBMC culture where cells were seeded in concentrations spanning $2*10^6$ and $1{,}25*10^5$ per well. CI peaks for all concentrations are reached approximately 1 h post activation (seen in the interval marked at 1-2h) and the CI values decrease in relative accordance with decreasing cell numbers. Wells without cells, with and without IgG pre-coat are seen in light grey. Only cell numbers to be used in the following experiments are shown in color. Only the first recorded 30 h of culture are depicted in the figure.

Two hundred thousand cells per well yield the highest CI value equal to CI=0.83, decreasing to a value of CI=0.3 after 12 h of cell culture where it stays throughout the 48-h assay. On the contrary, graphs for all cell numbers lower than $2*10^5$ cells progressively decrease towards CI=0. All following experiments on PBMCs were conducted with $2*10^5$ cells per well, while 10^5 cells were seeded during assays on Tregs.

Optimization of IL-2 concentration

Varying concentrations of IL-2 spanning between 2500 U/mL and no IL-2 in culture medium were tested it two separate experiments. A mean of two CI- values from parallel wells in a representative run was used to generate the graphs depicted in figure 4.3.

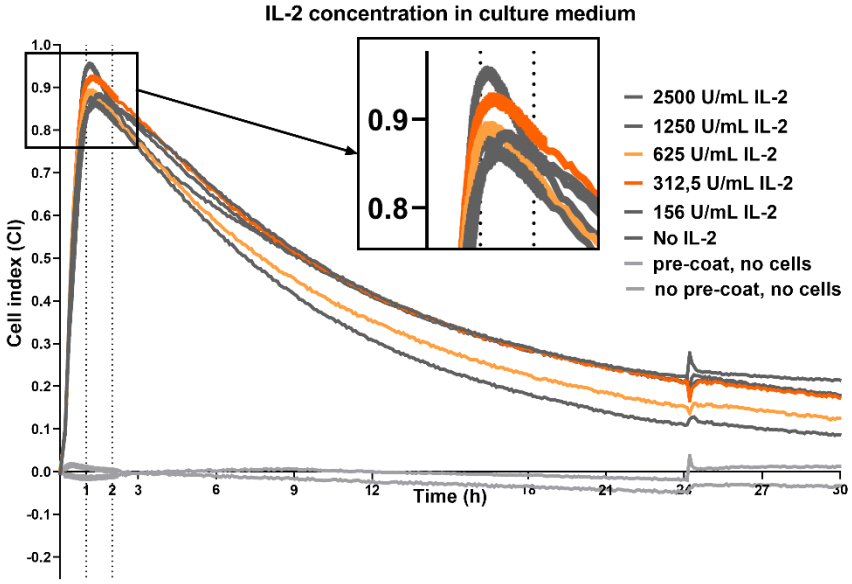

Figure 4.3 Cell index values recorded in real-time during 48 h PBMC culture with varying IL-2 concentrations. Similar peak values for all conditions are reached within 1-2 hours post-activation. IL-2 concentrations indicated by the orange graph was chosen for the rest of experiments to follow. Here, fresh culture medium with 50 U/mL IL-2 was added to all wells following 24 hours of cell culture. Wells without cells, with and without IgG pre-coat are seen in light grey.

No trends with regards to IL-2 concentrations were observed (fig. 4.3). Based on previous work done in the lab, a concentration of 500 U/mL IL-2 was chosen for future experiments on PBMCs, while 50 U/mL was used for Tregs.

4.3.2 Determination of optimal treatment concentrations of LMT-28 and Secukinumab

Six different concentrations of LMT-28 and five of Secukinumab were tested during three preliminary drug screening assays on PBMCs and Tregs from healthy controls. The drug response was assessed in real-time using xCELLigence RTCA, complemented by flow cytometric analysis for measuring cell survival and phenotype following 48-h culture. Of particular interest was any indications of the drugs' cytotoxicity possibly reflected by inhibited activation, lower cell numbers or increased cell death in treated samples compared to no drug controls. Additionally, the percentage of Tregs for each condition tested was also determined to see if there were any direct effect on the Treg number. Results from the drug concentration titrations on PBMCs are presented in figure 4.4 for LMT-28 and figure 4.5 for Secukinumab.

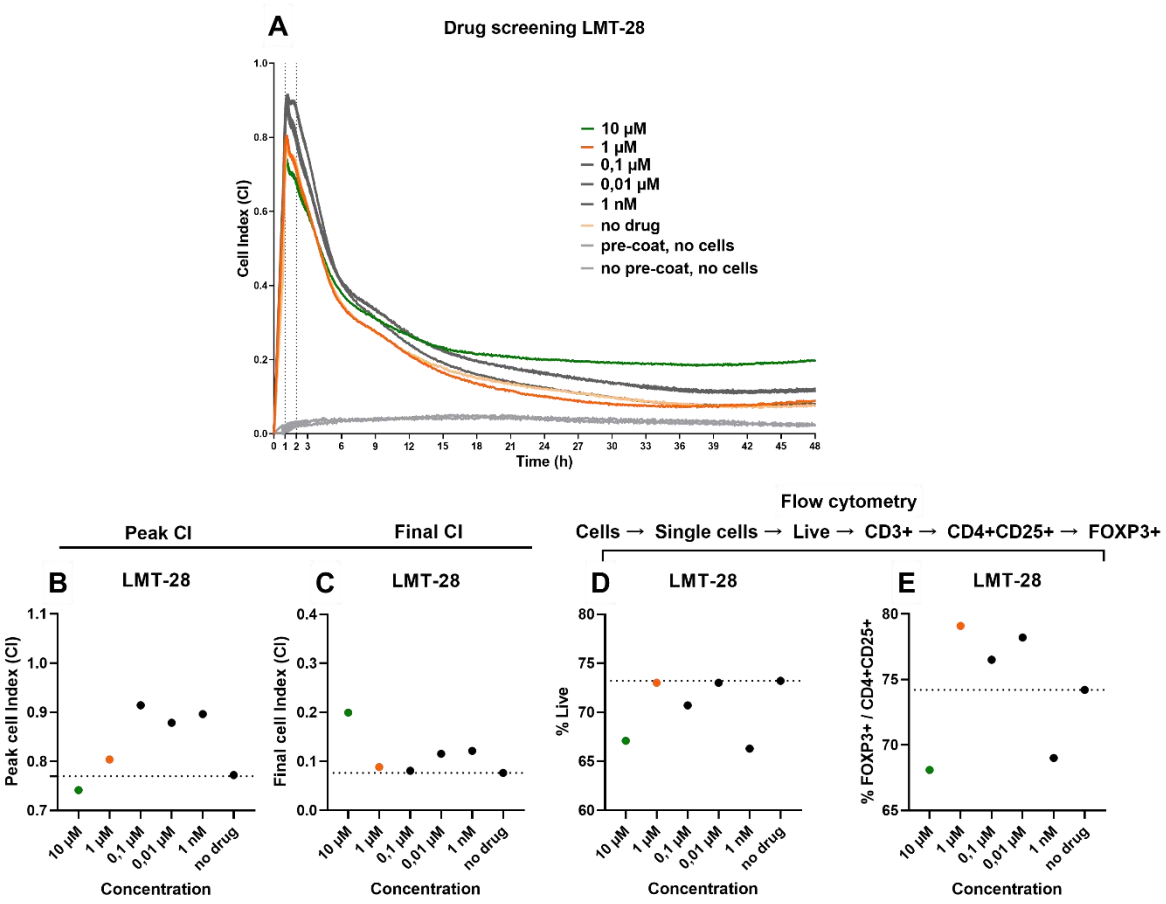

Figure 4.4 Comparison of cell behavior and survival following treatment with five different concentrations of LMT-28. A) xCELLigence graphs depicting a mean of CI values from two parallel wells for each concentration. B) Peak CI values reached 1-2 hours following activation and C) final CI values at 48 h. The highest concentration of LMT-28 (green graph) yielded the lowest activation peak and the highest final CI value. D) Percentage of live cells and E) percentage of Tregs in the CD4+CD25+ population assessed after culture with and without drug using flow cytometry; the gating strategy is stated above. The drug concentration chosen for future experiments on patient and control cells is highlighted in dark orange in all plots, while light orange in the xCELLigence graph and dotted lines in dot-plots mark the non-treated control. Data from a representative experiment is shown in this figure.

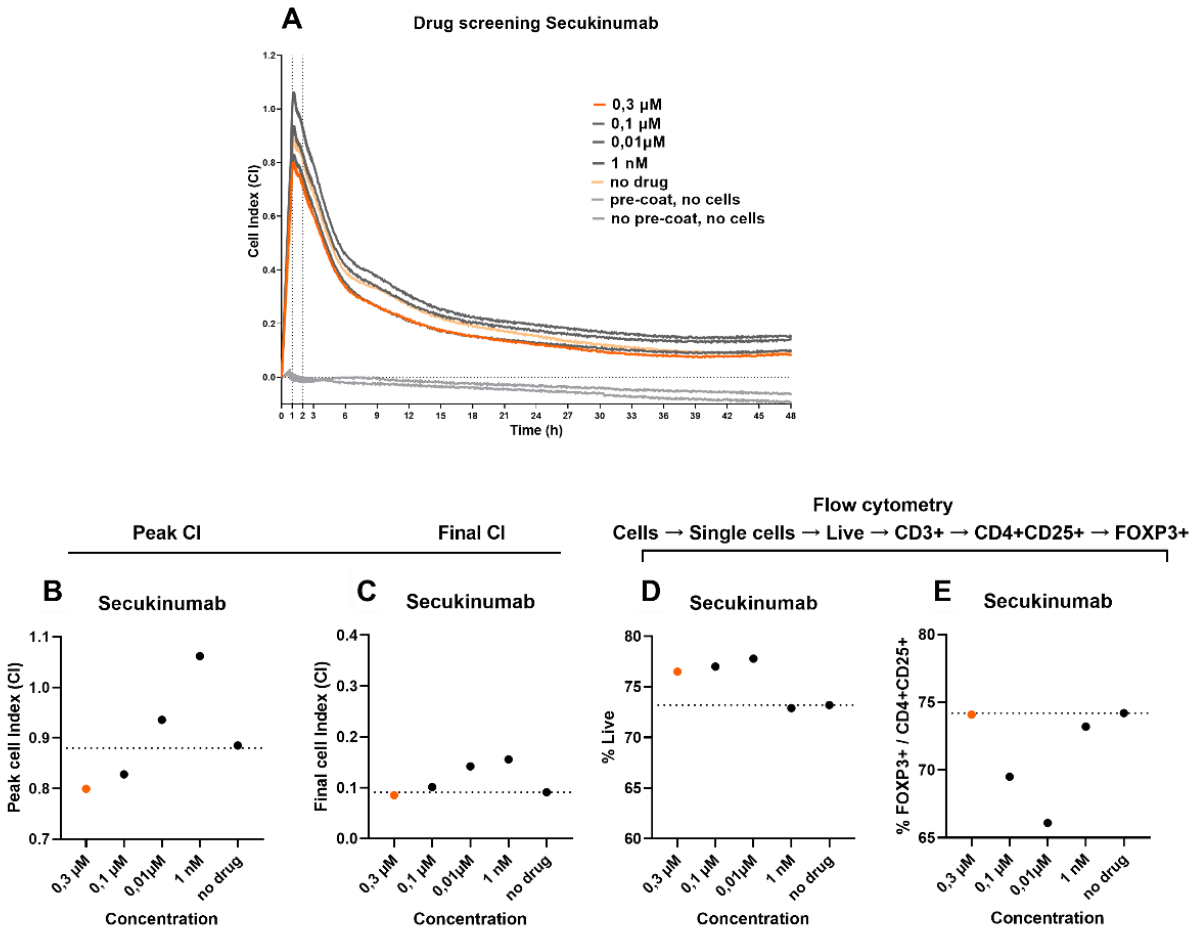

Figure 4.5 Comparison of cell behavior and survival following treatment with four different concentrations of Secukinumab. A) xCELLigence graphs depicting a mean of CI values from two parallel wells per concentration. B) Peak CI values reached 1-2 hours following activation and C) final CI values at 48 h. D) Percentage of live cells and E) percentage of Tregs in the CD4+CD25+ population assessed after culture with and without drug using flow cytometry, the gating strategy is stated above. The drug concentration chosen for future experiments on patient and control cells are highlighted in dark orange in all plots, while light orange in xCELLigence graph and dotted lines in dot-plots mark the non-treated control. Data from a representative experiment is shown in this figure.

No distinctive changes in the shapes of xCELLigence graphs were observed following treatment with drugs, indicating a lack of abrupt alterations to cell behavior (fig 4.4 A and 4.5 A). A variation in CI peaks could be seen, spanning 0,74-0,91 for LMT-28 (fig 4.4B) and 0,82-1,06 for Secukinumab (fig.4.5 B). Higher concentrations of the drugs generally yielded slightly lower CI peaks than the non-treated control. Inversely proportional CI values to drug concentrations were observed both during activation and at 48h following Secukinumab treatment (fig. 4.5 B-C). Little variation was seen in final CI values, with the only exception of 10 µM LMT-28 (fig. 4.4 C). Generally, the behavior of treated cells throughout the course of cell culture was comparable to that of non-treated control, with vastly all peak- and final CI values equal or higher for treated than non-treated cells.

Further, the survival of cells after culture was assessed by flow cytometry (fig 4.4 D and fig. 4.5 D) yielding values of live cells spanning 66,3-73,0% for LMT-28, and slightly higher 72,9-77,0% for Secukinumab. Non-treated control had the highest percentage of live cells compared to all LMT-28- treated samples, but no trend correlating to successive drug concentrations and percentage of live cells could be observed.

A larger variation was seen in the percentages of Tregs within the activated CD4+ T cell population. The LMT-28 treated samples (fig. 4.4 E) showed a span of 68,1-79,1% Tregs, while Secukinumab (fig. 4.5 E) had slightly lower Tregs-percentages (66,1-74,2%). A trend in LMT-28 treated cells could be observed, where concentrations with higher percentage of live cells subsequently had a higher proportion of Tregs within CD4+CD25+ T cells. For Secukinumab this held true for 0,3 µM, the only concentration where the percentage of Tregs was not lower than of non-treated sample.

Given the overall lack of clear indications of the drugs' cytotoxicity from xCELLigence data, the choice of concentrations was made on the background of live- and Treg cell fractions from flow analysis, where lower percentages have been observed in treated compared to non-treated samples. The highest concentrations of drugs that showed equal or higher percentages of live cells and Tregs were chosen, being 1 µM for LMT-28 and 0,3 µM for Secukinumab.

4.3.3 Assessment of real-time behavior of patient and healthy control cells after treatment with LMT-28 and Secukinumab

The xCELLigence RTCA platform was further used for real-time monitoring of PBMCs and Tregs from patients and healthy controls, during 96-h culture with LMT-28, Secukinumab or no drug present in the medium. Graphs generated for both PBMCs and Tregs were similar to the ones previously obtained during optimizations, exemplified in figure 4.6.

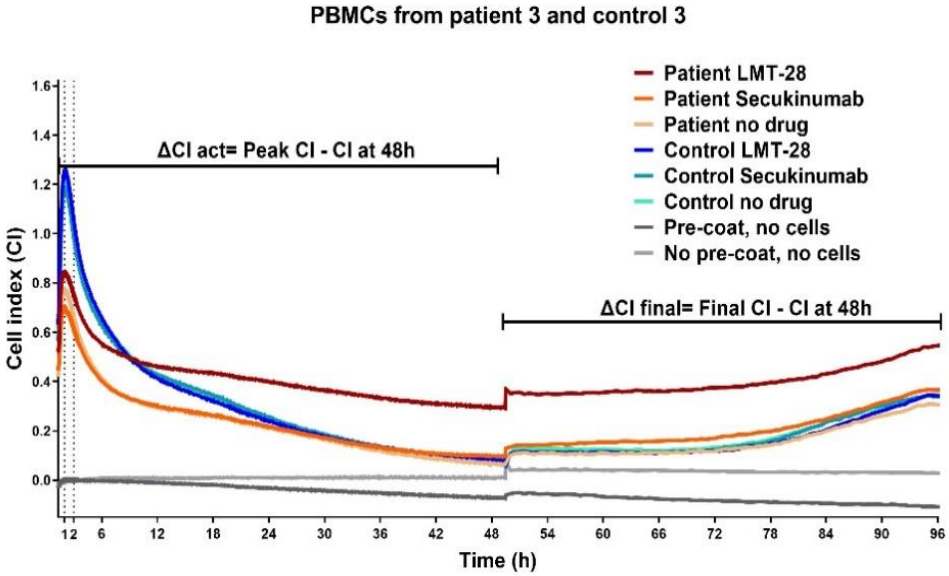

Figure 4.6 xCELLigence graphs of PBMCs from patient and healthy control three, treated with LMT-28 and Secukinumab as well as non-treated control, following 96-h culture. To evaluate whether addition of new medium at 48h leads to different effects on cell behavior than the initial treatment, two time intervals were studied separately: ΔCI act and ΔCI final, indicated in the figure. Mean of CI values from two parallel wells were used to generate the graphs.

Some variation in cell behavior following treatments compared to non-treated cells could be indicated, as seen for the LMT-28 treated patient sample in fig 4.6, where more stable CI values are observed in the first 48h of culture compared to non-treated control. Differences were also observed for peak CI values in-between individuals, exemplified by the much less prominent CI peak for patient than control in fig. 4.6. Overall, peak CI values spanning 0,677 and 1,6 (mean peak CI= 0,75) were observed for PBMCs and 0,15-3,1 for Tregs (mean peak CI= 0,66). Differences could also be indicated following addition of new media with or without treatments after 48 h of culture (seen as a nick in the graphs in figure 4.6). Net CI changes occurring in the first and last 48h were therefore studied separately. The time intervals are marked in figure 4.6 as ΔCI act= peak CI - CI at 48h and ΔCI final= final CI- CI at 48h. The effects of the treatments to changes in cell behavior are presented as normalized to the no drug control, by

diving the ΔCI value from treated- with ΔCI value non-treated sample, shown in fig. 4.7 for PBMCs and fig. 4.8 for Tregs.

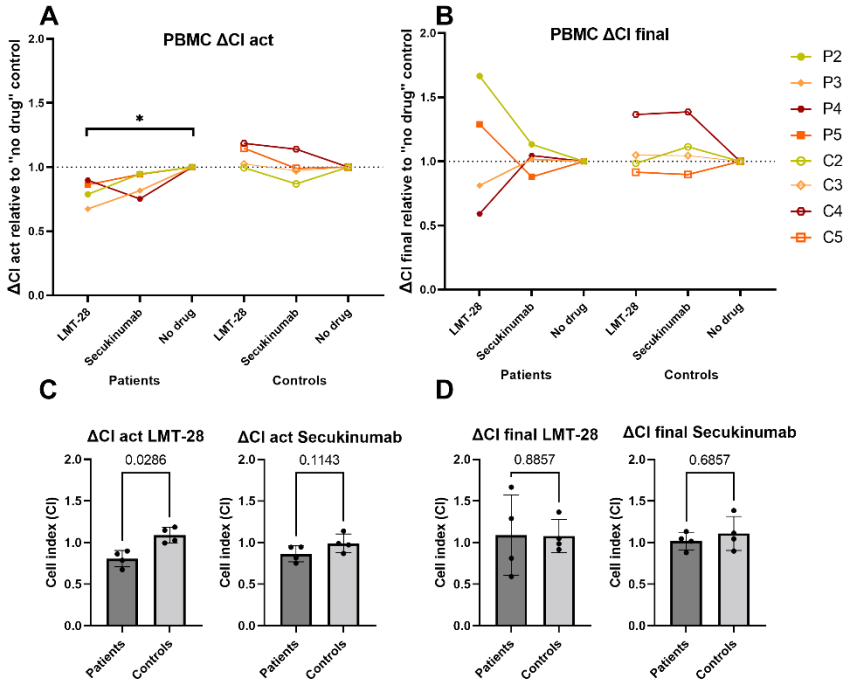

Figure. 4.7 The degree of change in CI values for PBMC from patients and healthy controls following treatment with LMT-28 and Secukinumab, expressed relative to the "no drug" control, indicated by the dotted line in A and B**.** ΔCI values > 1 show more pronounced differences in CI, while values <1 indicate less distinct changes to CI, as compared to the "no drug" control from the same individual. ΔCIs for two intervals have been evaluated**,** A) during the first 48 h of culture defined as the ΔCI act= peak CI - CI at 48h and B) ΔCI final= final CI - CI representing changes in the last 48 h. Statistical analysis on the differences between treated and non-treated cells in individual patients and controls was performed using paired one-way Anova (Friedman test). Comparison of patient and control groups regarding the relative changes to CI C) in the first 48h and D) last 48 h of culture was analyzed by unpaired, non-parametric t test. Mean values are indicated by boxes, while error bars show standard deviation. Patient and healthy control one were not analyzed due to lower cell numbers available. (See appendix XI)

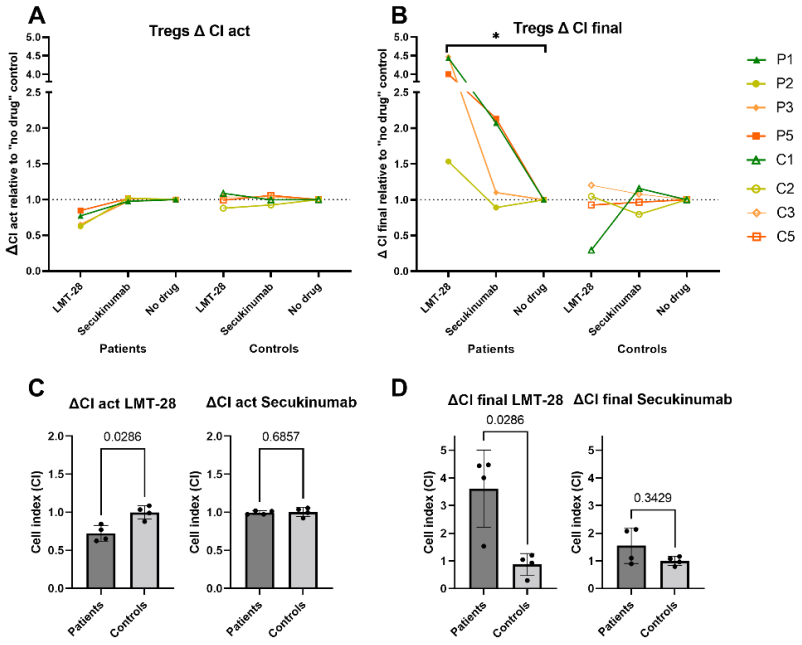

Figure. 4.8 The degree of change in the CI values for Tregs', following treatment with LMT-28 and Secukinumab, expressed relative to the "no drug" control, indicated by the dotted line in A and B**.** ΔCI values > 1 show more pronounced changes, while values <1 indicate less distinct changes in CI, as compared to the "no drug" control from the same individual. ΔCIs for two intervals have been evaluated**,** A) during the first 48 h of culture defined as the ΔCI act= peak CI - CI at 48h and B) ΔCI final= final CI - CI representing changes in the last 48 h. Statistical analysis on the differences between treated and non-treated cells in individual patients and controls performed using paired one-way Anova (Friedman test). Comparison of patient and control groups regarding the degree of changes to CI C) in the first 48h and D) last 48 h of culture was analyzed by unpaired, non-parametric t test. Mean values are indicated by boxes, while error bars show standard deviation. Patient and healthy control four were not analyzed due to lower cell numbers available. (See appendix XI)

A common trend in LMT-28 treated PBMCs from patients could be observed (fig.4.7 A), seen as a more gradual decline in CI graph during the first 48h of culture (alike the patient sample in fig. 4.6), yielding significantly lower ΔCI act as compared to non-treated cells (p-value 0,0267). The same effect of LMT-28 treatment was not observed in control PBMCs (fig. 4.7 C p-value: 0,0286). xCELLigence graphs of Secukinumab-treated cells usually "overlapped" better with that of non-treated cells, indicating less effect on cell behavior of this drug. More differential effects could be seen following repeated treatment at 48 h, indicated by ΔCI final, where both larger and less distinct deviations in CI could be seen in individual samples. No statistically significant differences for ΔCI final were observed, neither among the three conditions within patients and controls, nor across the two groups (fig. 4.7 D).

In line with results seen in PBMCs, a close to significant difference in ΔCI act was observed in LMT-28 treated Tregs from patients (p-value: 0,0678) (fig. 4.8 A). Upon repeated treatment at 48 h, all Treg cultures from patients experienced an altered behavior reflected by exaggerated ΔCI final values (fig.4.8 B), significantly higher after LMT-28 treatment (p-value: 0,0267). CI

changes in control cells were more apparent in the final- than the first 48 h, however most of the ΔCI final values were still relatively close to 1 (fig.4 B), indicating less apparent effects of the treatments on the cell behavior than in patients. When comparing the degree of changes in Tregs from patient and control groups, both significantly lower ΔCI act (p-value: 0,0286) and higher ΔCI final values (p-value: 0,0286) were seen in LMT-28 treated patients (fig.4.8 C-D).

Overall, real-time data from LMT-28-treated cells suggest that the drug alters the behavior of patient cells modestly, characterized by less distinct CI decrease during the first 48 h of culture and a more prominent increase in the last.

4.4 Flow cytometry analysis of patient and control PBMCs and Tregs after treatment with LMT-28 and Secukinumab.

4.4.1 Survival and proliferation of patient and control cells after treatment

After cell culture PBMCs and Tregs were harvested and stained for flow cytometry analysis, by which the survival and proliferation of treated and untreated cells were analyzed. The gating strategy used, is shown in figure 4.9.

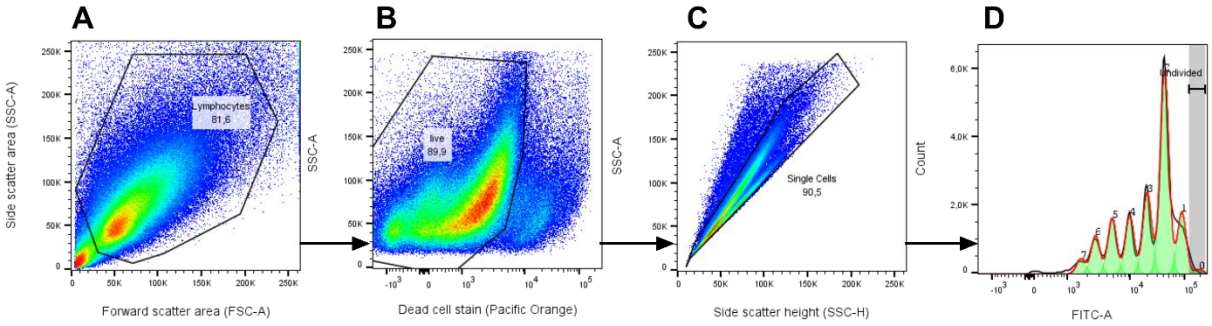

Figure 4.9 Gating strategy used on PBMCs and Tregs to assess the number of live cells and their proliferation profile, here shown for untreated PBMCs from healthy control one. A) A FSC versus SSC plot was used to exclude cell debris from the cell gate. B) Auto fluorescent dead cells with compromised plasma membranes permeable for the dead cell stain dye, were gated out using SSC versus dead cell stain plot. C) To only account for single cells, doublets were excluded using SSC area vs SSC height plot. D) Proliferation profile of single cells, stained with CFSE prior to cell culture, was generated using the "Proliferation modelling" tool in FlowJo. Undivided cells are marked by the grey bar, while subsequent green peaks represent every new generation, indicated by halved fluorescent intensity of CFSE (here in the FITC-channel).

Cell survival

To determine the effect on treatments on cell survival, the number and percentage of live cells in samples was assessed using the live cell gate (fig. 4.9 B). Varying numbers of live cells were achieved in each sample following harvesting and antibody staining, ranging between 9075-338277 (mean: 94680) for PBMCs and 10120-146092 (mean 22434) for Tregs. The

percentages of live cells were compared between the samples, shown for PBMCs and Tregs in fig. 4.10.

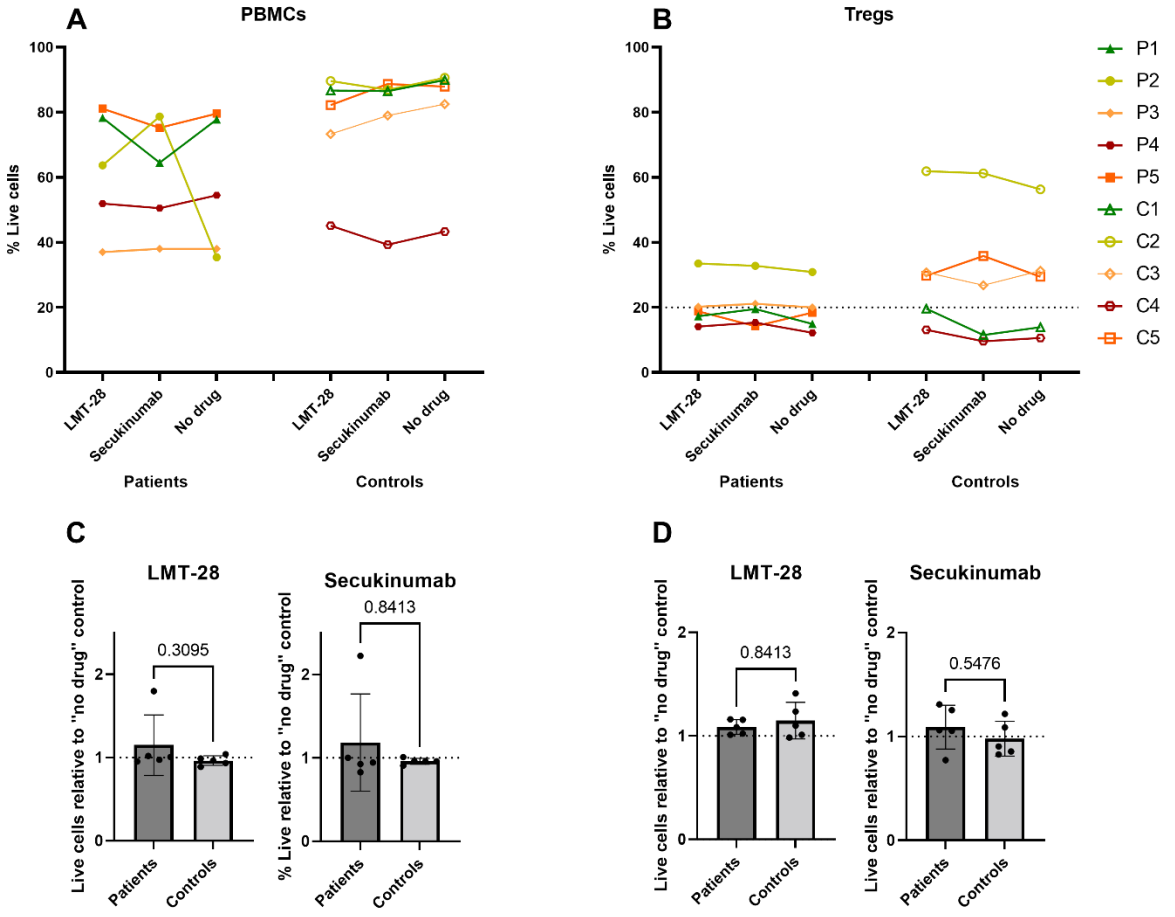

Figure 4.10 Percentages of live cells following culture with or without treatment for patient- and healthy control: A) PBMCs and B) Tregs. No statistically significant differences in cell survival were observed due to treatment with LMT-28 or Secukinumab when compared to non-treated cells in neither patients nor controls (One-way Anova, Friedman test). Comparison of cell survival between patient and control groups subjected to the same conditions for C) PBMCs and D) Tregs did not show significant differences using unpaired, non-parametric t test. Mean values are indicated by boxes, error bars show standard deviation, while the dotted line reflects the "no drug" baseline.

Relatively little variation and no trends were observed in the survival of treated as compared to non-treated cells from the same individuals, yielding no statistically significant differences. More distinct fluctuations were observed in-between individuals, spanning up to 40% in both PBMCs (fig. 4.10 A) and Tregs from controls (fig. 4.10 B). Low percentages of live cells were observed in cell samples from cultured Tregs, where only five individuals showed cell survival rates above 20% (fig 4.10 B). No differenced were indicated between patient and control groups (fig. 4.10 C and D).

For further proliferation analysis, we chose to exclude samples with live cell percentages lower than 20%, as autofluorescence from dead cells could interfere with the read-out of the CFSE dye.

Cell proliferation

Further, we investigated possible alterations of the treatments on the cell's proliferative capacity. The percentage of dividing cells among single cells was estimated (see appendix IV) and the mean number of cell divisions in the dividing population, defined as the Proliferation Index (PI), was calculated by the modelling tool in FlowJo (gated as shown in fig. 4.9).

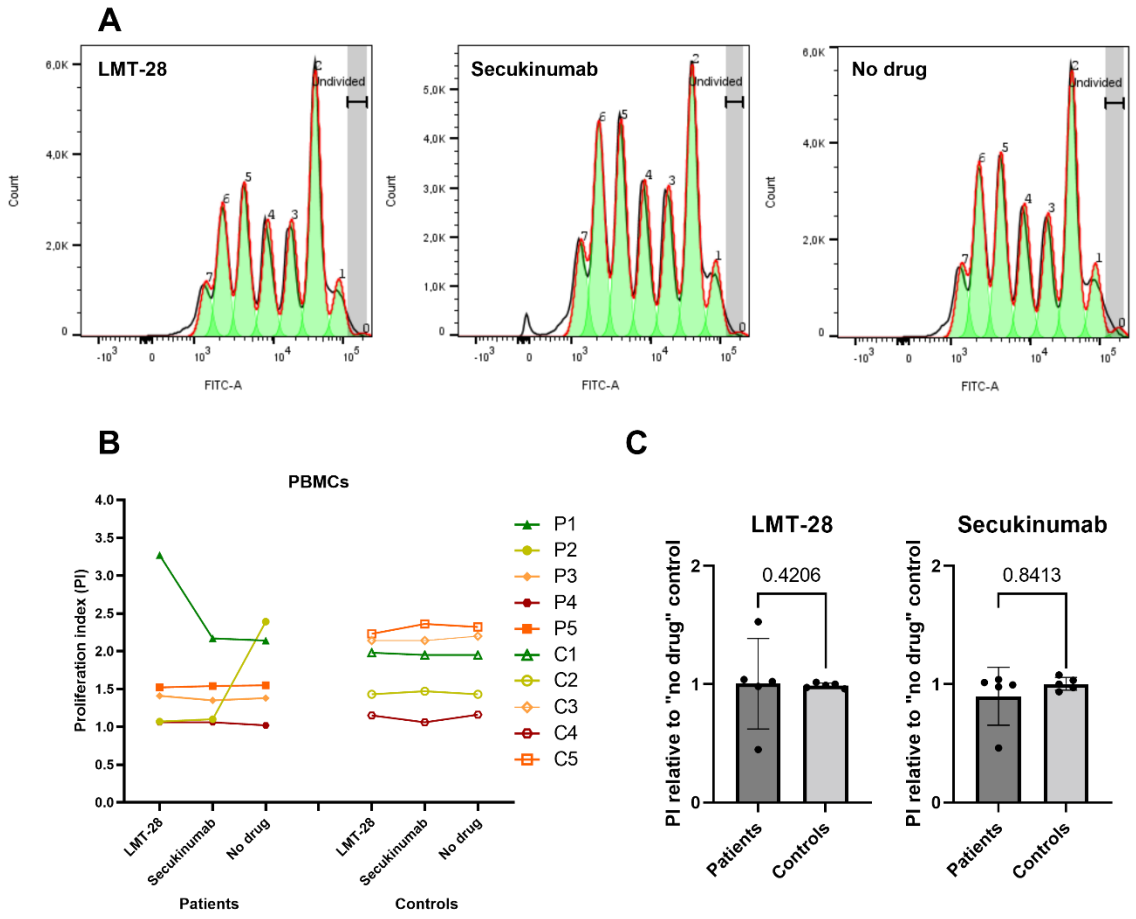

Figure 4.11 Cell proliferation in PBMC cultures, following treatment with LMT-28 and Secukinumab, A) Proliferation profiles for treated and non-treated samples, showing seven generations of dividing cells in samples from healthy control five B) Frequency of cell divisions among proliferating cells, indicated by the proliferation index, in cells from patients and healthy controls. C) A comparison of cell division frequencies in patient and healthy control groups, subjected to the same treatment. No significant differences were found neither between the three conditions in patients and controls (paired one-way Anova, Friedman test) nor when comparing normalized PI values between patient and control groups subjected to same treatment (unpaired, non-parametric t test). Mean values are indicated by boxes, while error bars show standard deviation.

Few differences were observed in cell proliferation after drug treatments, as exemplified by the highly similar proliferation profiles of LMT-28- and Secukinumab-treated cells compared to the no drug control (fig. 4.11 A). Distinguishable variation in PI values between individual patients and controls was observed. On the contrary, PI values across the three conditions in almost every individual were close to identical, (with two exceptions: LMT-28 treated cells from patient 1 and "no drug" control from patient 2), indicating that treated cells proliferate at a similar rate to non-treated cells. Consequently, no statistically significant differences for LMT-28- or Secukinumab-treated versus non-treated cells were found. Followingly, cell proliferation in patient and control groups is not shown to be affected differently by the respective treatments (fig. 4.11 C)

Tregs

Proliferation analysis was performed on Tregs from five individuals, as only these had percentages of live cells above 20%. The proliferation index values are presented in table 4.1

Table 4.1 Proliferation index values in Tregs from patients and healthy controls

	LMT-28	Secukinumab	No drug
Patient 2	1,74	1,84	1,70
Patient 3	1,66	1,58	1,59
Control 2	1,66	1,69	1,70
Control 3	1,23	1,22	1,22
Control 5	1,70	1,72	1,76

Alike in PBMCs, the PI values in Tregs are highly similar across the three conditions. Statistical analysis evaluating the effects of treatments on the proliferation of Tregs has not been performed due to few individuals represented.

4.6 Phenotypic analysis of patient and control cells after treatment with LMT-28 and Secukinumab

4.6.1 FOXP3+ Tregs in PBMCs

Further, we examined whether treatments influenced the frequencies of FOXP3 expressing Tregs in PBMC cultures (fig. 4.13), utilizing gating the strategy shown in fig 4.12. Additionally, the frequencies of CD14+ monocytes, CD20+ B cells and CD8+ cytotoxic T cells were also assessed (fig. 4.14). The optimal dilutions of CD14+ and CD20+ antibodies were

determined by antibody titrations prior to the analysis on patient and control cells, as shown in appendix V.

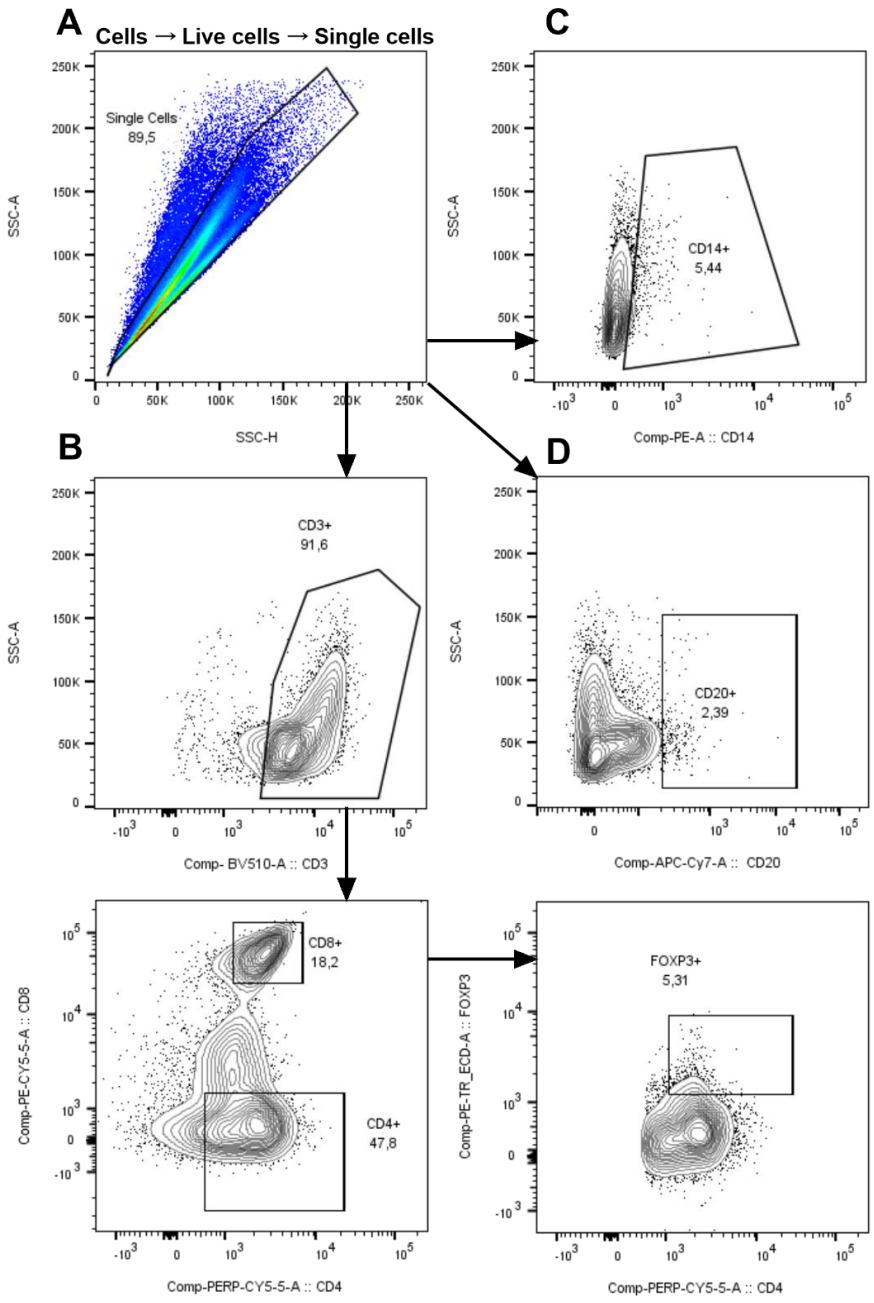

Figure 4.12 Gating strategy used to assess the frequencies of Tregs, cytotoxic T cells, monocytes, and B cells in treated and non-treated PBMCs from patients and healthy controls. A) Single cells (gating prior to single cells shown in fig. 4.9) B) were gated for CD3 expressing T cells using side scatter area versus BV510 fluorescence plot. Within the CD3+ gate, CD8+ and CD4+ T cell populations were separated by the fluorescence of PE-Cy5.5 and PerCP-Cy5.5 The CD4+ population was further gated towards FOXP3+ expressing CD4+ T cells by the fluorescence of PE-TR ECD dye (FOXP3) versus PerCP-Cy5.5 (CD4+), yielding Tregs. Single cells were also gated for C) CD14+ monocytes using SSC-A versus PE plot, and D) CD20+ B cells using SSC-A versus APC-Cy7 plot.

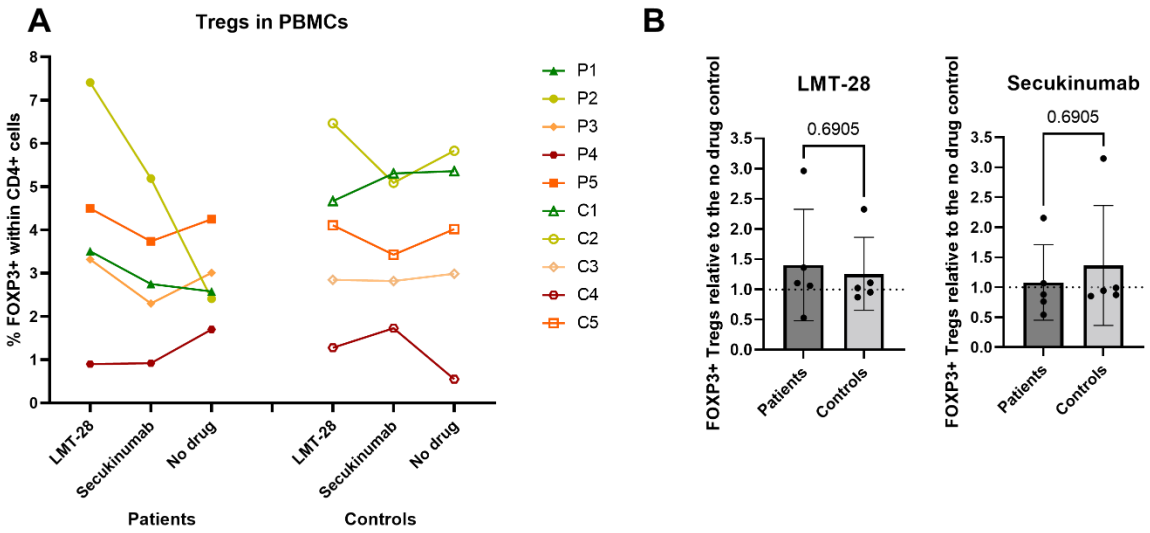

Figure 4.13 FOXP3+ Tregs within the CD4+ T cell population in treated and non-treated PBMC cultures from patients and healthy controls. A) Frequencies of Tregs in LMT-28 and Secukinumab treated cells compared to "no drug" control within each individual patient and control. No significant differences to the Treg cell fraction were seen in patients or controls when comparing LMT-28 and Secukinumab treated cells to the "no drug" controls (Paired one-way Anova, Friedman test) B) Frequencies of FOXP3+ in A, normalized to the "no drug" control were used to compare the response of patients and control groups to the same treatments, with no significance observed (unpaired, non-parametric t test). Mean values are indicated by boxes, error bars show standard deviation, while the dotted line reflects the "no drug" baseline.

Varying frequencies of Tregs within the CD4+ T cell population were observed after culture, ranging between 0,9-7,4% (mean: 3,42%) in patients and 0,55-6,5% (mean: 3,76%) in healthy controls. Both increase and decrease in the Treg populations were seen in Secukinumab treated cells. No statistically significant differences in Treg frequencies could be indicated upon LMT-28- (p-value patients: 0,418, controls: >0,99) or Secukinumab treatment (p-value patients: >0,99, controls: 0,685) when compared to non-treated cells from the same individual. No significant differential effects of the treatments on Treg frequencies between patient and healthy controls were observed (fig 4.13 B).

Low frequencies of monocytes and B cells were observed among the single cells from PBMCs cultured in T cell-stimulating conditions, as indicated in fig. 4.14. Frequencies of CD8+ (cytotoxic T cells) within the CD3+ T cells were estimated to 9,36±6,1% in patients, and 10,01±6,0% in controls (mean ± SD).

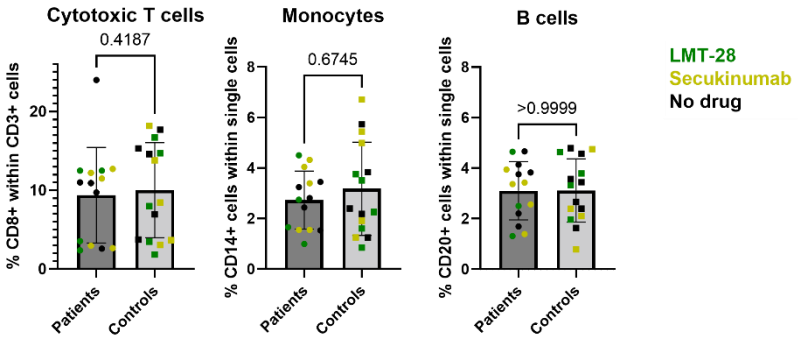

Figure 4.14 Frequencies of the major cell populations in PBMC cultures from patients and healthy controls. Type of treatment is shown in color, indicating that the variation observed across samples is alike for all three conditions. Mean values are indicated by boxes, while error bars show standard deviation.

Frequencies of the three cell populations was variable in-between individuals, indicated to be independent of the treatments as visualized in fig. 4.14.

4.6.2 Protein expression of selected markers in Tregs

The impact of treatments on the phenotypic and functional markers of Tregs' was assessed using the gating strategy shown in figure 4.15

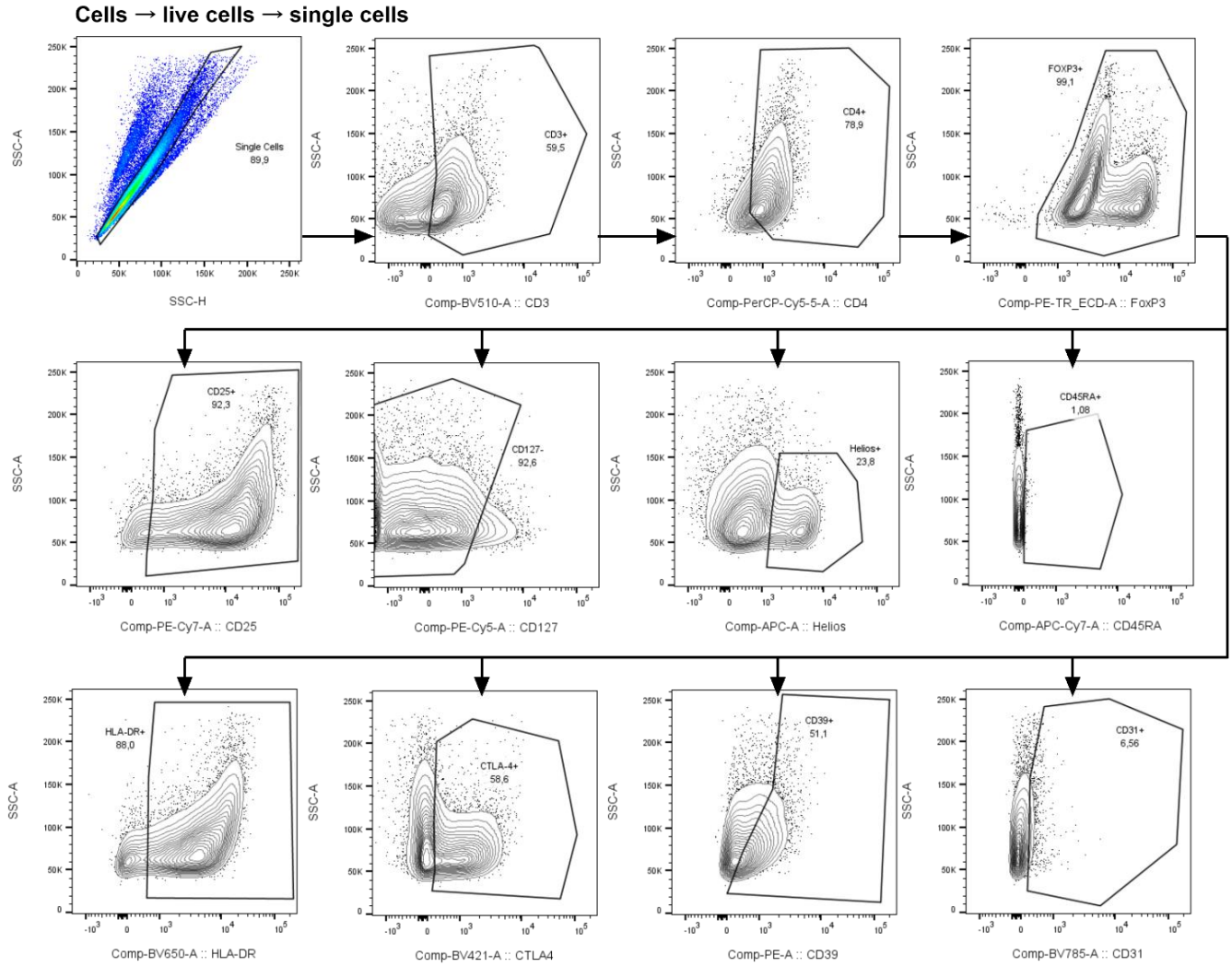

Figure 4.15 Gating strategy used to assess the phenotypic and functional markers on Tregs from patients and healthy controls following treatment with LMT-28 and Secukinumab, as well as non-treated controls. Single cells (gating prior to single cells shown in fig. 4.9) were gated for CD3+ T cells using SSC versus BV510 plot. Within the CD3+ population, CD4+ T cells were assessed using SSC versus PerCP-Cy5.5. CD4+ T cells positive for FOXP3, defined as Tregs, were distinguished using SSC versus PE-TR ECD dye plot. From the FOXP3+ Treg population, plots of SSC versus the fluorescence of the relevant fluorochrome were used to define Tregs positive for CD25, CD127, Helios, CD45RA, HLA-DR, CTLA-4, CD39 and CD31.

Highly variable frequencies of FOXP3+ T cells were found within CD4+ population harvested after Treg culture, ranging 12,6-85,8% (mean 42,15%) in patients and 8,8-99.1% (mean 58,56%) in controls (fig 4.16 A). A positive correlation between higher frequencies of FOXP3+ Tregs and the percentage of live cells (fig. 4.10 B) in Tregs was observed. When evaluating the effect of the treatments, significantly higher numbers of FOXP3+ cells were seen in all LMT-28 treated patients (p-value: 0,0288), suggesting a positive influence of the drug on the Treg phenotype. Similar positive effect was observed in cells from healthy controls treated with Secukinumab, but no significance was achieved (p-value: 0,228). Despite the mentioned

trends, no differential effect of the treatments on patient and healthy control Tregs was indicated (fig. 4.16 D).

The fraction of FOXP3+ Tregs positive for the phenotypic and functional Treg marker CD25 (fig. 4.16 B) showed few trends with regards to treatments in patients. In healthy controls, a subtle trend towards an increase in CD25+ Tregs was observed following Secukinumab treatment (p-value: 0,31). However, close to significant difference in the effect of Secukinumab on fractions of CD25+ Tregs in patients and controls could be seen (p-value: 0,0635) (4.16 E). Consistently across all individuals, almost all FOXP3+ Tregs were negative for the surface marker CD127, with no significant differences in the number of CD127- Tregs with regards to treatments (fig. 4.16 C) for neither patients, controls or when comparing the two groups (fig. 4.16 F)

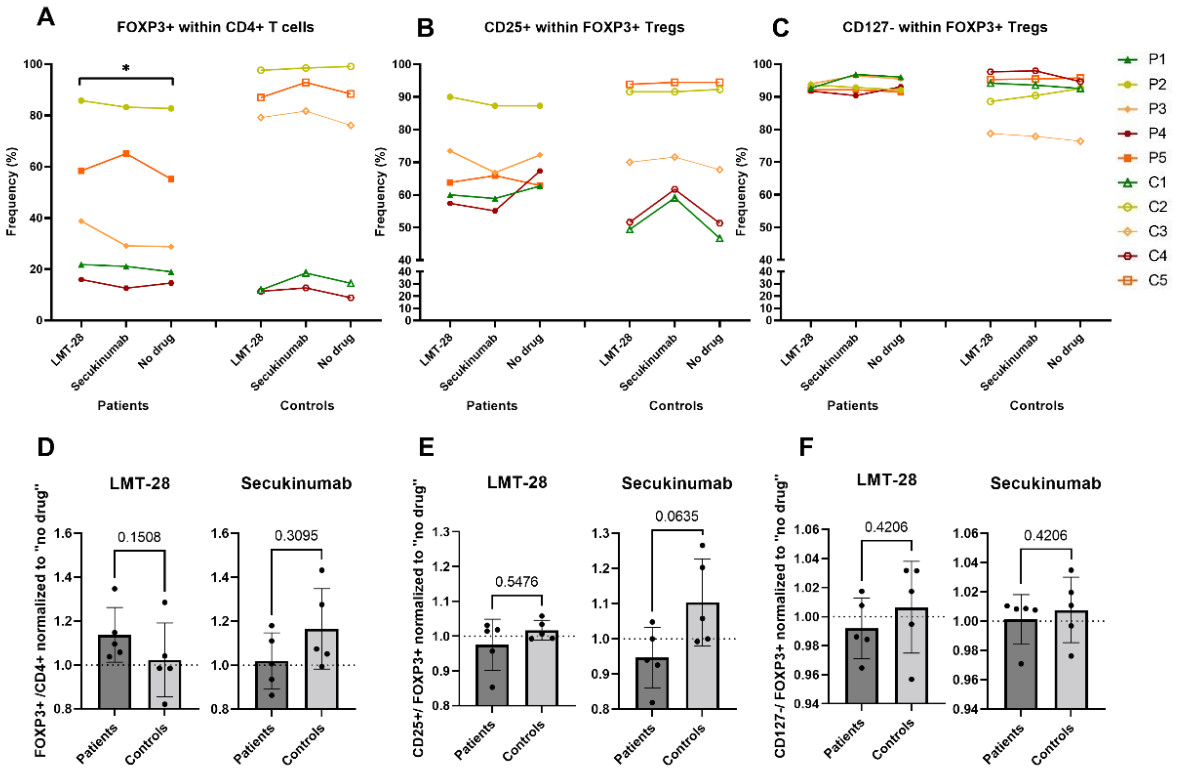

Fig 4.16 Frequencies of cells expressing the phenotypic Treg markers following treatments with LMT-28 and Secukinumab. Percentage of A) FOXP3+ Tregs within the CD4+ T cell population as well as B) CD25+ and C) CD127- within FOXP3 expressing Tregs. Significant increase in FOXP3+ Tregs was found in patients when treated with LMT-28 (paired One-way Anova, Friedman test). Relative increase/decrease in the fractions of D) CD4+ T cells positive for FOXP3 as well as E) CD25+ and F) CD127- Tregs after treatments, as normalized to "no drug" controls from the same individual. No differential effect of the treatments on the two groups was indicated by the statistical analysis performed (unpaired, non-parametric t test). Mean values are indicated by boxes, error bars show standard deviation, while the dotted line reflects the "no drug" baseline.

Frequency of FOXP3+ Tregs positive for CTLA-4 varied across individual samples but stayed relatively consistent in most treated compared to non-treated samples (fig 4.17 A) and no effect of treatments was suggested for patients, controls, or when their responses were compared (fig.

4.17 C). Surface expression of CD39 (ENTPD-1) on Tregs from patients showed both up- and downregulation following treatment (fig. 4.17 B). Intriguingly, almost all healthy controls saw higher numbers of CD39+ Tregs following treatments (mean: LMT-28: 56,06%, Secukinumab: 53,84%, no drug: 47,14%) yielding statistically significant p-values: 0,0146 for both drugs. The promotion of CD39+ Tregs in controls and decline in their frequencies in patients, in response to Secukinumab was shown statistically significant (p-value: 0,0159) (fig. 4.17 D)

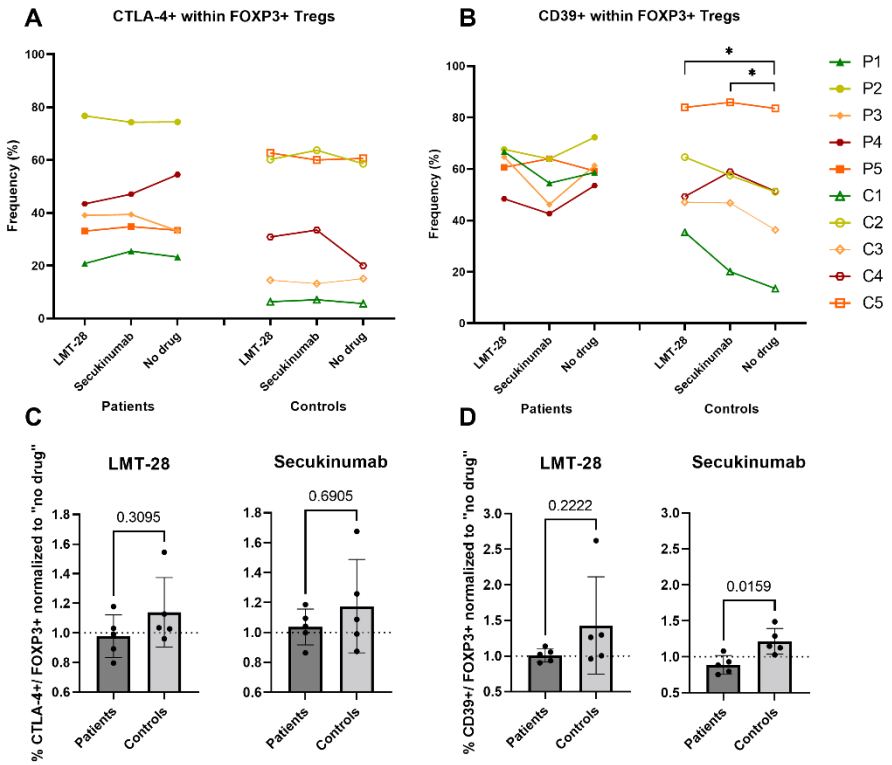

Fig 4.17 Frequencies of Tregs treated with LMT-28 and Secukinumab positive for the functional Treg markers A) CTLA-4 and B) CD39 as compared to non-treated "no drug" controls. Significant increase in the fraction of CD39+ Tregs was indicated for controls in response to both treatments (paired, one-way Anova Friedman test). Relative increase/decrease in the fractions of C) CTLA-4+ and D) CD39+ Tregs after treatments, as normalized to "no drug" controls from the same individuals. Significance difference in CD39+ Treg fraction in response to Secukinumab in patients and controls was observed (unpaired, non-parametric t test). Mean values are indicated by boxes, error bars show standard deviation, while the dotted line reflects the "no drug" baseline.

No significant effects of treatments were shown on the frequencies of FOXP3+ Tregs positive for the remaining markers CD31, CD45RA, HLA-DR and Helios (appendix VI fig.VIa) when compared to non-treated controls. When comparing the effect of treatments on patient and healthy control Tregs, significantly higher CD31+ Tregs were observed in LMT-28 cultures (appendix VI fig. VIb B). On average, healthy controls had higher frequencies of Tregs positive for the nine markers when compared to the non-treated controls both upon LMT-28 and Secukinumab treatment (fig. 4.16 D-F, fig. 4.17 C-D and appendix VI fig. VIb). The same trend was not observed in patients.

4.7 Gene expression analysis of patient and control cells after treatment with LMT-28 and Secukinumab

RNA from cultured PBMCs and Tregs was isolated, and the RNA concentrations estimated using Nanodrop, ranging between 7,3-146,78 ng/µL (mean: 43,5 ng/µL) for PBMCs and 16,39-171,43 (mean: 54,9 ng/µL) for Tregs. The purity of RNA was also assessed spectrophotometrically using 260/280 OD ratios, spanning 1,41-2,22 (mean: 1,82) for PBMCs and 1,45-2,13 (mean: 1,85) for Tregs.

4.7.1 Relative gene expression of T cell linage markers in treated and untreated PBMCs

SYBR green based qPCR assays were performed to assess the relative gene expression of T cell linage markers in PBMCs from 5 patients and 5 controls following culture with LMT-28 and Secukinumab. Specificity of the primers encoding: *FOXP3*, *RORγt*, *BCL6*, *EOMES*, *GATA3* and *TBET* was confirmed by the presence of a single peak in melting curve analyses after every run, further verified by gel electrolysis in a preliminary assay. Additionally, assay efficacy for cDNA inputs ranging 8,3 ng/µL-166 ng/µL was evaluated, showing a linear correlation between higher template concentrations and decrease in Ct values of the respective gene targets. Results from assay optimizations can be found in appendix VII. Mean Ct values for all six target genes spanned the range of 24,86-28,37 indicating a reliable amplification of the qPCR products.

Of particular interest were changes in *FOXP3* and *RORγt* expression, as their interrelation may indicate skewing in the Treg: Th17 ratio. Effect of the treatment on gene expression was analyzed as previously described (3.9.4). Generally, no trends regarding the effect of LMT-28 or Secukinumab on the expression of *FOXP3* or *RORγt* couth ld be observed (fig 4.6 A and B), as both upregulation and downregulation is seen in both patients and controls following treatment. As for *Rorγt* expression (fig. 4.6B), either up- or downregulation for the two treatments was seen in unison, in all individuals. Both genes were also relatively little expressed in non-activated cells “pre-culture”, yielding an almost significant difference in *FOXP3* (p-value: 0,0625) for both patients and controls. Paired, non-parametric t tests did not yield any significant differences when comparing LMT-28/no drug and Secukinumab/no drug samples within the same individuals in neither patients nor controls. No differential effect of

the respective drugs was seen on gene expression when comparing patients and control groups (fig 4.18D), although a trend towards lower expression of *RORγt* in LMT-28 treated healthy controls could be observed.

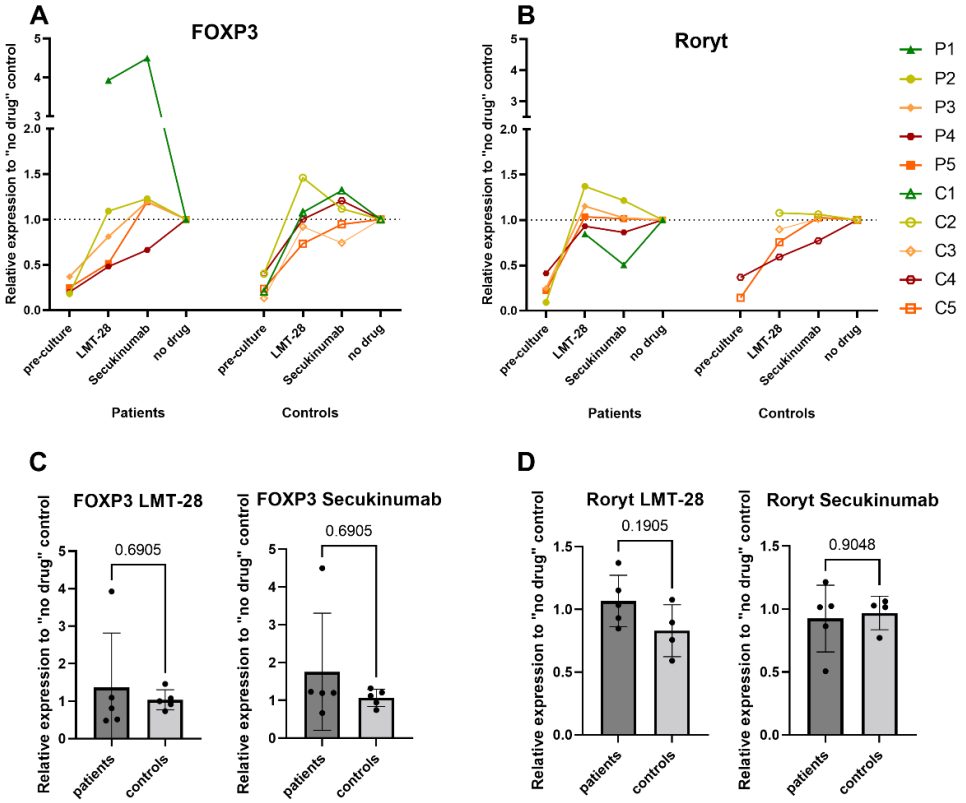

Figure 4.18 Relative changes in the expression of *FOXP3* and *Rorγt* after treatment with LMT-28 and Secukinumab, normalized to the non-treated control from the same individual, represented by a dotted line for A) *FOXP3* and B) *RORγt*. Samples from patients and matched controls are visualized in the same color, indicated in figure legend. Upregulation in gene expression is reflected by values higher than one on the y-axis, while the opposite shows downregulation. No effects of the treatments have been indicated for neither FOXP3, nor *Rorγt* (paired, non-parametric t tests). Comparison of C) *FOXP3* and D) *RORγt* expression between patient- and control groups, subjected to the same treatment. Mean values are indicated by boxes, while error bars show standard deviation. Statistical analyses (unpaired, non-parametric t tests) did not indicate differential effects of either drug on gene expression in the two groups. Samples with undetected values are shown in appendix XI

Expression of the other T linage markers: *BCL6*, *EOMES*, *GATA3* and *T-BET* shown in appendix VIII (fig. VIIIa), did not indicate any significant differences between treated and non-treated samples within individuals, neither among patients nor controls. Expression of *GATA3* and *T-bet* in treated samples from patient one showed a markable upregulation, as observed for *FOXP3*. Expression of *EOMES* in pre-culture samples from patients and controls was 20-80-fold higher when compared to activated, non-treated samples and gave a close-to significant p-value of 0.0625 for healthy controls. When comparing LMT-28 and Secukinumab-treated patient and control groups (appendix VIII fig 4. VIIIb), treated patients usually showed an equal or higher expression of *TBET*, *GATA3* and *EOMES* than the control group.

4.7.2 Relative gene expression of selected Treg markers in treated and untreated Tregs

TaqMan based qPCR assay was performed to assess the relative expression of Treg linage- and functional markers: *FOXP3*, *HELIOS*, *CTLA-4*, *ENTPD-1*, *ICOS* as well as *FASN* and *GPR15* from 4 patients and 4 controls following culture with LMT-28 and Secukinumab. Patient and control four were not included in the analysis due to limited cell material. Three conditions were evaluated for each individual patient and control: LMT-28- treated, Secukinumab-treated and a non-treated sample ("no drug" control). Mean Ct values for the seven target genes spanned the range of 25,01-28,13 indicating a reliable amplification of the targets. Results for *FOXP3*, *HELIOS*, *CTLA-4* can be found in fig. 4.19 while, *ENTPD-1*, *ICOS*, *FASN*, *GPR15* in fig. IX a and IX b (appendix IX)

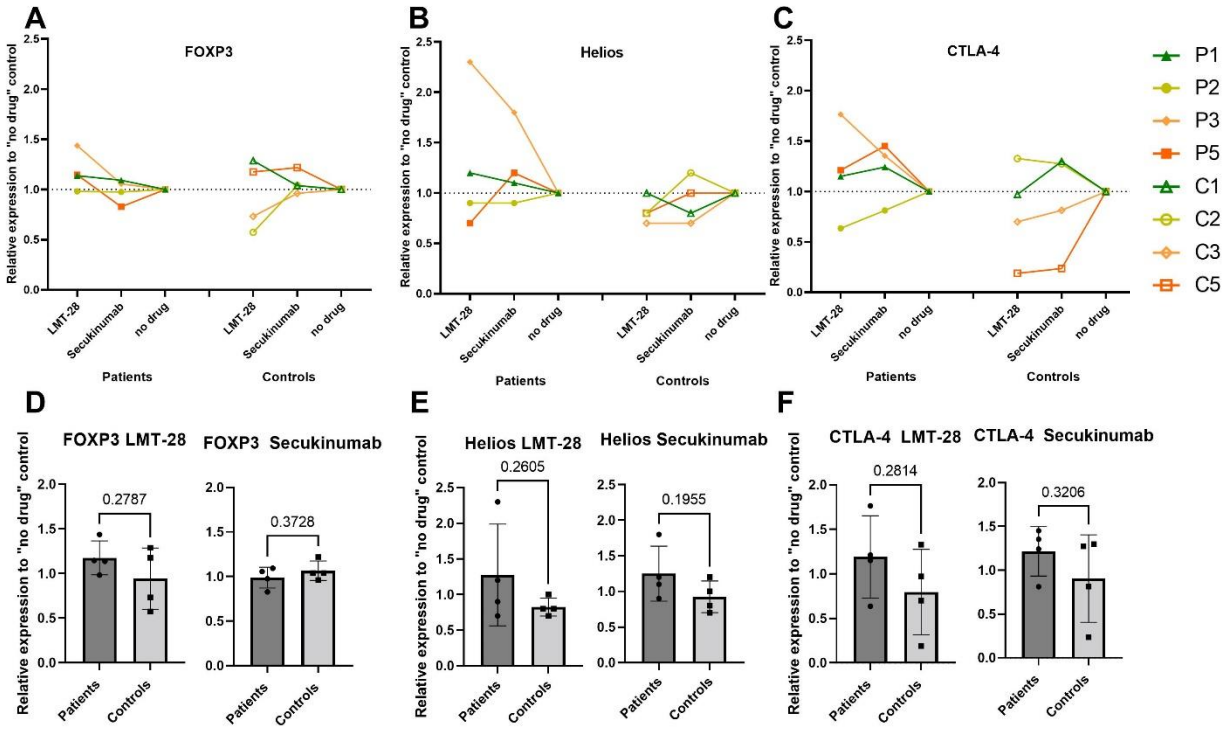

Figure 4.19 Relative changes in the expression of Treg markers after treatment with LMT-28 and Secukinumab, normalized to the non-treated control from the same individual, indicated by dotted lines for A) *FOXP3* B) *HELIOS* and C) *CTLA-4.* Samples from patients and matched controls are visualized in the same color, see figure legend. No clear trends with regards to the effect of the drugs can be indicated, as both up- and downregulation in seen for all three genes. Comparison of patient and healthy control groups and their expression of D) FOXP3, E) Helios or F) CTLA-4 following the same treatments. Mean values are indicated by boxes, while error bars show standard deviation.

Minimal changes on the expression of the two Treg linage markers: *FOXP3* (fig 4.19 A) and *HELIOS* (4.19 B) can be seen following treatment, spanning 0,5-1,5 fold of the expression in non-treated controls (except for patient 3 in 4.19 B). Up- and downregulation of all three targets

can be indicated, while the variation to "no drug" control is slightly more pronounced for *CTLA-4* (fig 4.19 C). Further, little correlation could be observed between increase or decrease in expression of *FOXP3/HELIOS* and the Treg-functional marker *CTLA-4* within individuals. Paired, non-parametric t tests did not yield any significant differences in A-C, when comparing LMT-28/no drug and Secukinumab/no drug samples within the same individuals for neither patients nor controls. Except for *FOXP3* following Secukinumab treatment (fig.4.19 D), a trend towards higher expression of all three targets can be indicated in patients' samples after both treatments, although no statistical significance was reached (fig. 4.19 D-F).

Relative expression of the other Tregs-genes: *FASN, GPR15, ICOS, ETNPD-1* seen in figure 4.IXa (appendix IX) showed somewhat less variation than the other targets. In the vast majority of both patient and control samples, similar or up-regulated expression can be seen following treatments (except healthy control samples in fig. IX A and C). No significant differences have been indicated of the drugs' effect when compared to non-treated samples (paired, non-parametric t tests), however close to significant differences in the expression of *FASN* and *ICOS* could be seen in LMT-28 treated patients compared to healthy controls (fig IXb A and C appendix IX) yielding p-values of 0,0271 and 0,062 respectively (paired, non-parametric t test).

4.7 Treg signature cytokines in cultured PBMCs and Tregs

Sandwich ELISA assays for TGF-β and IL-10 were utilized on cell culture supernatants to assess the immunsupressive function of Tregs in isolated cultures as well as in PBMCs.

4.7.1 Immunosuppressive cytokines produced by Tregs during expansion

Following the 14-day *in-vitro* expansion, functionality of Tregs from patients and healthy controls was confirmed by their ability to produce immunosuppressive cytokines. Concentrations of TGF-β and IL-10 in culture supernatants collected on the last day of expansion can be found in appendix 00. The most abundant cytokine, produced by all expanded Tregs was TGF-β (mean patients: 657,9 pg/mL, controls: 381,5 pg/mL). Concentrations of IL-10 (mean patients: 21,93 pg/mL controls: 14,22 pg/mL) was lower than of TGF-β and not detected in some samples analyzed (seen as dots on the x axis in appendix 00). As all expanded Tregs produced immunosuppressive cytokines, all were regarded functionable.

4.8 Levels of TGF-β and IL-10 in PBMCs and Tregs treated with LMT-28 and Secukinumab

TGF-β

Generally, considerably higher concentrations of TGF-β were detected in supernatants from PBMCs (mean: 322,7 pg/mL) than Treg cultures (mean: 170,1 pg/mL). Trends towards decreased levels of this cytokine were observed after Secukinumab treatment in all patient PBMCs (fig. 4.20 A) and nearly all patient Tregs (fig 4.20B) when compared to non-treated cells, however no significance was achieved (p-values: 0,125 and 0,25 respectively) (paired, non-parametric t tests). No similar trends were observed in cells from healthy controls. Lower levels of TGF-β in Secukinumab-treated patient Tregs almost reached significance when compared to healthy controls (p-value: 0,0635) (fig. 4.20 D)

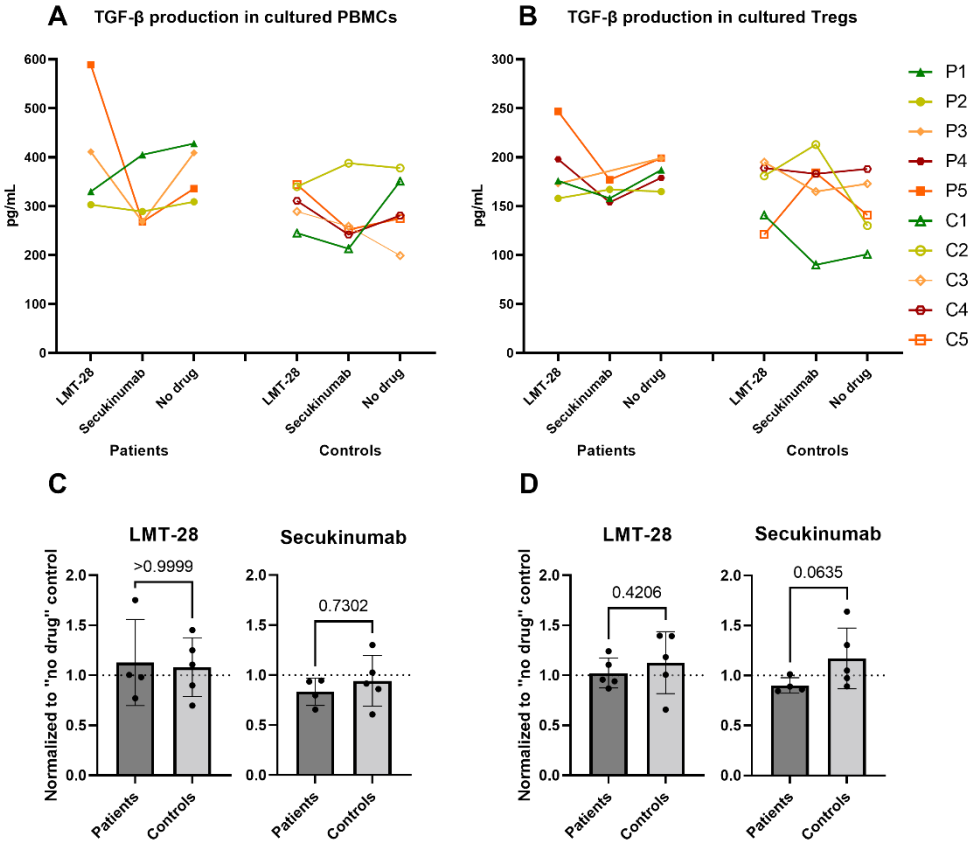

Figure 4.20 Levels of TGF-β detected in culture supernatants of LMT-28- and Secukinumab treated A) PBMCs and B) Tregs compared to non-treated "no drug" controls. The effect of the treatments was analyzed by multiple paired, non-parametric t tests, but no significance was achieved. Levels of TGF-β in treated C) PBMCs and D) Tregs, normalized to their respective "no drug" controls were used to compare the responses of patient and control groups. A close to significant value for Secukinumab-treated Tregs was shown implicating unpaired, non-parametric t test. Mean values are indicated by boxes, error bars show standard deviation, while the dotted line reflects the "no drug" baseline. Concentrations of TGF-β were not detected in supernatants from: patient four "no drug" PBMCs and patient five Secukinumab-treated Tregs.

IL-10

A high sensitivity ELISA kit was used to determine the concentrations of IL-10 in culture supernatants; however, the concentrations of this cytokine was still under the detectable limit (0,8-50 pg/mL) in most of the samples analysed. Supernatant samples in which the cytokine levels were detectable are shown in table 4.2.

Table 4.2 Concentrations of IL-10 (pg/mL) in cell culture supernatants of treated and non-treated PBMCs and Tregs from patients and healthy controls.

	Cultured PBMCs			Cultured Tregs		
	LMT-28	Secukinumab	No drug	LMT-28	Secukinumab	No drug
Patient 1	ND	ND	ND	ND	ND	1,010
Patient 2	ND	ND	ND	ND	ND	ND
Patient 3	0,906	ND	ND	ND	ND	ND
Patient 4	ND	ND	ND	ND	ND	ND
Patient 5	3,667	3,901	6,131	2,973	1,578	1,840
Control 1	ND	ND	ND	ND	ND	ND
Control 2	2,365	0,928	2,028	0,414	ND	ND
Control 3	0,845	ND	1,283	ND	ND	ND
Control 4	0,203	5,557	ND	ND	ND	ND
Control 5	6,840	5,426	4,972	2,880	3,013	3,206

ND= non-detectable

As only 22 out of 60 samples showed detectable IL-10 concentrations, statistical analysis determining the effect of treatments on Treg IL-10 production was not conducted.

5. Discussion

There is an instant urge to invent and improve treatment modalities for patients with autoimmune disorders, affecting millions of people worldwide. Importantly, optimised treatments should treat the cause, not only manage the symptoms. In the current project, we optimised methodology for *in vitro* studies of new potential targeted treatments for endocrine autoimmunity particularly focusing on T cells and the Tregs/Th17 balance. Cells from AAD-patients and healthy controls were then used to explore the effect of two drugs potentially affecting this T cell equilibrium, utilizing both real time monitoring and several endpoint-assays. The overall findings we present supports no major effect for the chosen drugs in *in vitro* cultures of PBMC or expanded Tregs. However, the functional marker CD39 within Tregs was modestly positively affected in controls but not patients for both drugs, and LMT-28 revealed small positive effects on the number of FOXP3+Tregs both within PBMC and Treg cultures in ADD patients. Tregs treated with LMT-28 also showed higher protein expression of the thymic recent emigrant marker CD31 in controls compared to patients, as well as higher levels of gene expression of the fatty acid synthase enzyme FASN in patients compared to controls. Since this is a preliminary study including only 5 patients and 5 controls, care must be taken when interpreting these findings.

Th17 cells have frequently been observed to be involved in pathogenicity of autoimmune disorders [151]. At the same time, reduced numbers or un-efficient Tregs are seen in autoimmune conditions [117] also in autoimmune polyendocrine syndromes where AAD is a frequent component [80, 120, 152, 153]. Notably, TGF-β is involved in inducing both these T cell subtypes[75], while IL-6 and IL-17A are involved in modulating the Treg/Th17 axis. The anti-IL17 monoclonal drug Secukinumab and the IL-6R inhibitor LMT-28 were chosen because they both have been shown to confer skewing of the Treg/Th17-axis towards Tregs.

The methodology chosen in this project is a combination of real time label-free monitoring of cell growth/behavior and multiple assays to measure how the drugs affect proliferation and functionality of the T cells. While the flow cytometry panel and parts of the qPCR techniques were available in house and the ELISA-assays were commercial ready-to-use kits, the use of the xCELLigence RTCA platform on primary T cell studies was new to the lab. It has not been explored to its full extent previously when investigating the literature, and therefore needed to be optimized and validated.

5.1 Optimize and investigate the utility of the xCELLigence RTCA platform for real time monitoring of T cells (in primary PBMC and Treg cultures)

The xCELLigence RTCA platform, allowing real-time study of cell behaviour during culture, was optimized for T cell studies. The impedance read-out generated by the biosystem is based on several physiological parameters (cell adherence, cell number and morphology) and thus circumvents the need for "unphysiological" (and often laborious) handling of cells connotated with labelling or staining, required by most conventional cell-based assays for cell viability or proliferation assessments. The continuous measurements also allow to detect transient responses to treatments missed by endpoint assays, aiding to pinpoint the exact timepoint at which the response is most pronounced. That information could be found useful when designing downstream functional assays that qualitatively assess the nature of any observed changes in cell behaviour.

Using xCELLigence, we optimized culturing conditions for the subsequent drug screening assays. The parameters chosen, were the ones yielding most pronounced CI values, as these were more sensitive to changes, and thus better reflects altered cell behaviour that may occur during treatment. The only exception was the chosen IL-2 concentration, where the highest CI peak corresponded to no IL-2 in the culture medium. Although not strictly required for initial activation (reflected by the CI values during the early hours of the assays), further T cell proliferation and survival is promoted by IL-2 [154]. In 96 h cultures on patient and control cells, the cytokine was used in concentrations based on previous experiences with PBMCs and Tregs cultures in the group.

The initial culturing optimizations also served as an orientation to what a CI profile for T cells looks like. Due to differences in cell size, morphology, adhesion- and migratory properties, CI graphs for different cell types usually have very different characteristics [142]. Adhesive cell lines which xCELLigence has been most widely used to study [142, 155-158], usually reach much higher CI values than what observed in our assays. Further, their proliferation is often indicated by a progressive CI increase following initial attachment, while compromise and cell death are explained by decrease in CI values, when these cells shrink and detach from the biosensor electrodes [142]. In the present study, the CI decreases dramatically after the CI activation peak; what this decline indicated is a matter of debate and was further discussed with the xCELLigence manufacturer. Cell death due to early reached confluence and lack of nutrients was deemed unlikely, given that even the lowest cell numbers in the cell titration experiment revealed the same CI reduction. Cell viability was later validated by flow cytometry

in subsequent drug screening assays, yielding satisfactory survival rates spanning 65-80%. A possible explanation could be that morphological changes promoting T cell-APC contact [14] during T cell activation induce a CI peak, while their subsequent retraction leads to the CI decrease observed. This hypothesis seems plausible, as similar xCELLigence curves have been shown in a study of T cell activation in a Jurkat cell line [147]. This underlines how interpretations of the CI curves should be done with caution (and regards to cell type studied), and that alterations to cell behaviour observed using xCELLigence should subsequently be validated by additional phenotypic and/or functional assays.

xCELLigence, in complement with flow cytometry, was followingly used for initial cytotoxicity screenings of LMT-28 and Secukinumab on PBMC and Treg cultures from healthy controls, aiming to determine the optimal concentrations of the drugs to be used in assays on patient and control cells. As cytotoxic effect of treatments with too high concentrations used would be expected to alter several aspects of T cell physiology including morphology, proliferation, and viability, we looked for distinctly altered CI profiles in treated cells compared to the "no drug" controls. Global assessment of CI graphs throughout 48-h of culture revealed no such indications. However, variable CI values during activation were observed, where the highest concentration for LMT-28 and two of the highest for Secukinumab revealed slightly lower peak CIs than the non-treated control, possibly indicating reduced or inhibited T cell activation [147]. We debated whether these were due to the mechanism of action of the drugs, a consequence of the drugs' possible cytotoxicity, or the drugs' alterations in cell-cell or cell-electrode attachments. For cells treated with the highest LMT-28 concentration 10 µM, the low peak CI in results from xCELLigence correlated with lower survival in flow cytometry assessment possibly suggesting cytotoxicity. In contrast, cultures with 0,3 µM and 0,1 µM Secukinumab showed higher percentages of live cells than the non-treated control, thereby indicating an unlikely negative effect on cell survival.

As we identified an increase in CI values after addition of fresh medium in some of the initial experiments with LMT-28 we wanted to incorporate the "final CI" values in the analysis pipeline. The hypothesis behind this was that this measure could be used as an indication of an increase in cell proliferation, which we subsequently validated using flow cytometry. Since no correlation was observed, most apparent by the discrepancy between final CI of 10 µM LMT-28 and the relatively low percentage of live cells in that sample, it was not deemed appropriate to use increased CI values to predict higher cell survival or cell numbers. In subsequent assays on patients and control cells we therefore chose to compare temporal changes in CI at after the

first- and second time drug treatment and interpreted them in a broader context, as reflection of changes to cell behaviour.

Since we did not see any larger deviations in cell behaviour/CI values regarding different drug concentration in xCELLigence data, we based our choice of concentrations on flow cytometry data for both drugs used. Lower fractions of live cells and Tregs in treated samples have been observed, an undesirable effect when attempting to promote the Treg population. It is however important to pinpoint that we could not observe trends or dose-dependency with the effects to increasing drug concentrations, which would be indicative of cell responsiveness to the treatments. It is possible that even the highest concentrations of treatments used here, were too low to induce changes in cell behaviour needed to be reflected using xCELLigence. Additionally, we suspect that because cells were treated and activated at the same time, any immediate effects of the drugs on cell behaviour could have been "hidden" under the prominent activation peak (which could then possibly explain the variable peak CI values observed). Since we were interested to alter T cell differentiation and the Treg/Th17 balance, events dictated during T cell activation, it is possible that addition of drugs to cells could have been conducted at a timepoint prior to the actual activation cocktail, to yield a better reflection of the drugs' impact on CI values during activation. During assays on patient and healthy control cells, the cells were treated twice; first time upon cell culture, followed by repeated addition of fresh medium with the same drug concentration after 48 h hours, to keep the concentration of the drugs' constant.

5.2 Utility of xCELLigence for real-time monitoring of immune cells

When implementing xCELLigence on non-adherent immune cells like T cells, a pre-coat must be used to facilitate cell attachment to the E-plate electrodes [159, 160]. The nature and strength of the binding between that pre-coating agent and the cells seeded, reflects the changes in CI detected by xCELLigence. In our assays we used goat anti-mouse IgG as the pre-coat, which subsequently binds functional antibodies used to activate the T cells: mouse anti-human CD3 and mouse anti-human CD28. This likely explains why the most prominent increase in CI is seen during T cell activation and subsequently why the increase in CI did not reflect proliferation, or CI decrease, cell death. These are the parameters we were hoping to observe during initial cytotoxicity screenings, and it is possible another pre-coating agent could have been used for these experiments. A possible alternative would be fibronectin fragments as used on Jurkat cells by Obr et.al [159], an extracellular matrix protein serving as a scaffold to "halt" migrating lymphocytes. The ability to use pre-coating agents to mediate the attachment, may

be of value to use xCELLigence in the studies of immune cells, many of which are non-adherent. Additionally, the biosensor has in the recent years frequently been employed in cancer immunotherapy research, to test the potency of immune mediated killing of both solid and haematological cancer cells [161-163].

As few changes to cell behaviour in treated and non-treated cells were observed in our drug screening assays compared to what has been indicated in existing literature [164, 165], we found it difficult to interpret the meaning of changes to CI in LMT-28- treated patients PBMCs and Tregs. To use this method to its full potential, further optimization would be required.

5.3 In vitro treatment with LMT-28 and Secukinumab did not alter cell survival or proliferation of cultured PBMC or Tregs

Flow cytometry analysis was used to investigate whether *in vitro* treatments with LMT-28 and Secukinumab influenced cell viability and -proliferation. No significant differences in the live cell fractions were observed for either of the drugs when compared to non-treated cells, indicating that the drugs did not lead to undesirable cell death in neither patient nor healthy control cells. We did however observe noticeable cell death (viability <20%) in Treg cultures from several individual patients and controls. These challenges were unlikely related to the drugs as similar live cell fractions were observed in both treated and non-treated cells. It is possible that cells from some individuals were more likely to experience exhaustion related to repeated stimulation, first during expansion and second during culture.

Proliferation index values generated from flow cytometry data, indicated that cells treated with both LMT-28 and Secukinumab were proliferating very similarly to non-treated cells, with close to identical PI values across all three conditions for most patients and controls. As no differences in cell survival and proliferation were indicated in treated samples by flow data, we believe that the altered cell behaviour reflected by xCELLigence does not reflect these parameters well. In samples from two outlies; “no drug” sample from patient two and LMT-28 sample from patient one, fewer cells made up the dividing population, thus likely “overstating” the mean of the undergone cell divisions. Overall, the cells were expanding well, with models indicating up to 7 generations, with no differences in the rate of cell division shown for patients and controls. Despite that only 5 out of 10 Treg samples had adequate fractions of live cells to be used to model PI values, no visible deviations in cell proliferation in cells cultured with drugs were observed. Although attempting to modulate T cell activation, the two drugs did not give any indications to negatively influence the cells’ subsequent proliferation.

5.4 The effect of LMT-28 on *in vitro* PBMC and Tregs cultures

LMT-28 targeting the gp130 signalling subunit of the IL-6R, is the first synthetic IL-6R inhibitor developed and has, to date, only been studied using *in vitro* and murine models [137] (no clinical trials have been reported in EudraCT or in ClinicalTrials.gov). It has been shown to reduce IL-6 induced phosphorylation and activation of STAT3 by 90% in luciferase assays [137], and to have a diminishing effect on autoinflammatory collagen-induced arthritis and pancreatitis in mice models it has been tested on [137]. It is therefore a promising alternative to anti IL-6/anti-IL-6R antibody (Ab) therapeutics, used in treatments of IL-6 driven autoimmune and autoinflammatory diseases including RA, where dysregulated Th17/Treg balance has been indicated [96]. *In vivo* inhibition of IL-6R with tocilizumab has been suggested to correct the Th17/Treg imbalance as found in peripheral blood of RA patients [96].

One of our main hypotheses was that LMT-28, similarly to tocilizumab, could have a positive effect on promoting Treg numbers by skewing of the Th17/Treg axis. To test this, we assessed the FOXP3+ Treg cell fractions in both PBMCs and Treg cultures by flow cytometry. Although modest, an increase in FOXP3+ Tregs frequencies within the CD4+ T cells in PBMCs was observed for almost all patients in LMT-28 cultures however no significance was achieved. Similar modest, but significant, increase in the FOXP3+ Tregs population within the CD4+ T cells in Treg cultures was observed for AAD patients as compared to non-treated cells, an effect not indicated in healthy controls. This is however complicated by the fact that no effect of LMT-28 was observed regarding cell numbers for the expanded Tregs in culture, which could be due to inaccurate estimation of cell numbers. For a more accurate assessment of cell numbers in flow analysis, counting beads could have been used. LMT-28 did not affect the numbers of other cell types present in PBMCs: monocytes, B-cells and CD8+ T cells, as indicated by flow cytometry using their respective markers CD14, CD20 and CD8. This further implies no undesired alterations in the frequencies of other immune cell populations. Similarly, no effects of the drug were observed for the gene expression of the linage transcription factors for T cell subpopulations in PBMCs: *FOXP3, RORγt, GATA3, T-BET, BCL-6 or EOMES*. Of note, no differences were observed in the expression of the Treg and Th17 markers, *FOXP3* and *RORγt*, in treated and non-treated samples, and neither between patients nor controls. As such, our data does not indicate that skewing of the Treg/Th17 axis has been achieved.

Ex vivo Tregs highly expressing the gp130 have been suggested to possess reduced suppressive capacity when compared to gp130 negative Tregs [166], indicated to be restored following culture with LMT-28 [166]. We therefore aimed to evaluate whether LMT-28 would lead to

improved function of Tregs from AAD patients. Although the functional behaviour was not assessed directly by coculture of Tregs with Teffs like in the previously mentioned study, we assessed the expression of Treg functional protein markers both on the protein and RNA level. None of the functional markers CD25, CTLA-4, HLA-DR nor Helios revealed any differences in LMT-28 treated cells when compared to non-treated cells. Although not significantly higher than in non-treated cultures, Tregs from patients showed an upregulation in *FASN* in LMT-28 cultures, found significantly more expressed than in healthy controls Tregs. *FASN* encodes fatty acid synthase (FAS) involved in fatty acid synthesis. It has previously been shown that Tregs require fatty acid metabolism to a greater extent, while Th17 cells are more reliant on glycolysis [81]. Our results indicate that this metabolism is upregulated within Tregs compared to "normal circumstances", although it's not clear to us what this might imply. Increase in the fraction of CD31+ expressing Tregs in healthy controls was further observed in LMT-28 treated cultures, however the difference was not significant when compared to non-treated cells, thus not indicative to be an effect of the drug. We did however observe a significant difference for this marker when comparing LMT-28 treated patients and healthy controls. As CD31 is marker of Tregs recently emigrated from the thymus [83], it is difficult to establish why this difference is observed in Tregs expanded in culture.

We also observed a significant increase in the protein expression levels of CD39 (ENTPD-1) in LMT-28 cultured Tregs from healthy controls, not observed in Tregs from AAD patients. Enhanced expression of this ATP to AMP converting enzyme has intriguingly also been indicated in Tregs of RA patients following tocilizumab treatment [167]. As this ectoenzyme has been indicated to have a role in the suppressive function of Tregs [168], it could potentially indicate that LMT-28 has a positive effect on the function of Tregs from healthy controls, which fails in AAD patients. However, higher expression level of the same molecule was not verified by qPCR analysis, revealing a discrepancy between the protein and RNA levels. As cell death was generally observed in Treg cultures it is difficult to assess whether the observed difference is reliable or if this finding is an artifact.

5.5 The effect of Secukinumab on *in vitro* PBMC and Tregs cultures

The IL-17A targeting antibody Secukinumab has been evaluated in the treatments of multiple autoimmune diseases including psoriasis, RA, and psoriatic arthritis, though to be driven by dysregulated Th17 cells [169]. Since there is a lack on in depth immune phenotypic studies on AAD in the literature, it is not known whether Th17 cells are also involved in pathological events of AAD. However, inhibition of IL-17A with Secukinumab has been indicated to restore

TGF-β expression and secretion of impaired psoriatic Tregs [127], cytokine crucial not only for Treg suppressive function, but also for the maintenance of *FOXP3* expression in the periphery [75] and the generation of induced Tregs [39]. It is therefore a potential modulator of the Treg/Th17 axis, of promise in promoting the Treg suppressive mechanisms and their numbers.

In this study, we did not observe increased TGF-β levels in supernatants of PBMC and Tregs cultured with Secukinumab, neither in cells from AAD patients, nor healthy controls. Followingly, flow cytometry analysis did not reveal any significant differences in the numbers of FOXP3+ Tregs in PBMCs or Tregs cultured with the drug when compared to non-treated cells, in line with no changes observed in the *FOXP3* expression, evaluated by qPCR. Subsequently, our data does not correlate with the Treg promoting effects observed in patients treated with Secukinumab, where both increased fractions of Tregs and increase in TGF-β production by Tregs have been indicated [127]. Since no effect of the drug could either be observed on the expression of Th17 linage marker *RORγt*, our data does not indicate that the balance between Tregs/Th17 has been altered.

Subsequently to assess whether Secukinumab potentiates the suppressive function of Tregs, functional Treg markers have been evaluated both on the protein and RNA level. No differences in the expression of the vast majority of markers have been found. The only exception was the protein expression of CD39 within FOXP3+ Tregs, which was higher in Secukinumab-treated healthy control cells, but not in patients, results not replicated by qPCR. As the same observation was indicated for LMT-28 treated cells, the relevance of its biology is the same as priorly discussed.

5.6 Conclusions

In summary, we have optimized the xCELLigence platform for real-time monitoring of T cell behaviour, and subsequently used it with established end-point assays for preliminary *in vitro* drug screenings on T cells and Tregs from AAD patients. Overall, real-time data suggested few alterations to cell behaviour in cultures with LMT-28 and Secukinumab, subsequently validated by flow cytometry, where no effect of the drugs on cell viability or proliferation were observed when compared to non-treated cells. A modest increase in the numbers of Tregs was indicated following LMT-28 treatment in AAD patients, however this finding was not supported at the RNA level, where no differences in *FOXP3* expression were seen for either of the drugs. Furthermore, no significant differences in the expression of the Th17 linage marker

Rorγt were observed, indicating that the Treg/Th17 balance was not altered by the *in vitro* treatments, in neither patients nor healthy controls

Regarding function, we did not observe many effects of treatments, indicated by the lack of changes in protein expression of the Treg markers: CD25, CTLA-4, HLA-DR as well as ICOS at the RNA level. Followingly, Treg production of the immunosuppressive cytokine TGF-β was not seen affected by the treatments. However, a significant increase in CD39+ Tregs following both treatments was observed in the healthy control population. Similar was not seen after either of the treatments in patients' cells, possibly suggesting that Tregs from patients failed to respond to this potentiating alteration. Although not replicated on the RNA level, this differential response could be an interesting lead to follow in subsequent studies involving more patients.

5.7 Limitations

Although relatively extensive, the assays employed in this project also proved to be time-consuming, restricting the number of patients and healthy controls feasible to include in this project, hence reducing the power of our statistical analyses. Due to the rarity of AAD and low volumes of blood that can be sampled from patients at a time, the access of PBMCs and Tregs from patients is limited. The cryopreservation step further likely leads to cell loss, and for some patients the number of cells retrieved after magnetic dead cell removal was too low be cultured for both xCELLigence RTCA and flow cytometry analyses. In these cases, culture for flow cytometry was prioritized.

External stressors related to freezing, thawing, and washing of cell samples might also affect cell viability, which we observed was variable in cell cultures from different individuals. Low viability was observed in Treg cultures in both treated and non-treated cultures, possibly due to exhaustion, which might be a reason to suspect that they did not respond optimally to drug treatments. Gene expression results obtained by qPCR from cultured cells where low live cell fraction was observed may therefore be less reliable. Although the Ct values obtained suggested a reliable amplification, the quality of RNA was only assessed spectrophotometrically, where measurement of RIN values using Tape Station would have been a preferred method. This was not performed due to limited availability of the kits required.

In this project we used relative gene expression of the different T cell linage markers: *FOXP3, RORγt, GATA3, T-BET*, *BCL-6* and *EOMES* on PBMCs to indicate whether drug treatments altered the Treg/Th17 cell balance, as well as the other T cell subsets. However, expression of

these transcription factors is not strictly restricted to CD4+ T cells, exemplified by FOXP3, which has been reported to also be expressed by minor populations of CD8+ T cells and B cells in PBMCs from RA patients [170, 171]. The linage transcription factors can also be found co-expressed in CD4+ T cells [172]. For a more reliable indication of the different linages, flow cytometry analysis could have been used. This would however require establishment of a new antibody panel needed to be optimized for intracellular targets, which was not feasible in this project.

Lastly, glucocorticoid replacements used to medicate AAD patients work as immunosuppressants. Since we do not know whether the patients have taken their medication prior to blood sampling, the responses of isolated immune cells to *in vitro* drug screenings may have been affected.

5.8 Future perspectives

Great efforts have been made to understand the underlying causes of AAD, but there is currently still a lack of in-depth immunophenotypic knowledge to develop targeted therapies. Recent technological advances may be used to facilitate their discoveries, exemplified by single-cell sequencing which can be used to define differentially expressed genes in cells that represent a small population like Tregs. Treg transcriptomes in AAD patients could then be compared to healthy controls, and upregulated/downregulated genes and their pathways potentially serve as novel therapy targets. Subsequent functional studies would then be needed to evaluate potential Treg dysfunctions, for instance by performing *in vitro* suppression assays, by which activated Tregs and Teffs are cocultered, and proliferation of Teffs is assessed using flow cytometry to determine Treg suppressiveness [171]. Furthering of the understanding of the Treg biology, what contributes to their destabilization and dysregulation in autoimmunity will certainly bring many breakthroughs and hopefully also novel therapies to better the quality of life of AAD patients

References

1. Rogatsky, I. and K. Adelman, *Preparing the first responders: building the inflammatory transcriptome from the ground up.* Molecular cell, 2014. **54**(2): p. 245-254.
2. Medzhitov, R. and C.J. Janeway, *Advances in immunology: Innate immunity.* The New England journal of medicine, 2000. **343**(5): p. 338-344.
3. Janeway, C., *Immunobiology 5 : the immune system in health and disease*, in *Immunobiology 5*. 2001, Garland Pub: Place of publication not identified.
4. Schwartz, R.H., *T-Lymphocyte Recognition of Antigen in Association with Gene Products of the Major Histocompatibility Complex.* Annual Review of Immunology, 1985. **3**(1): p. 237-261.
5. Marshall, J.S., et al., *An introduction to immunology and immunopathology.* Allergy, Asthma & Clinical Immunology, 2018. **14**(2): p. 49.
6. Zúñiga-Pflücker, J.C. and M.J. Lenardo, *Regulation of thymocyte development from immature progenitors.* Curr Opin Immunol, 1996. **8**(2): p. 215-24.
7. Klein, L., et al., *Positive and negative selection of the T cell repertoire: what thymocytes see (and don't see).* Nature Reviews Immunology, 2014. **14**(6): p. 377-391.
8. Anderson, M.S., et al., *Projection of an immunological self shadow within the thymus by the aire protein.* Science, 2002. **298**(5597): p. 1395-401.
9. Malchow, S., et al., *Aire Enforces Immune Tolerance by Directing Autoreactive T Cells into the Regulatory T Cell Lineage.* Immunity, 2016. **44**(5): p. 1102-1113.
10. Cain, J.A. and G.S. Deepe, Jr., *Interleukin-12 neutralization alters lung inflammation and leukocyte expression of CD80, CD86, and major histocompatibility complex class II in mice infected with Histoplasma capsulatum.* Infect Immun, 2000. **68**(4): p. 2069-76.
11. June, C.H., et al., *T-cell proliferation involving the CD28 pathway is associated with cyclosporine-resistant interleukin 2 gene expression.* Mol Cell Biol, 1987. **7**(12): p. 4472-81.
12. Boyman, O. and J. Sprent, *The role of interleukin-2 during homeostasis and activation of the immune system.* Nature Reviews Immunology, 2012. **12**(3): p. 180-190.
13. Aslaksen, S., S. Aslaksen, and i. Universitetet i Bergen Klinisk, *Functional characterization of genetic risk factors in autoimmune Addison's disease*. 2020, University of Bergen: Bergen, Norway.
14. Comrie, W.A. and J.K. Burkhardt, *Action and Traction: Cytoskeletal Control of Receptor Triggering at the Immunological Synapse.* Frontiers in Immunology, 2016. **7**.
15. Luckheeram, R.V., et al., *CD4$^+$T cells: differentiation and functions.* Clinical & developmental immunology, 2012. **2012**: p. 925135-925135.
16. Zhu, J., H. Yamane, and W.E. Paul, *Differentiation of effector CD4 T cell populations (*).* Annual review of immunology, 2010. **28**: p. 445-489.
17. Sakaguchi, S., et al., *Regulatory T Cells and Immune Tolerance.* Cell, 2008. **133**(5): p. 775-787.
18. Matos, T.R., et al., *Maturation and Phenotypic Heterogeneity of Human CD4+ Regulatory T Cells From Birth to Adulthood and After Allogeneic Stem Cell Transplantation.* Frontiers in Immunology, 2021. **11**.
19. Sakaguchi, S., et al., *Immunologic self-tolerance maintained by activated T cells expressing IL-2 receptor alpha-chains (CD25). Breakdown of a single mechanism of self-tolerance causes various autoimmune diseases.* J Immunol, 1995. **155**(3): p. 1151-64.
20. Sakaguchi, S., et al., *Organ-specific autoimmune diseases induced in mice by elimination of T cell subset. I. Evidence for the active participation of T cells in natural self-tolerance; deficit of a T cell subset as a possible cause of autoimmune disease.* Journal of Experimental Medicine, 1985. **161**(1): p. 72-87.

21. Sakaguchi, S., T. Takahashi, and Y. Nishizuka, *Study on cellular events in post-thymectomy autoimmune oophoritis in mice. II. Requirement of Lyt-1 cells in normal female mice for the prevention of oophoritis.* Journal of Experimental Medicine, 1982. **156**(6): p. 1577-1586.
22. Fontenot, J.D., M.A. Gavin, and A.Y. Rudensky, *Foxp3 programs the development and function of CD4+CD25+ regulatory T cells.* Nat Immunol, 2003. **4**(4): p. 330-6.
23. Hori, S., T. Nomura, and S. Sakaguchi, *Control of Regulatory T Cell Development by the Transcription Factor Foxp3.* Science, 2003. **299**(5609): p. 1057-1061.
24. Liu , W., et al., *CD127 expression inversely correlates with FoxP3 and suppressive function of human CD4+ T reg cells.* Journal of Experimental Medicine, 2006. **203**(7): p. 1701-1711.
25. Maloy, K.J. and F. Powrie, *Regulatory T cells in the control of immune pathology.* Nature Immunology, 2001. **2**(9): p. 816-822.
26. Hsieh, C.-S., H.-M. Lee, and C.-W.J. Lio, *Selection of regulatory T cells in the thymus.* Nat Rev Immunol, 2012. **12**(3): p. 157-167.
27. Jordan, M.S., et al., *Thymic selection of CD4+CD25+ regulatory T cells induced by an agonist self-peptide.* Nat Immunol, 2001. **2**(4): p. 301-6.
28. Apostolou, I., et al., *Origin of regulatory T cells with known specificity for antigen.* Nat Immunol, 2002. **3**(8): p. 756-63.
29. Singer, A., et al., *CD28 costimulation of developing thymocytes induces Foxp3 expression and regulatory T cell differentiation independently of interleukin 2.* Nat Immunol, 2005. **6**(2): p. 152-162.
30. Burchill, M.A., et al., *IL-2 Receptor beta-Dependent STAT5 Activation Is Required for the Development of Foxp3+ Regulatory T Cells.* J Immunol, 2007. **178**(1): p. 280-290.
31. Lio, C.W. and C.S. Hsieh, *A two-step process for thymic regulatory T cell development.* Immunity, 2008. **28**(1): p. 100-11.
32. Chinen, T., et al., *An essential role for the IL-2 receptor in Treg cell function.* Nature immunology, 2016. **17**(11): p. 1322-1333.
33. Li, J., et al., *DNA demethylation switches the drivers of Foxp3 expression to maintain regulatory T cell identity.* bioRxiv, 2020: p. 2020.12.16.423137.
34. Yadav, M., S. Stephan, and J.A. Bluestone, *Peripherally induced tregs - role in immune homeostasis and autoimmunity.* Front Immunol, 2013. **4**: p. 232.
35. Chen, W., et al., *Conversion of peripheral CD4+CD25- naive T cells to CD4+CD25+ regulatory T cells by TGF-beta induction of transcription factor Foxp3.* J Exp Med, 2003. **198**(12): p. 1875-86.
36. Gottschalk, R.A., E. Corse, and J.P. Allison, *TCR ligand density and affinity determine peripheral induction of Foxp3 in vivo.* J Exp Med, 2010. **207**(8): p. 1701-11.
37. Chen, Q., et al., *IL-2 controls the stability of Foxp3 expression in TGF-beta-induced Foxp3+ T cells in vivo.* J Immunol, 2011. **186**(11): p. 6329-37.
38. Hsu, P., et al., *IL-10 Potentiates Differentiation of Human Induced Regulatory T Cells via STAT3 and Foxo1.* The Journal of Immunology, 2015. **195**(8): p. 3665.
39. Zheng, S.G., *The Critical Role of TGF-beta1 in the Development of Induced Foxp3+ Regulatory T Cells.* International journal of clinical and experimental medicine, 2008. **1**(3): p. 192-202.
40. Takimoto, T., et al., *Smad2 and Smad3 are redundantly essential for the TGF-beta-mediated regulation of regulatory T plasticity and Th1 development.* J Immunol, 2010. **185**(2): p. 842-855.
41. Tone, Y., et al., *Smad3 and NFAT cooperate to induce Foxp3 expression through its enhancer.* Nature Immunology, 2008. **9**(2): p. 194-202.
42. Fantini, M.C., et al., *Cutting edge: TGF-beta induces a regulatory phenotype in CD4+CD25- T cells through Foxp3 induction and down-regulation of Smad7.* J Immunol, 2004. **172**(9): p. 5149-53.

43. Josefowicz, S.Z., C.B. Wilson, and A.Y. Rudensky, *Cutting Edge: TCR Stimulation Is Sufficient for Induction of Foxp3 Expression in the Absence of DNA Methyltransferase 1.* The Journal of Immunology, 2009. **182**(11): p. 6648.
44. Round, J.L. and S.K. Mazmanian, *Inducible Foxp3⁺ regulatory T-cell development by a commensal bacterium of the intestinal microbiota.* Proc Natl Acad Sci U S A, 2010. **107**(27): p. 12204-12209.
45. Curotto de Lafaille, M.A. and J.J. Lafaille, *Natural and Adaptive Foxp3 + Regulatory T Cells: More of the Same or a Division of Labor?* Immunity, 2009. **30**(5): p. 626-635.
46. Thornton, A.M., et al., *Expression of Helios, an Ikaros transcription factor family member, differentiates thymic-derived from peripherally induced Foxp3+ T regulatory cells.* J Immunol, 2010. **184**(7): p. 3433-41.
47. Yadav, M., et al., *Neuropilin-1 distinguishes natural and inducible regulatory T cells among regulatory T cell subsets in vivo.* J Exp Med, 2012. **209**(10): p. 1713-22, s1-19.
48. Hill, J.A., et al., *Foxp3 Transcription-Factor-Dependent and -Independent Regulation of the Regulatory T Cell Transcriptional Signature.* Immunity, 2007. **27**(5): p. 786-800.
49. Schmidt, A., N. Oberle, and P. Krammer, *Molecular Mechanisms of Treg-Mediated T Cell Suppression.* Frontiers in Immunology, 2012. **3**.
50. Yamaguchi, T., et al., *Construction of self-recognizing regulatory T cells from conventional T cells by controlling CTLA-4 and IL-2 expression.* Proceedings of the National Academy of Sciences, 2013. **110**(23): p. E2116-E2125.
51. Sakaguchi, S., et al., *Foxp3+ CD25+ CD4+ natural regulatory T cells in dominant self-tolerance and autoimmune disease.* Immunol Rev, 2006. **212**: p. 8-27.
52. Papiernik, M., et al., *Regulatory CD4 T cells: expression of IL-2R alpha chain, resistance to clonal deletion and IL-2 dependency.* Int Immunol, 1998. **10**(4): p. 371-8.
53. O'Gorman, W.E., et al., *The initial phase of an immune response functions to activate regulatory T cells.* J Immunol, 2009. **183**(1): p. 332-9.
54. Pandiyan, P., et al., *CD4+CD25+Foxp3+ regulatory T cells induce cytokine deprivation-mediated apoptosis of effector CD4+ T cells.* Nat Immunol, 2007. **8**(12): p. 1353-62.
55. Krummel, M.F. and J.P. Allison, *CD28 and CTLA-4 have opposing effects on the response of T cells to stimulation.* Journal of Experimental Medicine, 1995. **182**(2): p. 459-465.
56. Wu, Y., et al., *FOXP3 Controls Regulatory T Cell Function through Cooperation with NFAT.* Cell, 2006. **126**(2): p. 375-387.
57. Gavin, M.A., et al., *Foxp3-dependent programme of regulatory T-cell differentiation.* Nature, 2007. **445**(7129): p. 771-775.
58. Perkins, D., et al., *Regulation of CTLA-4 expression during T cell activation.* The Journal of Immunology, 1996. **156**(11): p. 4154.
59. van der Merwe, P.A., et al., *CD80 (B7-1) Binds Both CD28 and CTLA-4 with a Low Affinity and Very Fast Kinetics.* Journal of Experimental Medicine, 1997. **185**(3): p. 393-404.
60. Thompson, C.B. and J.P. Allison, *The Emerging Role of CTLA-4 as an Immune Attenuator.* Immunity, 1997. **7**(4): p. 445-450.
61. Marengère, L.E.M., et al., *Regulation of T Cell Receptor Signaling by Tyrosine Phosphatase SYP Association with CTLA-4.* Science, 1996. **272**(5265): p. 1170-1173.
62. Onishi, Y., et al., *Foxp3+ natural regulatory T cells preferentially form aggregates on dendritic cells in vitro and actively inhibit their maturation.* Proc Natl Acad Sci U S A, 2008. **105**(29): p. 10113-8.
63. Qureshi, O.S., et al., *Trans-Endocytosis of CD80 and CD86: A Molecular Basis for the Cell-Extrinsic Function of CTLA-4.* Science, 2011. **332**(6029): p. 600-603.
64. Wing, K., et al., *CTLA-4 control over Foxp3+ regulatory T cell function.* Science, 2008. **322**(5899): p. 271-5.
65. Kuehn, H.S., et al., *Immune dysregulation in human subjects with heterozygous germline mutations in CTLA4.* Science, 2014. **345**(6204): p. 1623-1627.

66. Caridade, M., L. Graca, and R. Ribeiro, *Mechanisms Underlying CD4+ Treg Immune Regulation in the Adult: From Experiments to Models.* Frontiers in Immunology, 2013. **4**.
67. Deaglio, S., et al., *Adenosine generation catalyzed by CD39 and CD73 expressed on regulatory T cells mediates immune suppression.* J Exp Med, 2007. **204**(6): p. 1257-65.
68. Jarvis, L.B., et al., *Therapeutically expanded human regulatory T-cells are super-suppressive due to HIF1A induced expression of CD73.* Communications Biology, 2021. **4**(1): p. 1186.
69. Fletcher, J.M., et al., *CD39+Foxp3+ regulatory T Cells suppress pathogenic Th17 cells and are impaired in multiple sclerosis.* J Immunol, 2009. **183**(11): p. 7602-10.
70. Han, L., et al., *Phenotypical analysis of ectoenzymes CD39/CD73 and adenosine receptor 2A in CD4(+) CD25(high) Foxp3(+) regulatory T-cells in psoriasis.* Australas J Dermatol, 2018. **59**(1): p. e31-e38.
71. Ranges, G.E., et al., *Inhibition of cytotoxic T cell development by transforming growth factor beta and reversal by recombinant tumor necrosis factor alpha.* Journal of Experimental Medicine, 1987. **166**(4): p. 991-998.
72. Gilbert, K.M., et al., *Transforming growth factor-ß1 induces antigen-specific unresponsiveness in naive t cells.* Immunological investigations, 1997. **26**(4): p. 459-472.
73. Collison, L.W., et al., *The inhibitory cytokine IL-35 contributes to regulatory T-cell function.* Nature, 2007. **450**(7169): p. 566-569.
74. Saraiva, M., P. Vieira, and A. O'Garra, *Biology and therapeutic potential of interleukin-10.* Journal of Experimental Medicine, 2019. **217**(1).
75. Marie , J.C., et al., *TGF-ß1 maintains suppressor function and Foxp3 expression in CD4+CD25+ regulatory T cells.* Journal of Experimental Medicine, 2005. **201**(7): p. 1061-1067.
76. Chaudhry, A., et al., *Interleukin-10 Signaling in Regulatory T Cells Is Required for Suppression of Th17 Cell-Mediated Inflammation.* Immunity, 2011. **34**(4): p. 566-578.
77. Kochetkova, I., et al., *IL-35 Stimulation of CD39⁺ Regulatory T Cells Confers Protection against Collagen II-Induced Arthritis via the Production of IL-10.* The Journal of Immunology, 2010. **184**(12): p. 7144.
78. Baecher-Allan, C., E. Wolf, and D.A. Hafler, *MHC class II expression identifies functionally distinct human regulatory T cells.* J Immunol, 2006. **176**(8): p. 4622-31.
79. Li, D.-Y. and X.-Z. Xiong, *ICOS+ Tregs: A Functional Subset of Tregs in Immune Diseases.* Frontiers in Immunology, 2020. **11**.
80. Berger, A.H., et al., *Transcriptional Changes in Regulatory T Cells From Patients With Autoimmune Polyendocrine Syndrome Type 1 Suggest Functional Impairment of Lipid Metabolism and Gut Homing.* Front Immunol, 2021. **12**: p. 722860.
81. Cluxton, D., et al., *Differential Regulation of Human Treg and Th17 Cells by Fatty Acid Synthesis and Glycolysis.* Frontiers in Immunology, 2019. **10**.
82. Ammitzbøll, C., et al., *GPR15(+) T cells are Th17 like, increased in smokers and associated with multiple sclerosis.* J Autoimmun, 2019. **97**: p. 114-121.
83. Kimmig , S., et al., *Two Subsets of Naive T Helper Cells with Distinct T Cell Receptor Excision Circle Content in Human Adult Peripheral Blood.* Journal of Experimental Medicine, 2002. **195**(6): p. 789-794.
84. Santegoets, S.J., et al., *Monitoring regulatory T cells in clinical samples: consensus on an essential marker set and gating strategy for regulatory T cell analysis by flow cytometry.* Cancer Immunol Immunother, 2015. **64**(10): p. 1271-1286.
85. Chung, Y., et al., *Critical regulation of early Th17 cell differentiation by interleukin-1 signaling.* Immunity, 2009. **30**(4): p. 576-87.
86. Korn, T., et al., *IL-21 initiates an alternative pathway to induce proinflammatory T(H)17 cells.* Nature, 2007. **448**(7152): p. 484-487.
87. Bettelli, E., et al., *Reciprocal developmental pathways for the generation of pathogenic effector TH17 and regulatory T cells.* Nature, 2006. **441**(7090): p. 235-238.

88. Kimura, A. and T. Kishimoto, *IL-6: Regulator of Treg/Th17 balance.* European Journal of Immunology, 2010. **40**(7): p. 1830-1835.
89. Ivanov, I.I., et al., *The Orphan Nuclear Receptor RORγt Directs the Differentiation Program of Proinflammatory IL-17+ T Helper Cells.* Cell, 2006. **126**(6): p. 1121-1133.
90. West, N.R., *Coordination of Immune-Stroma Crosstalk by IL-6 Family Cytokines.* Front Immunol, 2019. **10**: p. 1093.
91. Chen, J., et al., *IL-17A Induces Pro-Inflammatory Cytokines Production in Macrophages via MAPKinases, NF-κB and AP-1.* Cellular Physiology and Biochemistry, 2013. **32**(5): p. 1265-1274.
92. Camporeale, A. and V. Poli, *IL-6, IL-17 and STAT3: a holy trinity in auto-immunity?* Front Biosci (Landmark Ed), 2012. **17**(6): p. 2306-26.
93. Langrish , C.L., et al., *IL-23 drives a pathogenic T cell population that induces autoimmune inflammation.* Journal of Experimental Medicine, 2005. **201**(2): p. 233-240.
94. Lee, Y., et al., *Induction and molecular signature of pathogenic TH17 cells.* Nat Immunol, 2012. **13**(10): p. 991-9.
95. Han, L., et al., *Th17 cells in autoimmune diseases.* Front Med, 2015. **9**(1): p. 10-9.
96. Samson, M., et al., *Brief report: inhibition of interleukin-6 function corrects Th17/Treg cell imbalance in patients with rheumatoid arthritis.* Arthritis Rheum, 2012. **64**(8): p. 2499-503.
97. Wang, L., F.S. Wang, and M.E. Gershwin, *Human autoimmune diseases: a comprehensive update.* J Intern Med, 2015. **278**(4): p. 369-95.
98. Ermann, J. and C.G. Fathman, *Autoimmune diseases: genes, bugs and failed regulation.* Nature Immunology, 2001. **2**(9): p. 759-761.
99. Hellesen, A., E. Bratland, and E.S. Husebye, *Autoimmune Addison's disease – An update on pathogenesis.* Annales d'endocrinologie, 2018. **79**(3): p. 157-163.
100. Skov, J., et al., *Heritability of Addison's disease and prevalence of associated autoimmunity in a cohort of 112,100 Swedish twins.* Endocrine, 2017. **58**(3): p. 521-527.
101. Winqvist, O., F.A. Karlsson, and O. Kämpe, *21-hydroxylase, a major autoantigen in idiopathic Addison's disease.* The Lancet, 1992. **339**(8809): p. 1559-1562.
102. Bratland, E., et al., *T Cell Responses to Steroid Cytochrome P450 21-Hydroxylase in Patients with Autoimmune Primary Adrenal Insufficiency.* The Journal of Clinical Endocrinology & Metabolism, 2009. **94**(12): p. 5117-5124.
103. Wolff, A.B., et al., *The natural history of 21-hydroxylase autoantibodies in autoimmune Addison's disease.* European journal of endocrinology, 2021. **184**(4): p. 607-615.
104. Hahner, S., et al., *High Incidence of Adrenal Crisis in Educated Patients With Chronic Adrenal Insufficiency: A Prospective Study.* J Clin Endocrinol Metab, 2015. **100**(2): p. 407-416.
105. White, K. and W. Arlt, *Adrenal crisis in treated Addison's disease: a predictable but under-managed event.* European Journal of Endocrinology, 2010. **162**(1): p. 115.
106. Røyrvik, E.C. and E.S. Husebye, *The genetics of autoimmune Addison disease: past, present and future.* Nature Reviews Endocrinology, 2022.
107. Eriksson, D., et al., *GWAS for autoimmune Addison's disease identifies multiple risk loci and highlights AIRE in disease susceptibility.* 2021.
108. Øksnes, M., et al., *Quality of Life in European Patients with Addison's Disease: Validity of the Disease-Specific Questionnaire AddiQoL.* The Journal of Clinical Endocrinology & Metabolism, 2012. **97**(2): p. 568-576.
109. Erichsen, M.M., et al., *Normal overall mortality rate in Addison's disease, but young patients are at risk of premature death.* European journal of endocrinology, 2009. **160**(2): p. 233.
110. Ehlers Mario, R., *Who let the dogs out? The ever-present threat of autoreactive T cells.* Science Immunology, 2018. **3**(20): p. eaar6602.
111. Danke, N.A., et al., *Autoreactive T Cells in Healthy Individuals.* The Journal of Immunology, 2004. **172**(10): p. 5967.

112. Bennett, C.L., et al., *The immune dysregulation, polyendocrinopathy, enteropathy, X-linked syndrome (IPEX) is caused by mutations of FOXP3.* Nature Genetics, 2001. **27**(1): p. 20-21.
113. Gambineri, E., T.R. Torgerson, and H.D. Ochs, *Immune dysregulation, polyendocrinopathy, enteropathy, and X-linked inheritance (IPEX), a syndrome of systemic autoimmunity caused by mutations of FOXP3, a critical regulator of T-cell homeostasis.* Curr Opin Rheumatol, 2003. **15**(4): p. 430-435.
114. Brunkow, M.E., et al., *Disruption of a new forkhead/winged-helix protein, scurfin, results in the fatal lymphoproliferative disorder of the scurfy mouse.* Nature Genetics, 2001. **27**(1): p. 68-73.
115. Bonelli, M., et al., *Quantitative and qualitative deficiencies of regulatory T cells in patients with systemic lupus erythematosus (SLE).* Int Immunol, 2008. **20**(7): p. 861-8.
116. Takahashi, M., et al., *An Inverse Correlation of Human Peripheral Blood Regulatory T Cell Frequency with the Disease Activity of Ulcerative Colitis.* Digestive Diseases and Sciences, 2006. **51**(4): p. 677-686.
117. Crispin, J.C., A. Martínez, and J. Alcocer-Varela, *Quantification of regulatory T cells in patients with systemic lupus erythematosus.* J Autoimmun, 2003. **21**(3): p. 273-6.
118. Brusko, T.M., et al., *Functional Defects and the Influence of Age on the Frequency of CD4+CD25+ T-Cells in Type 1 Diabetes.* Diabetes, 2005. **54**(5): p. 1407-1414.
119. van Roon, J.A., et al., *Numbers of CD25+Foxp3+ T cells that lack the IL-7 receptor are increased intra-articularly and have impaired suppressive function in RA patients.* Rheumatology (Oxford), 2010. **49**(11): p. 2084-9.
120. Kriegel, M.A., et al., *Defective suppressor function of human CD4+ CD25+ regulatory T cells in autoimmune polyglandular syndrome type II.* J Exp Med, 2004. **199**(9): p. 1285-91.
121. Sugiyama, H., et al., *Dysfunctional blood and target tissue CD4+CD25high regulatory T cells in psoriasis: mechanism underlying unrestrained pathogenic effector T cell proliferation.* J Immunol, 2005. **174**(1): p. 164-73.
122. Nie, H., et al., *Phosphorylation of FOXP3 controls regulatory T cell function and is inhibited by TNF-α in rheumatoid arthritis.* Nat Med, 2013. **19**(3): p. 322-8.
123. Goodman, W.A.W.A., et al., *IL-6 Signaling in Psoriasis Prevents Immune Suppression by Regulatory T Cells1.* The Journal of immunology (1950), 2009. **183**(5): p. 3170-3176.
124. Hirota , K., et al., *T cell self-reactivity forms a cytokine milieu for spontaneous development of IL-17+ Th cells that cause autoimmune arthritis.* Journal of Experimental Medicine, 2007. **204**(1): p. 41-47.
125. Munn, D.H., M.D. Sharma, and T.S. Johnson, *Treg Destabilization and Reprogramming: Implications for Cancer Immunotherapy.* Cancer Res, 2018. **78**(18): p. 5191-5199.
126. Chen, Z., et al., *The Ubiquitin Ligase Stub1 Negatively Modulates Regulatory T Cell Suppressive Activity by Promoting Degradation of the Transcription Factor Foxp3.* Immunity, 2013. **39**(2): p. 272-285.
127. Liu, Y., et al., *A novel role of IL-17A in contributing to the impaired suppressive function of Tregs in psoriasis.* J Dermatol Sci, 2021. **101**(2): p. 84-92.
128. Jorn Bovenschen, H., et al., *Foxp3+ Regulatory T Cells of Psoriasis Patients Easily Differentiate into IL-17A-Producing Cells and Are Found in Lesional Skin.* Journal of Investigative Dermatology, 2011. **131**(9): p. 1853-1860.
129. Raffin, C., L.T. Vo, and J.A. Bluestone, *Treg cell-based therapies: challenges and perspectives.* Nature Reviews Immunology, 2020. **20**(3): p. 158-172.
130. Scalapino, K.J., et al., *Suppression of Disease in New Zealand Black/New Zealand White Lupus-Prone Mice by Adoptive Transfer of Ex Vivo Expanded Regulatory T Cells.* The Journal of Immunology, 2006. **177**(3): p. 1451.
131. Bluestone, J.A., et al., *Type 1 diabetes immunotherapy using polyclonal regulatory T cells.* 2015.

132. Marek-Trzonkowska, N., et al., *Administration of CD4+CD25highCD127- regulatory T cells preserves β-cell function in type 1 diabetes in children.* Diabetes Care, 2012. **35**(9): p. 1817-20.
133. Trzonkowski, P., et al., *Hurdles in therapy with regulatory T cells.* Sci Transl Med, 2015. **7**(304): p. 304ps18.
134. Trzonkowski, P., et al., *First-in-man clinical results of the treatment of patients with graft versus host disease with human ex vivo expanded CD4+CD25+CD127— Tregulatory cells.* Clinical immunology (Orlando, Fla.), 2009. **133**(1): p. 22-26.
135. Dall'Era, M., et al., *Adoptive Treg Cell Therapy in a Patient With Systemic Lupus Erythematosus.* Arthritis & Rheumatology, 2019. **71**(3): p. 431-440.
136. Esensten, J.H., et al., *Regulatory T-cell therapy for autoimmune and autoinflammatory diseases: The next frontier.* Journal of Allergy and Clinical Immunology, 2018. **142**(6): p. 1710-1718.
137. Hong, S.-S., et al., *A Novel Small-Molecule Inhibitor Targeting the IL-6 Receptor β Subunit, Glycoprotein 130.* J Immunol, 2015. **195**(1): p. 237-245.
138. Choy, E.H., et al., *Translating IL-6 biology into effective treatments.* Nat Rev Rheumatol, 2020. **16**(6): p. 335-345.
139. Rendon, A. and K. Schäkel, *Psoriasis Pathogenesis and Treatment.* International journal of molecular sciences, 2019. **20**(6): p. 1475.
140. Grossman, R.M., et al., *Interleukin 6 is expressed in high levels in psoriatic skin and stimulates proliferation of cultured human keratinocytes.* Proc Natl Acad Sci U S A, 1989. **86**(16): p. 6367-71.
141. Goodman, W.A., et al., *IL-6 signaling in psoriasis prevents immune suppression by regulatory T cells.* J Immunol, 2009. **183**(5): p. 3170-6.
142. Kho, D., et al., *Application of xCELLigence RTCA Biosensor Technology for Revealing the Profile and Window of Drug Responsiveness in Real Time.* Biosensors (Basel), 2015. **5**(2): p. 199-222.
143. Guimet, D., et al., *Real-Time Quality Control Functional Assessment of Mesenchymal Stem Cells for Cellular Therapies*. 2019.
144. Kierano, *Schematic of a flow cytometer, from sheath focusing to data acqusition*. 2012.
145. Livak, K.J. and T.D. Schmittgen, *Analysis of relative gene expression data using real-time quantitative PCR and the 2(-Delta Delta C(T)) Method.* Methods, 2001. **25**(4): p. 402-8.
146. Smith, C.J. and A.M. Osborn, *Advantages and limitations of quantitative PCR (Q-PCR)-based approaches in microbial ecology.* FEMS microbiology ecology, 2009. **67 1**: p. 6-20.
147. Guan, N., et al., *Label-free monitoring of T cell activation by the impedance-based xCELLigence system.* Mol Biosyst, 2013. **9**(5): p. 1035-43.
148. Li, Y. and R.J. Kurlander, *Comparison of anti-CD3 and anti-CD28-coated beads with soluble anti-CD3 for expanding human T cells: Differing impact on CD8 T cell phenotype and responsiveness to restimulation.* Journal of Translational Medicine, 2010. **8**(1): p. 104.
149. Lyons, A.B. and C.R. Parish, *Determination of lymphocyte division by flow cytometry.* Journal of Immunological Methods, 1994. **171**(1): p. 131-137.
150. Heimli, M., *Characterization of regulatory T cells in Autoimmune Polyendocrine Syndrome type I, a model disease for autoimmunity*. 2018, The University of Bergen.
151. Yasuda, K., Y. Takeuchi, and K. Hirota, *The pathogenicity of Th17 cells in autoimmune diseases.* Semin Immunopathol, 2019. **41**(3): p. 283-297.
152. Kekäläinen, E., et al., *A Defect of Regulatory T Cells in Patients with Autoimmune Polyendocrinopathy-Candidiasis-Ectodermal Dystrophy.* The Journal of Immunology, 2007. **178**(2): p. 1208.
153. Arstila, P. and H. Jarva, *Human APECED; a Sick Thymus Syndrome?* Frontiers in Immunology, 2013. **4**.

154. Kelly, E., et al., *IL-2 and related cytokines can promote T cell survival by activating AKT.* J Immunol, 2002. **168**(2): p. 597-603.
155. Atienzar, F.A., et al., *The Use of Real-Time Cell Analyzer Technology in Drug Discovery: Defining Optimal Cell Culture Conditions and Assay Reproducibility with Different Adherent Cellular Models.* J Biomol Screen, 2011. **16**(6): p. 575-587.
156. Urcan, E., et al., *Real-time xCELLigence impedance analysis of the cytotoxicity of dental composite components on human gingival fibroblasts.* Dent Mater, 2010. **26**(1): p. 51-8.
157. Yu, N., et al., *Real-Time Monitoring of Morphological Changes in Living Cells by Electronic Cell Sensor Arrays: An Approach To Study G Protein-Coupled Receptors.* Analytical Chemistry, 2006. **78**(1): p. 35-43.
158. Atienza, J.M., et al., *Dynamic and label-free cell-based assays using the real-time cell electronic sensing system.* Assay Drug Dev Technol, 2006. **4**(5): p. 597-607.
159. Obr, A., et al., *Real-time monitoring of hematopoietic cell interaction with fibronectin fragment: the effect of histone deacetylase inhibitors.* Cell Adh Migr, 2013. **7**(3): p. 275-82.
160. Martinez-Serra, J., et al., *xCELLigence system for real-time label-free monitoring of growth and viability of cell lines from hematological malignancies.* Onco Targets Ther, 2014. **7**: p. 985-94.
161. Au - Xi, B., et al., *A Real-time Potency Assay for Chimeric Antigen Receptor T Cells Targeting Solid and Hematological Cancer Cells.* JoVE, 2019(153): p. e59033.
162. Lisby, A.N., et al., *Evaluation of CAR-T cell cytotoxicity: Real-time impedance-based analysis.* Methods Cell Biol, 2022. **167**: p. 81-98.
163. Cerignoli, F., et al., *In vitro immunotherapy potency assays using real-time cell analysis.* PloS one, 2018. **13**(3): p. e0193498-e0193498.
164. Atienza, J.M., et al., *Label-free and real-time cell-based kinase assay for screening selective and potent receptor tyrosine kinase inhibitors using microelectronic sensor array.* J Biomol Screen, 2006. **11**(6): p. 634-43.
165. Guan, N., et al., *Label-free monitoring of T cell activation by the impedance-based xCELLigence system.* Mol Biosyst, 2013. **9**(5): p. 1035-1043.
166. Bin Dhuban, K., et al., *Signaling Through gp130 Compromises Suppressive Function in Human FOXP3+ Regulatory T Cells.* Frontiers in Immunology, 2019. **10**.
167. Thiolat, A., et al., *Interleukin-6 receptor blockade enhances CD39+ regulatory T cell development in rheumatoid arthritis and in experimental arthritis.* Arthritis Rheumatol, 2014. **66**(2): p. 273-83.
168. Gu, J., et al., *Human CD39hi regulatory T cells present stronger stability and function under inflammatory conditions.* Cellular & Molecular Immunology, 2017. **14**(6): p. 521-528.
169. Patel, D.D., et al., *Effect of IL-17A blockade with secukinumab in autoimmune diseases.* Annals of the Rheumatic Diseases, 2013. **72**(suppl 2): p. iii116.
170. Ellis, S.D.P., et al., *Induced CD8+FoxP3+ Treg Cells in Rheumatoid Arthritis Are Modulated by p38 Phosphorylation and Monocytes Expressing Membrane Tumor Necrosis Factor α and CD86.* Arthritis & Rheumatology, 2014. **66**(10): p. 2694-2705.
171. Guo, Y., et al., *Changes in peripheral CD19(+)Foxp3(+) and CD19(+)TGFβ(+) regulatory B cell populations in rheumatoid arthritis patients with interstitial lung disease.* Journal of thoracic disease, 2015. **7**(3): p. 471-477.
172. Mirlekar, B., *Co-expression of master transcription factors determines CD4+ T cell plasticity and functions in auto-inflammatory diseases.* Immunology Letters, 2020. **222**: p. 58-66.

6. Appendix

Appendix I Additional information about the patients and healthy controls included in this project

Patient, sex and year of birth		Matched healthy control, sex and year of birth	
P1	F-1965	C1	F-1962
P2	F-1952	C2	F-1955
P3	M-1946	C3	M-1949
P4	M-1967	C4	M-1963
P5	F-1963	C5	F-1958

Appendix II Overview of antibodies for flow cytometry including their targets, cell type stained, fluorochromes, and wavelengths for excitation and collection of emission

Target	Marker of	Cell type stained	Dilution factor	Fluorochrome	Filter for emittance BP= band pass
CD3	T cells	Both	1:20	V500	670/30 BP
CD4	Helper T cells	Both	1:100	PerCP-Cy5.5	695/40 BP
CD8	Cytotoxic T cells	PBMC	1:100	PE-Cy5	582/15 BP
CD14	Monocytes	PBMC	1:100	PE	582/15 BP
CD20	B cells	PBMC	1:100	APC-Cy7	780/60 BP
CD25 (IL-2RA)	Tregs, activated T cells	Tregs	1:40	PE-Cy7	780/60 BP
CD31 (PECAM-1)	Recent thymic emigrants	Tregs	1:160	BV785	780/60 BP
CD39 (ENTPD-1)	Highly suppressive Tregs	Tregs	1:500	PE	582/15 BP
CD45RA	Naïve/resting T cells	Tregs	1:80	APC-H7	780/60 BP
CD127	Inversely proportional to FoxP3 expression	Tregs	1:50	PE-Cy5	661/20 BP
CD152 (CTLA-4)	Tregs (upregulated in activated T cells)	Tregs	1:20	BV421	450/50 BP
HLA-DR	Activated T cells/ Tregs	Tregs	1:100	BV650	670/30 BP
FOXP3	Tregs	Both	1:10	PE-CF594	610/20 BP
IKZF2 (Helios)	Tregs	Tregs	1:40	APC	670/14 BP

Dead cell stain	Dead cells	Both	1:1000	BV570	585/42 BP
CFSE	Cell proliferation	Both	-	FITC	530/30 BP

Appendix III Overview of primer sequences used in the SYBR green PBMC panel

Gene target	Forward	Reverse
β-actin	5'- GCATGGGTCAGAAGGATTCCT	5'- TCGTCCCAGTTGGTGACGAT
Bcl-6	5'- CATGCAGAGATGTGCCTCCACA	5'- TCAGAGAAGCGGCAGTCACACT
Eomes	5'- AGGCGCAAATAACAACAACACC	5'- ATTCAAGTCCTCCACGCCATC
FOXP3	5'- ATGCACCAGCTCTCAA	5'- AGTGGGTAGGAGCTCT
Gata-3	5'- GTCCTGTGCGAACTGTCA	5'- GATGCCTTCCTTCTTCATAGTCA
Rorγt	5'- TGGACCACCCCCTGCTGAGAAGG	5'- CTTCAATTTGTGTTCTCATGACT
T-bet	5'- GATGCGCCAGGAAGTTTCAT	5'- GCACAATCATCTGGGTCACATT

Appendix IV

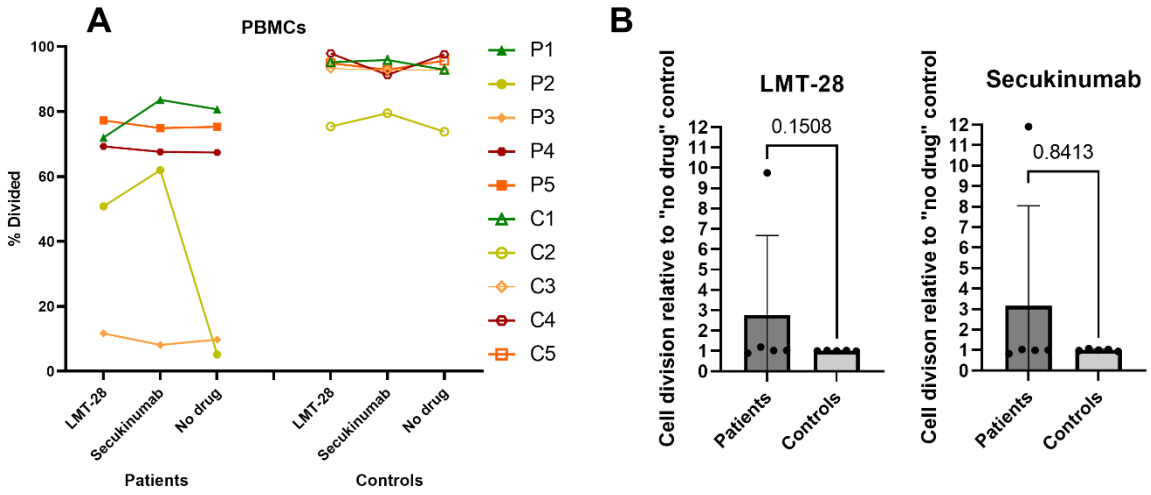

Figure. IV Percentage of dividing cells in treated and non-treated PBMCs from patients and healthy controls. A) Frequency of live, single cells that have undergone at least one cell division, making up the dividing population. B) Percentage of dividing cells in treated cells normalized to the "no drug" control within each individual were used to compare the impact of respective treatments on patients and healthy controls. Treatments were not shown to alter the size of the dividing cell population differentially in the two groups (unpaired, non-parametric t test).

Appendix V

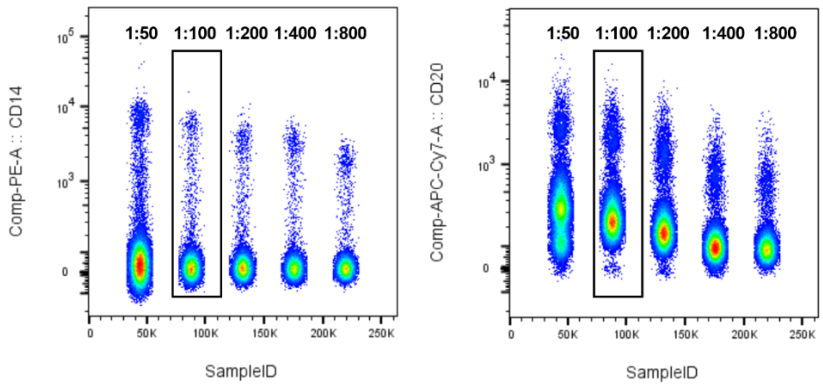

PBMC samples stained with different concentrations of CD14- and CD20 targeting antibodies spanning 1:50 to 1:800 of cell sample volume. Dilution yielding the best separation of populations positive and negative for the markers were chosen, indicated in the figure by boxes

Appendix VI

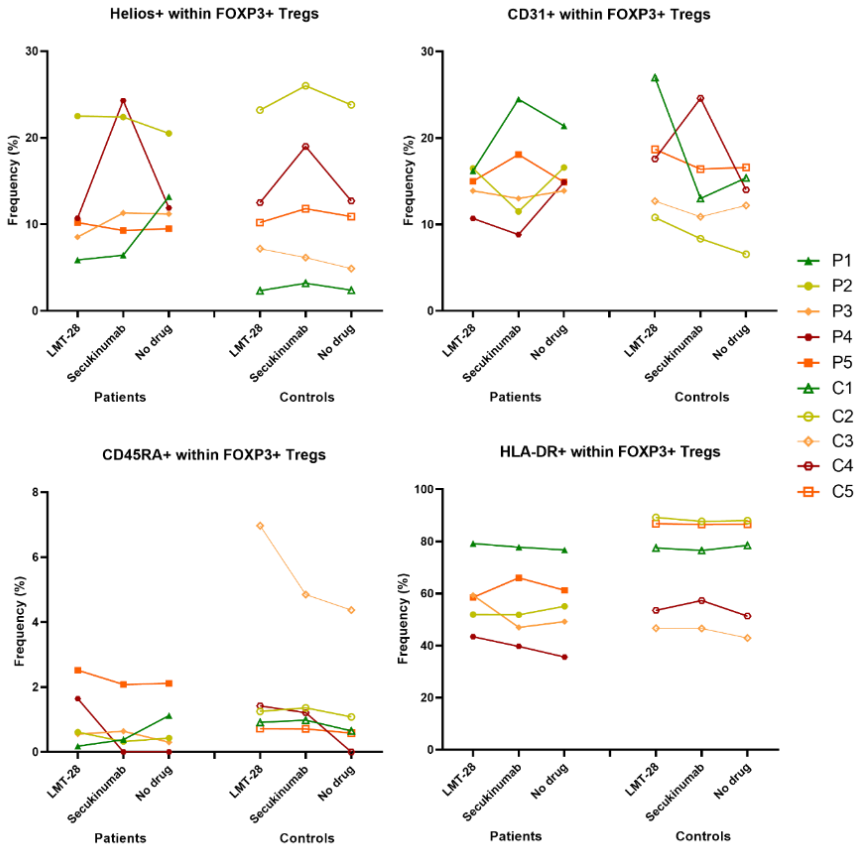

Figure VI a Frequencies of Tregs treated with LMT-28 and Secukinumab positive for the Treg markers A) Helios B) CD31 C) CD45RA and D) HLA-DR compared to non-treated "no drug" controls. No significant differences in the fractions of these markers on Tregs was indicated for patients or controls in response to both treatments (paired, one-way Anova, Friedman test).

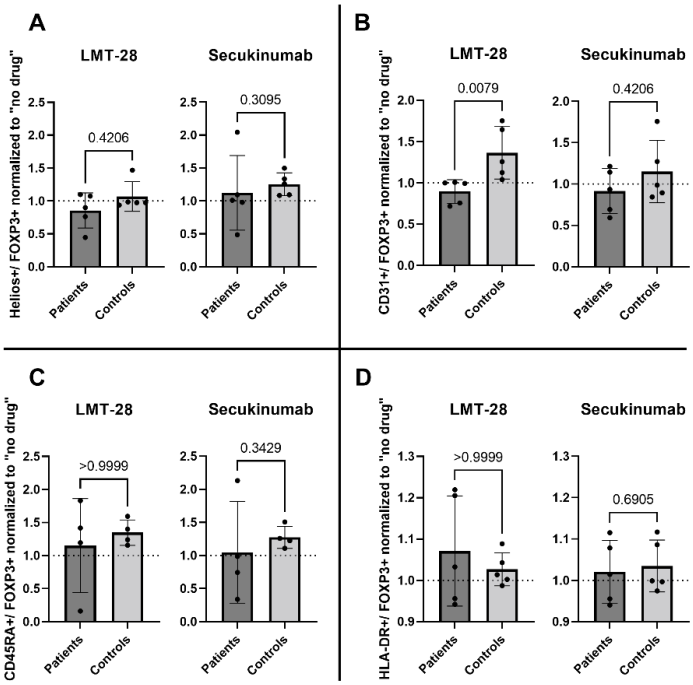

Figure VI b Relative increase/decrease in the fractions of A) Helios+ B) CD31+ C) CD45RA and D) HLA-DR+ Tregs after treatments, normalized to "no drug" controls from the same individuals. Differential effect of LMT-28 was seen on patients and controls when comparing CD31+ fraction of Tregs after treatment, (unpaired, non-parametric t test). Mean values are indicated by boxes, error bars show standard deviation, while the dotted line reflects the "no drug" baseline.

Appendix VII

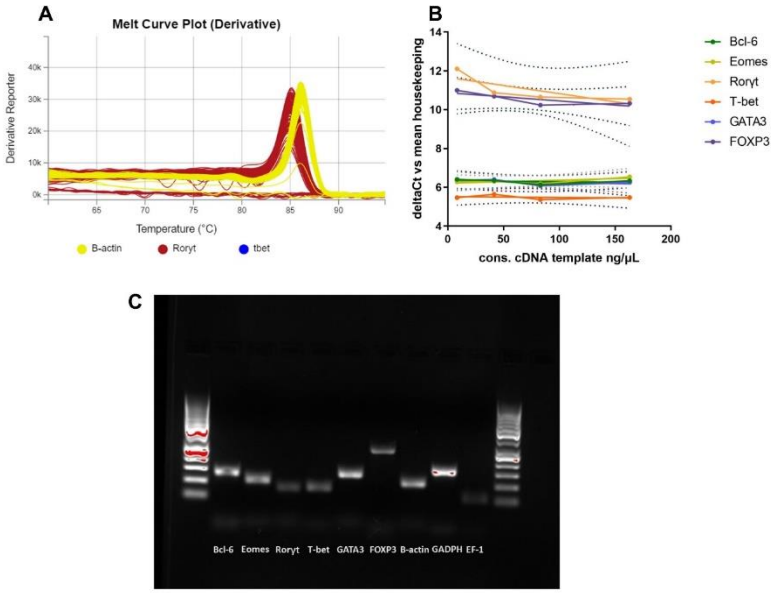

Figure VII Optimization of the efficacy and specificity of SYBR green primers A) Exemplary melting curve plots for B-actin and Rorγt showing a single peak at melting temperatures of the double strands for the amplified products. B) Primer verified for cDNA inputs between 8,33-166 ng/µL by achieving a close-to linear correlation between (ΔCt gene of interest relative to ΔCt housekeeping gene) and cDNA templates from a 4-fold diluted cDNA sample. C) Single bands indicating one qPCR product for each of the six targets, as well as B-actin (selected) and two other housekeeping genes that were considered. 50-1000 bp ladder present in first and last well of the gel.

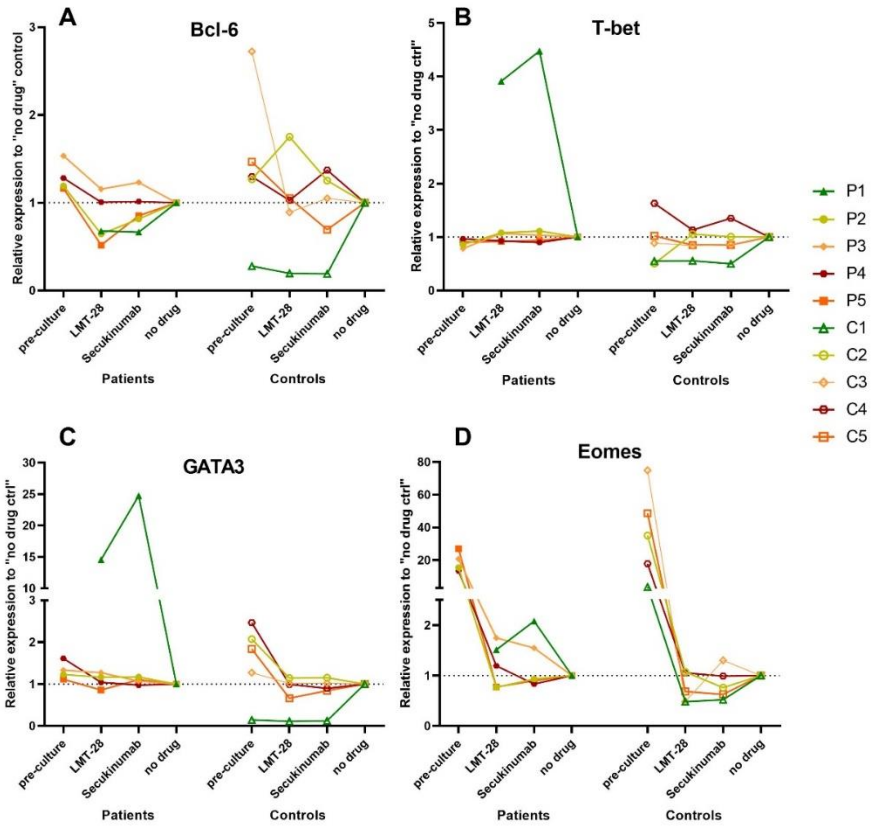

Figure VIII a Relative changes in the expression of *Bcl-6, T-bet, GATA3 and Eomes* after treatment with LMT-28 and Secukinumab, normalized to the non-treated control from the same individual, represented by dotted lines. Upregulation in gene expression is indicated by values higher than one on the y-axis, while the opposite shows downregulation. Samples from patients and matched controls are visualized in the same color, indicated in figure legend. No statistically significant differences were found (paired, non-parametric t tests) regarding the effect of LMT-28 and Secukinumab within neither patients nor controls.

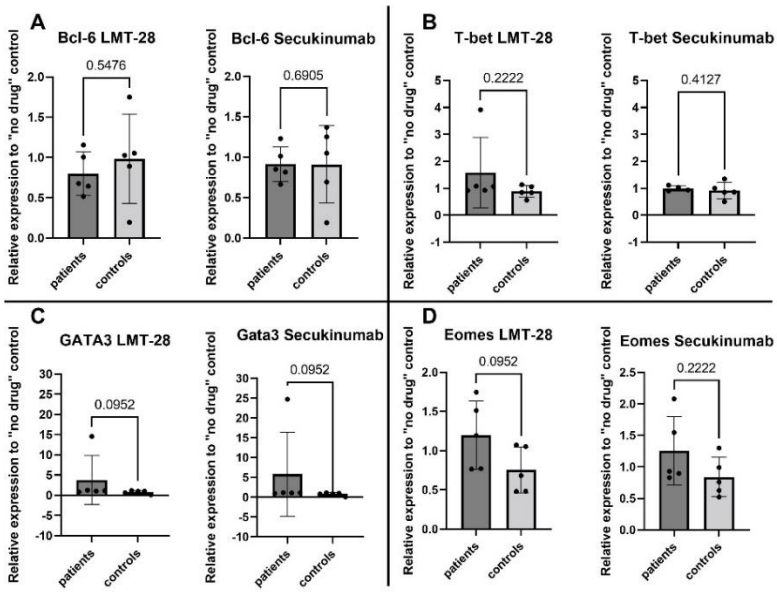

Figure VIII b Comparison of the effect of LMT-28 and Secukinumab treatment on differential expression of target genes in patient- and control groups Changes in expression relative to the "no drug" sample from each individual for A) Bcl-6 B) T-bet C) GATA3 and D) Eomes were compared between patient and control groups, indicating no statistically significant differences (unpaired, non-parametric t tests)

Appendix IX

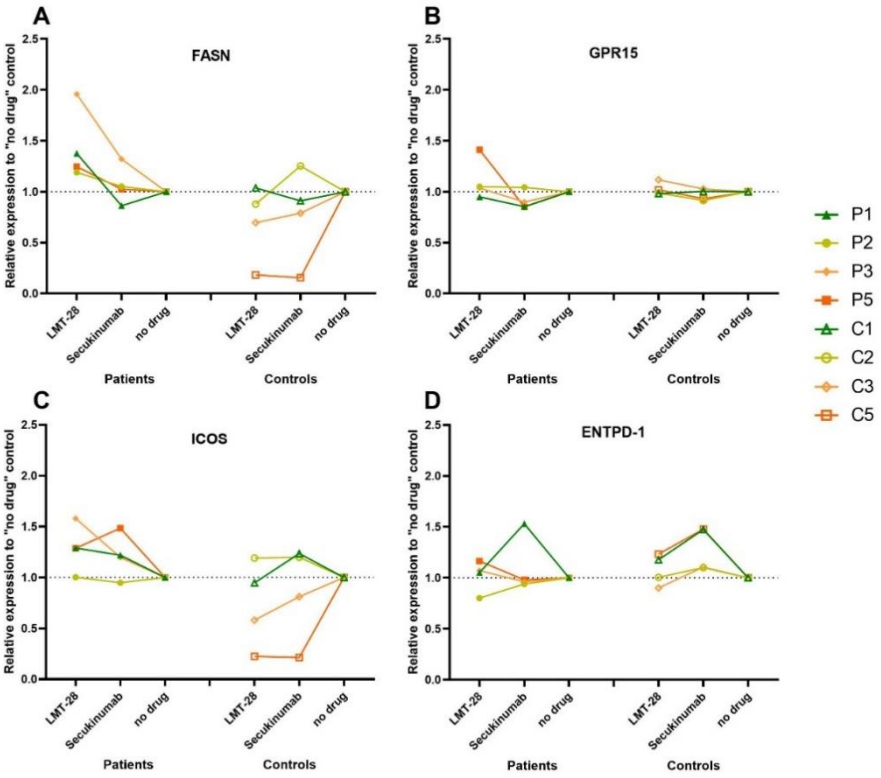

Figure 4.IX a Relative changes in the expression of A) ***FASN B) GPR15 C) ICOS and D) ENTPD-1*** **after treatment with LMT-28 and Secukinumab, normalized to the non-treated control from the same individual**, represented by dotted lines. Upregulation in gene expression is indicated by values higher than one on the y-axis, while the opposite shows downregulation. Samples from patients and matched controls are visualized in the same color, indicated in figure legend. No statistically significant differences were found (paired, non-parametric t tests) on the effect of both treatments on gene expression of all four targets.

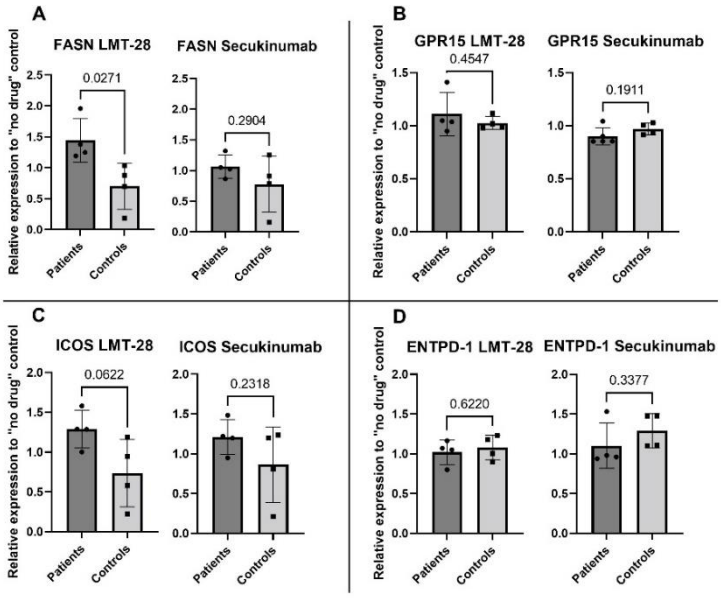

Fig 4 IX b Comparison of the effect of LMT-28 and Secukinumab treatment on differential expression of target genes in patient- and control groups Fold changes relative to the "no drug" sample from each individual for A) *FASN* B) *GPR15* C) *ICOS and* D) *ENTPD-1* were compared, indicating no statistically significant differences (unpaired, non-parametric t tests), although close-to significant p-values were found for FASN (A) and ICOS (B) after LMT-28 treatment.

Appendix X

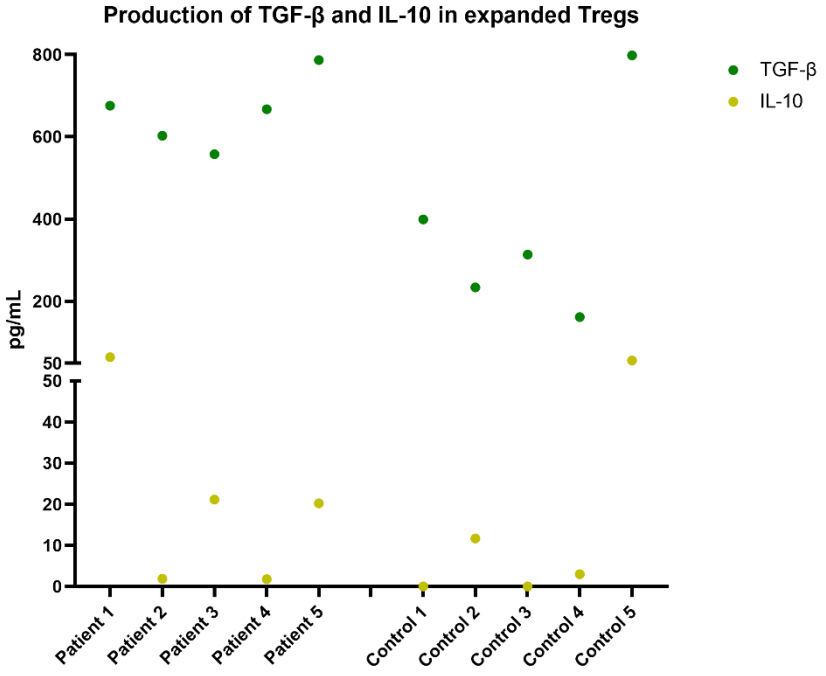

Figure X Concentrations of Treg signature cytokines in culture supernatant collected on the last day of 14-day *in vitro* expansion used to asses the functionality of patient and control Tregs.

Appendix XI

	xCELLigence RTCA	qPCR on PBMCs	qPCR on Tregs
Patient 1	NA: PBMCs	*Rorγt:* ****ND All gene targtets:**NA*	
Patient 2			
Patient 3			
Patient 4	NA: Tregs		All targets: NA
Patient 5			
Control 1	NA:PBMCs	*Rorγt:* *ND	
Control 2		*Rorγt:* *ND	
Control 3		*Rorγt:** ND	
Control 4	NA: Tregs		All targets: NA
Control 5			

NA: Not analyzed ND: Not determined *Pre-culture ** LMT-28 ***Secukinumab ****no drug control